COORDINATED MULTI-AGENT MOTION PLANNING UNDER REALISTIC CONSTRAINTS

A Dissertation

by

D. H. ASANKA MAITHRIPALA

Submitted to the Office of Graduate Studies of
Texas A&M University
in partial fulfillment of the requirements for the degree of

DOCTOR OF PHILOSOPHY

August 2008

Major Subject: Mechanical Engineering

COORDINATED MULTI-AGENT MOTION PLANNING UNDER REALISTIC CONSTRAINTS

A Dissertation

by

D. H. ASANKA MAITHRIPALA

Submitted to the Office of Graduate Studies of
Texas A&M University
in partial fulfillment of the requirements for the degree of

DOCTOR OF PHILOSOPHY

Approved by:

Chair of Committee,	Suhada Jayasuriya
Committee Members,	Aniruddha Datta
	Alexander Parlos
	Tamas Kalmar-Nagy
Head of Department,	Dennis O'Neal

August 2008

Major Subject: Mechanical Engineering

ABSTRACT

Coordinated Multi-agent Motion Planning Under Realistic Constraints. (August 2008)

D. H. Asanka Maithripala, B.S., University of Peradeniya;

M.S., Texas A&M University

Chair of Advisory Committee: Suhada Jayasuriya

Considered is a class of cooperative control problems that has a special affine characterization. Included in this class of multi-agent problems are the so called radar deception problem, formation keeping and formation reconfiguration. An intrinsic geometric formulation of the associated constraints unifies this class of problems and it is the first time such a generalization has been presented. Based on this geometric formulation, a real-time motion planning algorithm is proposed to generate dynamically feasible reference trajectories for the class. The proposed approach explicitly considers actuator and operating constraints of the individual agents and constrained dynamics are derived intrinsically for the multi-agent system which makes these constraints transparent. Deriving the constrained dynamics eliminates the need for nonlinear programming to account for the system constraints, making the approach amenable to real-time control. Explicit consideration of actuator and operating limitations and nonholonomic constraints in the design of the reference trajectories addresses the important issue of dynamic feasibility. The motion planning algorithm developed here is verified through simulations for the radar deception, rigid formation keeping and formation reconfiguration problems.

A key objective of this study is to advocate a change in paradigm in the approach to formation control by addressing the key issues of dynamic feasibility and computational complexity. The other important contributions of this study are: Uni-

fying formulation of constrained dynamics for a class of problems in formation control through the intrinsic geometry of their nonholonomic and holonomic constraints; Deriving these constrained dynamics in any choice of frame that can even be coordinate free; Explicit consideration of actuator and operating limits in formation control to design dynamically feasible reference trajectories and Developing a real-time, distributed, scalable motion planning algorithm applicable to a class of autonomous multi-agent systems in formation control.

ACKNOWLEDGMENTS

The following is my heartfelt appreciation to all those who gave me inspiration, advise, direction and insight to begin, conduct and complete this dissertation.

Naturally, my greatest appreciation goes to my advisor, Dr. Suhada Jayasuriya for his guidance, support, motivation and patience without which, these pages would not have been written. I consider myself very fortunate to have had the opportunity to work with him.

With great pleasure, I extend my gratitude to Dr. Alexander Parlos, Dr. Anirudda Datta, Dr. Tamas Kalmar-Nagy and Dr. Shankar Bhattacharyya who willingly agreed to be on my graduate committee and sit at the final examination in spite of their busy schedules.

I would like to extend my deepest gratitude and appreciation to my parents, two brothers and my sister for their relentless support and unselfish love. I also take this opportunity to thank all my friends here and back home for being an inspiration in all my work.

TABLE OF CONTENTS

CHAPTER Page

LIST OF FIGURES

FIGURE Page

CHAPTER I

INTRODUCTION

Cooperating multi-agent systems have received increased attention in the recent past, due primarily to technological advancements, and have applications in exploration and mapping, search and rescue, surveillance, cooperative manipulation, automated highways and network centric warfare. Autonomous, distributed and real-time control is an important if not imperative feature for the successful implementation of such multi-agent systems. Some of the other more important desirable features of multi-agent systems include, scalability in the number of agents, minimal communication, local sensing and communication, fault tolerance and learning behavior [1, 2]. In all the above paradigms of cooperative control one is interested in motion planning for a group of agents and in most cases involves some sort of formation control of the agents and our attention in this study is drawn only to such formation control problems in cooperating multi-agent systems. Formation control can be defined as a particular spatial arrangement of a group of agents through a common control strategy. Some of the problems in formation control that have been investigated are; formation feasibility [3], moving into formation [4], maintaining formation shape [5], and switching between formations [6].

Two main approaches can be seen in the literature on formation control. One approach is to formulate the formation control problem as a constrained optimization problem while the other approach is to formulate it in the framework of a tracking control problem. The main limiting characteristic of many existing motion planning algorithms utilizing the former approach is the computational complexity [7] where

---

The journal model is *IEEE Transactions on Automatic Control*.

even those proposed for real-time path planning lead to the solution of an optimization problem using nonlinear programming [8, 9]. The typical approach in constrained optimization is to cast the problem in a framework to find a trajectory of a nonlinear dynamic system (i.e. $\dot{x} = f(x, u)$ with x : states and u : controls) that minimizes a cost function ($J(x, u)$) subject to constraints possibly on the states, trajectory, initial time and final time. For the so called radar deception problem considered in this study the optimization approach reduces to solving a nonlinear two point boundary value problem using one of the standard numerical approaches of the *shooting method*, *finite difference method* or *projection method*, all of which are computationally intense processes at best. On the other hand, most approaches that formulate formation control as a tracking control problem assume the reference trajectory for the group as a whole is known a priori rather than designed in real-time to include the individual agent dynamics and constraints. This approach generally does not work well for a system having dynamic constraints at the individual agent level since we are likely attempting to track a trajectory of the system that may be dynamically infeasible. For example, in [10, 11] the phantom trajectory being generated by a coordinating team of UAVs engaged in a radar deception task is assumed rather than designed and reference trajectories of the individual agents are found through inverse kinematics. However the dynamic feasibility of tracking these reference trajectories quickly becomes a difficult issue and this was first pointed out in [12]. A leader following approach is used in [13, 14] for formation control where the trajectory of the leader is assumed. In leader following approaches, the leader-robot is required to follow a given trajectory while the follower robots are responsible for changing the formation. A leader-following approach for a system consisting of nonholonomic robots is presented in [15]. The concept of *virtual structure* (VS), introduced in [16] allowing a group of agents to behave as if they were embedded in a rigid body, is used in

[16, 17, 18] for the rigid formation keeping problem. The dynamic constraints of the individual agents are incorporated in the group behavior to a certain degree in [17, 18] where the VS slows down or speeds up along its assumed path depending on how well the formation is maintained. In all the above approaches, the resulting formation tracking error necessarily depends on a desired reference path/trajectory assumed rather than designed for the leader, the phantom or the VS. An exception to this is the work presented in [5], designing reference trajectories for the rigid formation keeping problem, which can theoretically result in zero tracking error for the mobile agents maintaining formation. However dynamic constraints are captured only to the extent that the designed reference trajectories will be smooth. Other notable approaches to formation control include behavior-based control [19], potential field approaches [20] and geometric control methods [21, 22].

In order to put in perspective the importance of designing trajectories that are dynamically feasible by each of the agents in the multi-agent system, let us now consider a scenario where three robots are maintaining an equally spaced line formation. If all three agents are restricted to have the same speed they *must* have common velocity directions to maintain this line formation. This corresponds to pure translational motion (parallel motion) of the formation line. In fact multi-agents constrained to have the same speed can have only one of two stable formations; parallel motion characterized by common velocity directions of agents (with arbitrary relative spacing) or circular motion characterized by circular orbits of the agents about a common fixed point [23, 24]. For the three agent line formation, a rotation of the line formation, no matter how small, will necessarily demand the agents to have differential speeds. The amount of dynamically feasible rate of rotation of the formation line will be a nonlinear function of the allowable differential speeds and the spacing between agents and will generally be considerably less than the allowable rate of turn of the individ-

ual agents. This simple example shows that the dynamic constraints that limit the maneuverability of a single agent can have a magnified effect in limiting the maneuverability of a formation as a whole. Parallel motion of a formation, while escaping this fact, will generally be too restrictive to be useful in practical applications. This is particularly so for example in the box pushing or formation flight scenarios. The issue of real-time trajectory generation under actuator and operating constraints is addressed for a constrained system in [8, 9] and in the multi-agent formation control setting in [25]. However these methods end up solving a constrained optimization problem using nonlinear programming to generate feasible trajectories, which is a computationally intense process.

The critical role played by dynamic constraints in formation control problems that do not allow flexibility in their formation constraints has been over looked in most approaches to formation control. Approaches that do consider dynamic constraints do so by solving a constrained optimization problem using nonlinear programming. One of the main goals of this study is to advocate a change in paradigm in the approach to formation control that would address the key issues of dynamic feasibility and computational complexity. Dynamic feasibility is especially critical for formation control problems that have little flexibility in their formation constraints.

A. A Class of Problems in Formation Control

We look at the class of problems in formation control that can be defined by a formation constraint (configuration constraint) and where the individual agent dynamics and constraints can be captured through an affine control form having inequality constraints on the affine control functions. At a minimum this class comprises of the following three general problems in formation control, each of which involves coor-

dinated motion planning of multi-agents to achieve a team goal in the presence of configuration and dynamic constraints. For convenience of presentation, the class of problems in formation control is identified by these three example problems though the results and analysis of this study are applicable to a broader class in general.

- Radar deception problem
- Rigid formation keeping
- Formation reconfiguration

The first problem, which we shall call the radar deception problem, serves as a motivating example in formation control involving a rather unique constraint on the system configuration. In this problem a team of fixed winged UAVs cooperate to deceive a ground radar network into seeing a spurious phantom track in its radar space. It is assumed that each UAV engaging a radar it is assigned to has the capability to intercept, introduce a time delay and re-transmit the radar's transmitted pulses thereby making the radar detect a target at a false range. The problem essentially involves all the extended lines of sight, from the radars to the UAVs engaging them, intersecting at a common point and tracing a path in space, which is a constraint on the system configuration space. The radar deception problem first appeared in [26, 10] while the essential role dynamic feasibility plays in this problem was first pointed out in [12]. Subsequently it has been studied in [11, 27, 28, 29, 30] for the 2D scenario while the only known 3D results are in [31]. The radar deception scenario is illustrated in Fig.1 for the case of four UAVs engaging a radar network having four radar stations.

The second problem we consider, rigid formation keeping, requires the relative distances of all the agents in the system to be fixed which is again a constraint on the

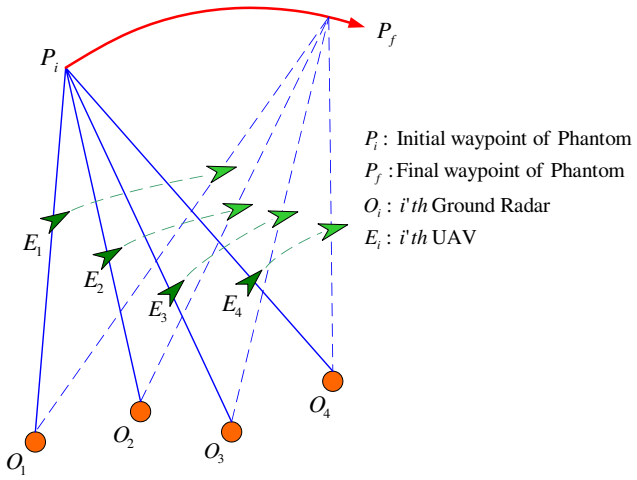

Fig. 1. Radar deception through phantom track generation.

configuration space. This problem has applications in formation flying [32, 33, 34], box pushing (also known as load transportation) [16, 35], cooperative sensing [36] and in scouting [19, 37]. In box pushing a group of robots uniformly surround a rigid object and may or may not grasp the object. By guaranteeing the shape of the formation, the surrounded or grasped object can be kept "trapped" amidst the robots and moved to a desired location. The robots are required to maintain a rigid geometric relationship with its load while in motion, as loose adherence will result in uneven load distribution [16, 35]. In close formation flight, an aircraft can benefit in terms of fuel efficiency from a reduction in drag if it can continue to stay in the "hot spot" of a vortex created by an aircraft in front of it [32, 33]. This requires that the group of aircraft fly in a rigid formation with considerable precision especially since separation of aircraft can be as little as a few meters while flying at very high speeds.

Rigid formation keeping can in general be too restrictive for an environment with obstacles and therefore formation reconfiguration, the third problem we consider, becomes important. In this problem we treat the time-invariant constraints defining

a rigid formation as time varying constraints to allow the formation to change from one fixed formation to another. Formation reconfiguration is also crucially important for the initial deployment of the multi-agents to form a rigid formation since it is unreasonable to assume the initial position of agents to be consistent with the desired rigid formation. Examples of rigid formation keeping and formation reconfiguration are illustrated in Fig.2.

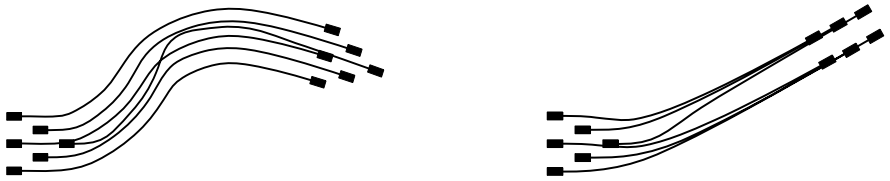

Fig. 2. Rigid formation keeping and formation reconfiguration.

Motion planning for the above three problems require satisfying constraints on the configuration of the multi-agent system while also satisfying constraints on the dynamics of the individual agents. At a minimum, constraints on individual agent dynamics will come through limitations on actuator capabilities. Dynamic constraints can also often include nonholonomic constraints, for example when the multi-agents are wheeled robots where the no slip condition at the wheel base is essentially a nonholonomic constraint on the agent dynamics. We show for the first time that the multi-agent motion planning for the above three problems are intrinsically geometric problems in the configuration space-time and can be expressed in a unifying manner. This is because, as will be shown later, these three problems can be defined through geometric constraints on the system configuration space-time. Hence from a geometric control point of view, the above three problems in formation control have a similar intrinsic geometry to them. The radar deception problem highlights the role of actuator and operating constraints in the feasibility of coordinated motion planning while

by considering the latter two problems, we in effect investigate the formation control problems of formation feasibility, moving into formation, maintaining formation and switching between formations.

Although a lot of research has been done on each of the formation control problems of formation flying [34, 32], box pushing [16, 35], scouting [19, 37], formation reconfiguration [6, 15], moving into formation [38, 39] and radar deception [11, 28, 31], we are unaware of any motion planning work that unifies these problems while also ensuring dynamic feasibility of such results. The class of problems in formation control we consider in this study encompasses and unifies all the above mentioned problems in formation control. We propose a motion planning algorithm applicable for the above class of problems in formation control, which also addresses the issue of dynamic feasibility.

The approach we propose in here is to embed the configuration and dynamic constraints of formation control into the design of reference trajectories to be used simultaneously by the tracking controllers of the individual agents. Theoretically (in the absence of model uncertainty, and external disturbances) this can result in zero tracking error. Based on this approach, we develop a real-time motion planning algorithm for the above class of problems to design formation trajectories that can ideally result in zero formation error at the tracking control stage. At the heart of the proposed algorithm is the explicit consideration of actuator and operating constraints of the individual agents and the derivation of constrained dynamics of the multi-agent system that makes these constraints transparent, thereby addressing the key issues of dynamic feasibility and computational complexity in formation control. In particular the actuator constraints we consider include lower bounds (with strictly positive bounds) for the individual robot speeds which we believe is imperative in aircraft/UAV applications.

Theoretical merit. Unifying formulation of constrained kinematics/dynamics for a class of problems in formation control through the intrinsic geometry of their nonholonomic and holonomic constraints. Deriving these constrained dynamics in any choice of frame that can even be coordinate free.

Practical merit. Explicit consideration of actuator and operating limits in multi-agent motion planning to design dynamically feasible reference trajectories. Developing a real-time, distributed, scalable motion planning algorithm applicable to a class of autonomous multi-agent systems in formation control.

B. Dissertation Outline

The work presented here is organized into eight chapters of which this introduction is Chapter-I. Chapter-II motivates the proposed motion planning algorithm for formation control through a kinematic analysis of the radar deception problem. The proposed motion planning algorithm for the class of formation control problems considered in this study is outlined in Chapter-III next. Chapter-IV formulates the constrained dynamics intrinsically and presents the main theoretical result of this study. The motion planning algorithm is next applied to the radar deception, the rigid formation keeping and the formation reconfiguration problem in Chapters V through VII. Chapter-VIII concludes with a discussion of proposed future work and conclusions of the study.

CHAPTER II

THE RADAR DECEPTION PROBLEM, A MOTIVATING EXAMPLE IN FORMATION CONTROL

The radar deception problem serves as a motivating example in formation control involving a rather unique constraint on the configuration space of the multi-agent system. Here a team of fixed winged UAVs cooperate to deceive a ground radar network into seeing a spurious phantom track in its radar space. A radar detects the presence of a target by listening into the echoes of its transmitted radio waves, bouncing off of the target. Measurements of the round-trip time and comparison of the frequency of the transmitted pulses to that of the moving target enables it to determine the range as well as the range-rate of the target [40]. Each UAV engaging a radar it is assigned to has the capability to intercept, introduce a time delay and re-transmit the radar's transmitted pulses thereby making the radar detect a target at a false range. This capability of intercepting and digitally storing and returning encoded pulses is known as range delay in Electronic Warfare [41, 27]. We assume each UAV to have stealth capability so as to remain hidden from the radar network and we assume the radar stations to be stationary. The challenge is to deceive the entire radar network into seeing a single coherent phantom track. This essentially involves all the extended lines of sight, from the radars to the UAVs engaging them, intersecting at a common point and tracing a path in space. By introducing the appropriate time delays to the radar signals, this path being traced is exactly what the radar network falsely detects as a target trajectory and hence the name phantom track. Based on this principle of range delay technique, Fig.3 illustrates how a team of four UAVs can be used to generate a phantom track to deceive a radar network. In this example scenario, there are four ground radars that share information about

the phantom track and four UAVs, one assigned to each radar. From an operational

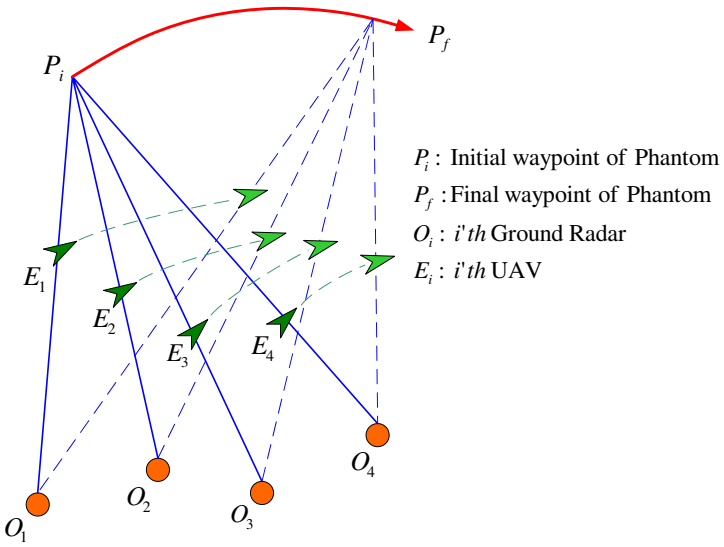

Fig. 3. Phantom track generation through a team of four UAVs.

point of view in the event a UAV fails, the radar it engaged will no longer detect the phantom and a loitering UAV can be brought in to re-engage the particular radar. The temporary loss of detection by one of the radars may not be detrimental for the deception process since often a radar network decides on the targets they detect based on majority ruled voting. However we emphasize that the radar deception scenario addressed here is not meant for operational significance but is more importantly intended as a motivating example to address the issue of finding dynamically feasible real-time solutions to formation control. In this study we assume that there are always as many UAVs as there are radars.

The requirement that all the lines of sight intersect at a common point is a constraint on the system configuration space, a constraint seemingly unique to this problem. Designing trajectories that satisfy the above configuration space constraint while operating within flight operating and actuator constraints of the UAVs makes

this a difficult but at the same time an interesting problem in formation control. In fact satisfying operating and actuator constraints becomes the most limiting or restricting factor in designing these trajectories. Satisfying these constraints is however essential for the trajectories to be dynamically feasible for the UAVs. This fact that the radar deception problem highlights the need to explicitly consider operating constraints and actuator limitations is exactly why we choose this particular problem as a motivating example. The radar deception problem was chosen in this study for several reasons: 1) it serves as a motivating example of multi-agent formation control, 2) demands a shift in paradigm to formation control to address the issues of feasibility and real-time control, 2) presents a problem in nonholonomic mechanics where the system can never be brought to rest making the vast majority of available results on nonholonomic systems inapplicable, 3) has all the typical issues that accompany multi-agent systems from scalability to real-time control.

Let us consider the radar deception problem that is restricted to the $2D$ plane. Suppose there are N-UAVs engaging N-radars and also suppose that we assign an imaginary UAV to mimic the motion of the phantom aircraft to make the phantom track realistic. The multi-agent system is decoupled into N-subsystems corresponding to the N radar-UAV pairs. Each subsystem (N of them) now only has two UAVs, one representing the phantom and the other the UAV engaging the radar. The configuration space of the i-th subsystem has the structure of a manifold, which we shall call Q_i, and we assign the local coordinates $q_i = (R_i, \vartheta_i, \varphi, r_i, \theta_i, \phi_i)$ as shown in Fig.4. Here, (R_i, ϑ_i) gives the position of the phantom in polar coordinates and φ gives its orientation in a global inertial frame. Similarly, (r_i, θ_i, ϕ_i) gives the position and orientation of the UAV engaging the radar. Without loss of generality, the radar is assumed to be at the origin of the local polar coordinate system q_i. The subscript i denotes the i-th subsystem. V and V_i denote the speed of the i-th UAV and the UAV

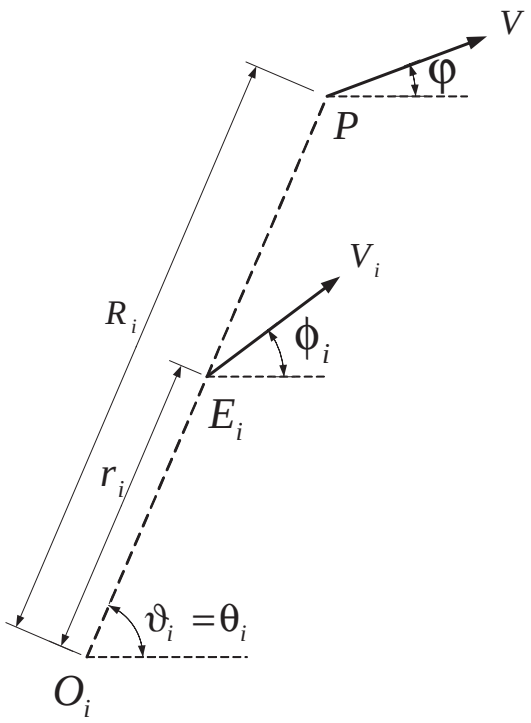

Fig. 4. Configuration of i-th subsystem in polar coordinates.

representing the phantom, respectively. When a coordinate or a function is global, having the same meaning in each of the N local coordinate systems, and there is no need to identify it with a particular subsystem we shall simply not use a subscript.

The requirement that the UAV has to be in-line with its corresponding radar and the phantom gives rise to a line of sight(LOS) constraint;

$$\vartheta_i = \theta_i. \tag{2.1}$$

We assume the dynamics of a UAV can be captured reasonably well, through the

following nonholonomic constraints of a unicycle;

$$\begin{aligned} \dot{R}_i \sin(\varphi - \vartheta_i) - R_i \dot{\vartheta}_i \cos(\varphi - \vartheta_i) = 0 \\ \dot{r}_i \sin(\phi_i - \theta_i) - r_i \dot{\theta}_i \cos(\phi_i - \theta_i) = 0. \end{aligned} \tag{2.2}$$

The above nonholonomic constraints of Eq.(2.2) define the following equivalent control system on Q_i;

$$\begin{aligned} \dot{R}_i &= V \cos(\varphi - \vartheta_i) \\ \dot{\vartheta}_i &= V \frac{\sin(\varphi - \vartheta_i)}{R_i} \\ \dot{\varphi} &= U \\ \dot{r}_i &= V_i \cos(\phi_i - \theta_i) \\ \dot{\theta}_i &= V_i \frac{\sin(\phi_i - \theta_i)}{r_i} \\ \dot{\phi}_i &= U_i \end{aligned} \tag{2.3}$$

and can be written in the compact form;

$$\dot{q}_i = f_V(q_i)V + f_U(q_i)U + f_{V_i}(q_i)V_i + f_{U_i}(q_i)U_i. \tag{2.4}$$

As evident, the above equivalent control form is affine in the functions V, U, V_i, U_i and these functions are nothing but the kinematic controls corresponding to speed and turn rate of the unicycle model we considered. Dynamic constraints due to actuator and flight operating limitations are explicitly captured through constraints on these kinematic controls $\mu_i = (V, U, V_i, U_i)$ of the above equivalent control system. Note that these constraints are explicitly associated with the equivalent control form of Eq.(2.4). The admissible control range of the forward speed V of a UAV is a strictly positive range due to the stall speed constraint of fixed winged UAVs while the admissible range of the steer control U is assumed symmetric. Hence, flight and

actuator constraints are assumed to be as follows;

$$\begin{aligned} V^{min} \leq \quad & V \quad & \leq V^{max} \\ -U^{max} \leq \quad & U \quad & \leq U^{max} \\ V_i^{min} \leq \quad & V_i \quad & \leq V_i^{max} \\ -U_i^{max} \leq \quad & U_i \quad & \leq U_i^{max}. \end{aligned} \tag{2.5}$$

A. Feasible Trajectory Solutions

The formation configuration constraint given in Eq.(2.1) can be written in the following compact form

$$G_i(q_i) = 0 \tag{2.6}$$

while the dynamic constraints of the UAVs given by Eq.(2.3) can be written in the compact form

$$\dot{q}_i = \mathcal{F}_i(q_i, \mu_i). \tag{2.7}$$

Also the actuator and operating constraints given in Eq.(5.5) can be written in the compact form

$$\mu_i \in \Pi_i \tag{2.8}$$

where $\mu_i = (V, U, V_i, U_i)$.

Consider a multi-agent system $\mathcal{A}$ separable to N subsystems where each i-th subsystem can be completely described by configuration constraints $G_i(q_i) = 0$, dynamic constrains $\dot{q}_i = \mathcal{F}_i(q_i, \mu_i)$ and operating and actuator constraints $\mu_i \in \Pi_i$. Such a generalization allows us to consider and comment on the rigid formation keeping problem and the formation reconfiguration problem in addition to the radar deception

problem that is considered in this chapter. Let us formally define what we mean by feasible solutions to $\mathcal{A}$ next.

Feasibility. *Feasible solutions for the multi-agent system $\mathcal{A}$ are defined as those solutions that satisfy individual agent dynamic constraints given by $\dot{q}_i = \mathcal{F}_i(q_i, \mu_i)$, formation configuration constraints given by $G_i(q_i) = 0$ subject to actuator and operating constraints given by $\mu_i \in \Pi_i$ for $i = 1, \ldots, N$.*

We derive the constrained kinematics that retain the control functions μ_i since we need to explicitly satisfy the actuator constraints $\mu_i \in \Pi_i$. The two equations $\dot{q}_i = \mathcal{F}(q_i, \mu_i)$ and $\mathcal{G}_i(\dot{q}_i, q_i) := \frac{d}{dt}(G_i(q_i)) = 0$ can be solved to yield $\mathcal{H}_i(q_i, \mu_i) = 0$.

Consider the partition of controls $\mu_i = (w^i, u^i)$ such that the dimension of w^i is equal to the dimension (number of equations, call it s) of $\mathcal{H}_i(q_i, \mu_i)$. Then, *if* the jacobian matrix $|\frac{\partial \mathcal{H}_i}{\partial w^i}| \neq 0$ for $(q_i, \mu_i) \in Q_i \times \Pi_i$, the implicit function theorem assures us that we can solve $\mathcal{H}_i(q_i, w^i, u^i) = 0$ for the w^is in terms of the u^is;

$$\begin{aligned} w_1^i &= H_{i,1}(q_i, u^i) \\ &\vdots \\ w_s^i &= H_{i,s}(q_i, u^i) \end{aligned} \tag{2.9}$$

and we get the constrained kinematic system affine in u^i, where u^i are the only independent controls. The constrained kinematic control system affine in the controls u^i can be written in the following compact form;

$$\dot{q}_i = \tilde{\mathcal{F}}_i(q_i, u^i) \tag{2.10}$$

and the multi-agent system $\mathcal{A}$ is now completely described by $\dot{q}_i = \tilde{\mathcal{F}}_i(q_i, u^i), \mu_i \in \Pi_i$ where $\mu_i = (w^i, u^i)$ and $w^i = H_i(q_i, u^i)$.

Suppose $\tilde{\mathcal{F}}_i$ of Eq.(2.10) are piecewise continuous in time and Lipschitz in its configuration variables q_i. Then given any initial condition $q_i(0) \in Q_i$ and controls

$u^i(0) \in \Pi_i$, there exists a time δt such that $\forall\, t \in [0, \delta t]$ a unique trajectory exists for $\dot{q}_i = \tilde{\mathcal{F}}_i(q_i, u^i)$ given by Eq.(2.10). Hence for feasibility of solutions we only need to guarantee that the controls $\mu_i = (w^i, u^i)$ are in the admissible control space, i.e. $\mu_i \in \Pi_i$, subject to $w^i = H_i(q_i, u^i)$ given by Eq.(2.9).

Suppose the control form $\dot{q}_i = \tilde{\mathcal{F}}_i(q_i, u^i)$ satisfies the Lie Algebra Rank Condition. Such a system is said to satisfy the accessibility property. If the set Π_i contains the origin, the control form $\dot{q}_i = \tilde{\mathcal{F}}_i(q_i, u^i)$ represented by Eq.(2.10) is also a symmetric system and hence will be small time controllable. Finding controls u^i that ensure $\mu_i \in \Pi_i$ for small time controllable systems will not be difficult since rest to rest motion is allowed and thus feasibility of solutions will not be an issue. For details on the accessibility property and small time controllability we refer the reader to [42]. Assume that the admissible control space of the system $\mathcal{A}$, Π_i, is such that Π_i is a compact and dense set not containing the origin as is the case for the radar deception problem we consider. Hence it will be a system that will not be small time controllable. In fact feasibility of solutions by itself becomes an issue. Consider piecewise constant controls u^i. For initial conditions $q_i(0) \in Q_i$, if $w_i(0)$ is within its control set bounds, then there exists a time $\delta_i t$ and admissible controls u^i such that $\forall\, t \in [0, \delta_i t]$, $w_i(t)$ continues to stay within its admissible range subject to $w^i = H_i(q_i, u^i)$ given by Eq.(2.9). If however $w_i(0)$ is at the boundary of Π_i, we require arbitrary control over the signature of $\frac{d}{dt}[H_{i,s}(q_i, u^i)]$ for $\forall s$ to ensure the existence of such a time $\delta_i t$. Based on the above, we have the following proposition for feasibility of solutions to the system $\mathcal{A}$, [29].

Proposition 1. *If (1)* $|\frac{\partial \mathcal{H}_i}{\partial w^i}| \neq 0$, *(2)* $H_{i,s}(q_i, u^i)$ *are continuous and (3)* $sgn\big(\dot{H}_{i,s}(q_i, u^i)\big)$ *can be arbitrarily controlled with admissible controls* $\forall s$ *and* $\forall\, i = 1, \ldots, N$ *then the system* $\mathcal{A}$ *has feasible solutions.*

The rest of this chapter will deal exclusively with the radar deception problem

and when we say the multi-agent system $\mathcal{A}$, we will be referring to the team of UAVs engaging a radar network. For the radar deception problem $\mathcal{H}_i(q_i, \mu_i) := V_i R_i \sin(\phi_i - \theta_i) - V r_i \sin(\varphi - \vartheta_i) = 0$ and for the partition of controls $\mu_i = (w^i, u^i)$ where $w^i = V_i$, $u^i = (V, U, U_i)$ we have $|\frac{\partial \mathcal{H}_i}{\partial w^i}| \neq 0$.

$w^i = H_i(q_i, u^i)$ only has one equation and is given by;

$$V_i = V \frac{r_i \sin(\varphi - \vartheta_i)}{R_i \sin(\phi_i - \theta_i)}. \tag{2.11}$$

The constrained kinematic system $\dot{q}_i = \tilde{\mathcal{F}}_i(q_i, u^i)$ is of the form;

$$\dot{q}_i = \tilde{f}_V(q_i)V + \tilde{f}_U(q_i)U + \tilde{f}_{U_i}(q_i)U_i \tag{2.12}$$

where $u^i = (V, U, U_i)$ are the only independent controls.

We pause to note that the above constrained kinematics expressed explicitly in terms of the kinematic controls u^i was possible because $|\frac{\partial \mathcal{H}_i}{\partial w^i}| \neq 0$, a luxury we do not see in the other two formation control problems we consider.

Consider constant V leaving U, U_i as the only independent controls. Taking the first derivative of $H_i(q_i, u^i)$ we get

$$\dot{H}_i = a(q_i)U + b(q_i)\left[U_i - c(q_i)\right] \tag{2.13}$$

where

$$\begin{aligned} a(q_i) &= V r_i R_i \sin(\varphi - \theta_i)\cos(\phi_i - \theta_i) \\ b(q_i) &= -V r_i R_i \sin(\varphi - \theta_i)\cos(\phi_i - \theta_i) \\ c(q_i) &= \frac{V(\sin(\varphi - \phi_i) + \cos(\varphi - \phi_i))}{R_i \cos(\phi_i - \theta_i)}. \end{aligned} \tag{2.14}$$

Note from Eq.(2.5) that U can always be set to zero. Hence from Prop.1 if $|U_i^{max}| > \sup c(q_i)$, we have arbitrary control over the signature of $\dot{H}_i$ to ensure feasibility of solutions to $\mathcal{A}$. This result, which is a sufficient but not necessary

condition for the existence of feasible solutions to $\mathcal{A}$, provides the basis to a trajectory generating algorithm we develop for this example problem.

B. Straightening of Trajectories

Consider the following constraints, which act as obstacles on the configuration manifold Q_i.

$$| \varphi - \theta_i | < \frac{\pi}{2}, \qquad | \phi_i - \theta_i | < \frac{\pi}{2} \tag{2.15}$$

For all meaningfully realizable trajectories we have

$$\varphi > \theta_i \iff \phi_i > \theta_i \qquad and \qquad \theta_i > \varphi \iff \theta_i > \phi_i. \tag{2.16}$$

We can also easily derive the following relationship;

$$\frac{d}{dt}\left(\frac{r_i}{R_i}\right) = \frac{r_i}{R_i^2}\frac{sin(\varphi - \phi_i)}{sin(\phi_i - \theta_i)}V. \tag{2.17}$$

Equation (2.15), Eq.(2.16) and Eq.(2.17) yield the following;

$$\begin{aligned} \frac{d}{dt}\left(\frac{r_i}{R_i}\right) > 0 \qquad & when \qquad \frac{r_i}{R_i} < \frac{V_i}{V} \\ \frac{d}{dt}\left(\frac{r_i}{R_i}\right) < 0 \qquad & when \qquad \frac{r_i}{R_i} > \frac{V_i}{V} \\ \frac{d}{dt}\left(\frac{r_i}{R_i}\right) = 0 \qquad & \iff \qquad \frac{r_i}{R_i} = \frac{V_i}{V}. \end{aligned} \tag{2.18}$$

Thus we have $\lim_{t\to\infty}\left(\frac{r_i}{R_i}\right) = \left[\frac{V_i^{min}}{V^{max}}, \frac{V_i^{max}}{V^{min}}\right]$. Furthermore forcing V to be continuous ensures $\frac{V_i}{V}$ to be continuous. Then as $t \to \infty$, for some $t = T_i$, we see that $\frac{r_i}{R_i} = \frac{V_i}{V}$ at least once, instantaneously. This results in $\lim_{t\to\infty} | \varphi - \phi_i | = 0$ at least once instantaneously and we say asymptotically the flow of trajectories, locally, straighten out with respect to the orientation angle φ. We draw on this point to give a controllability result that we present next for the radar deception problem.

C. Controllability Result

Suppose at $t = T_i$ (maybe a very large time) we have $\frac{r_i(T_i)}{R_i(T_i)} = \frac{V_i(T_i)}{V(T_i)}$ for the system satisfying the inequality constraints of Eq.(2.15), described in the earlier section. This implies $\theta_i(T_i) = \theta(T_i)$. We then freeze the controls $V_i \equiv V_i(T_i),\ V \equiv V(T_i)$, make $U_i(t) \equiv U(t),\ \forall t \geq T_i$ and update the control bounds $U^{max} = \min[U^{max},\ U_i^{max}]$, resulting in $\phi_i(t) \equiv \varphi(t),\ \forall t \geq T_i$. Then the equivalent control system given by Eq.(2.3), for $\forall t \geq T_i$ simplifies to the following control system;

$$\begin{aligned}
\dot{R}_i &= cos(\varphi - \theta_i)V(T_i) \\
\dot{r}_i &= cos(\varphi - \theta_i)V_i(T_i) \\
\dot{\theta}_i &= \frac{sin(\varphi - \theta_i)}{R_i}V(T_i) \\
\dot{\varphi} &= U \\
\dot{\phi}_i &= U.
\end{aligned} \tag{2.19}$$

The control system of Eq.(2.19) gives the coupled dynamics of two Dubins' cars represented by (R_i, θ_i, φ) and (r_i, θ_i, φ). The only control of it is U since $V(T_i)$ and $V_i(T_i)$ are now constants. A result due to Dubins in [43] states that this system is controllable on the submanifold (R_i, θ_i, φ) or on the submanifold (r_i, θ_i, φ). These results extend to the case of the N-UAV system $\mathcal{A}$ given by Eq.(2.1), Eq.(2.3), Eq.(5.5) and we make the following conclusion.

Proposition 2. *The multi-agent system $\mathcal{A}$ satisfying $|\varphi - \vartheta_i| < \frac{\pi}{2},\ |\varphi_i - \theta_i| < \frac{\pi}{2}$ is asymptotically controllable on the submanifold $(R_i, \vartheta_i, \varphi)$ or (r_i, θ_i, ϕ_i) where $i = 1, \ldots, N$.*

D. Motion Planning Algorithm for the Radar Deception Problem

Based on the results presented above, an algorithm was developed that generated trajectories online and in real-time for a team of N-UAVs engaging their corresponding radars to generate a coherent phantom track. The algorithm computes piecewise constant controls along with the time periods over which these controls are to be applied, and incrementally steps forward in time in a receding horizon framework until the goal waypoint of the phantom trajectory is reached.

The system is decoupled into N-subsystems for the N-UAVs engaging their corresponding N-radars as described earlier in this chapter. The algorithm is presented in the form of a flow chart in Fig.5. The decoupling causes the phantom kinematics $(R_i, \vartheta_i, \varphi)$ to appear in all the N-subsystems resulting in some redundancies in the computations but is justified by the advantage it offers in way of distributed control. We assume that the team of UAVs starts off with an admissible control-configuration combination. Here an admissible control-configuration combination is any system configuration along with a set of admissible controls that satisfies the LOS constraint together with the constraints derived in Eq.(2.11).

For simplicity the control V is assumed fixed at $(V^{min}+V^{max})/2$. Equation (2.13) along with Prop.1 provides the basis to the algorithm which computes piecewise constant controls U and U_i that continually drive the V_is of Eq.(2.11) to $(V_i^{min} + V_i^{max})/2$, the mean of their admissible bounds, for $\forall i = 1, \ldots, N$. Depending on the current value of V_i, the gradient of H_i, $\frac{d}{dt}(H_i)$, might have to be made either positive or negative to drive V_i towards its mean value. Each UAV estimates, the *range* of controls of U and U_i that would ensure the desired signature of $\frac{d}{dt}(H_i)$. Call these ranges $\bar{U}_{ph,i}, \bar{U}_i$. Note that $\bar{U}_{ph,i}$ estimated by each UAV always has zero included, and hence the intersection of these $\bar{U}_{ph,i}$ for $i = 1, \ldots, N$ will never be empty. Next the

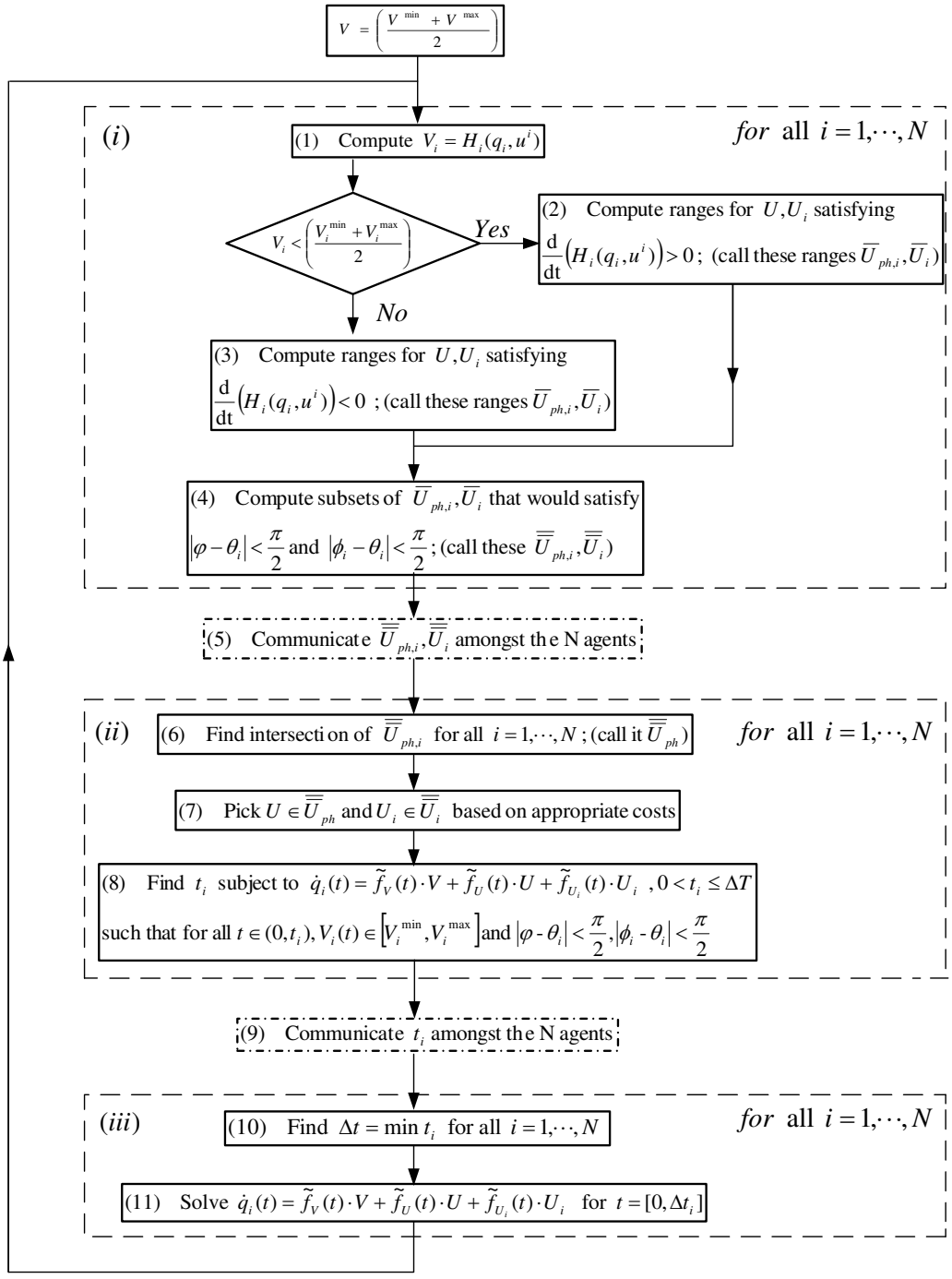

Fig. 5. Flow Chart: Algorithm used in generating real-time trajectories.

subsets of these ranges of $\bar{U}_{ph,i}, \bar{U}_i$ that would satisfy $\mid \varphi - \theta_i \mid < \pi/2, \mid \phi_i - \theta_i \mid < \pi/2$ are computed with the objective of straightening out the trajectories as detailed out in a previous section. Call these subsets $\bar{\bar{U}}_{ph,i}, \bar{\bar{U}}_i$. However not being able to satisfy the above inequalities it appears, would only slow the straightening of trajectories and will not affect feasibility. In the event these subsets or the intersection of $\bar{\bar{U}}_{ph,i}$ for $i = 1, \ldots, N$ is found to be empty, the above step (4th block of Fig.5) is simply ignored. Although theoretically it is not clear to us as to why these subsets would not be empty, simulation results have shown that for the most part they are indeed non empty. Simulation results have shown that for any given time interval the cumulative time over which the above constraints are not satisfied is either zero or is only a fraction of the time interval considered. Hence the net effect is for $\frac{r_i}{R_i}$ to converge to $\frac{V_i}{V}$. However we refrain from making a strong claim of this for the lack of a formal proof.

Next the intersection of $\bar{\bar{U}}_{ph,i}$ for $i = 1, \ldots, N$ is computed and final controls are determined for U and U_i based on cost functions. The cost function associated with calculating U attempts to minimize the phantom heading angle required to reach the final goal waypoint. This merely assists in keeping the phantom track directed as close to the the final waypoint as possible while it is the straightening of the trajectories and the consequent controllability of the phantom track that ensures the goal way point can be ultimately reached. The cost function associated with computing U_i minimizes the relative angle $\mid \varphi - \phi_i \mid$ to quicken the straightening of trajectories. Once the controls U, U_i are selected, each UAV estimates its maximum time t_i over which these controls can be applied before; V_i exceeds its admissible bounds or either $\mid \varphi - \theta_i \mid < \pi/2$ or $\mid \phi_i - \theta_i \mid < \pi/2$ is violated, which ever occurs first. Then $\Delta t = \min_i t_i$ is selected as the time period over which the selected constant controls are applied for each of the N-UAVs in the team.

The computations shown in the blocks (i),(ii) and (iii) of the flow-chart are performed in parallel by each of the N-UAVs and hence scaling of the number of UAVs has minimal effect on the computation time. The communication architecture of the algorithm is distributed as evident from Fig.5 though it requires global communication, meaning each UAV needs to communicate with each of the other UAVs. The ranges $\bar{U}_{ph,i}$ estimated by each of the UAVs and the times t_i are the only pieces of information that have to be communicated amongst the team agents and this has to happen only twice in each cycle of the algorithm as seen by the 5th and 9th blocks of Fig.5. Some of the key attributes of the algorithm are; (i) scalable in the number of UAVs (ii) suited for real time computation, as the search for the 2D case is reduced to single parameter searche over U, U_i (iii) low communication between agents (iv) implementable as an autonomous team of agents (v) the feedback structure of the proposed receding horizon approach provides inherent robustness.

E. Simulation Results

The algorithm produced the trajectories shown in Fig.6 in real-time for the case of 4-UAVs engaging 4-radars. Here we assumed a phantom speed of $400 \pm 40m/s$, UAV speeds of $100 \pm 15m/s$ and minimum turn radii of $5000m$ and $1500m$ for the phantom and the UAVs, respectively. The straightening of the trajectories, where the phantom and all the UAVs converge to a common orientation angle φ is seen in the latter part of the trajectory evolution in Fig.6. The convergence of $\frac{r_i}{R_i}$ to $\frac{V_i}{V}$ as explained in Section B is illustrated in Fig.7 for the 4th UAV. As soon as $\frac{r_i}{R_i} = \frac{V_i}{V}$, the control U_i is locked onto U as explained in Section C, resulting in $\frac{r_i}{R_i}$ being fixed as seen in the latter part of the time history of Fig.7. Obviously if all UAVs start off with initial admissible control-configuration combinations such that $\frac{r_i}{R_i} = \frac{V_i}{V}$ for $i = 1, \ldots, N$,

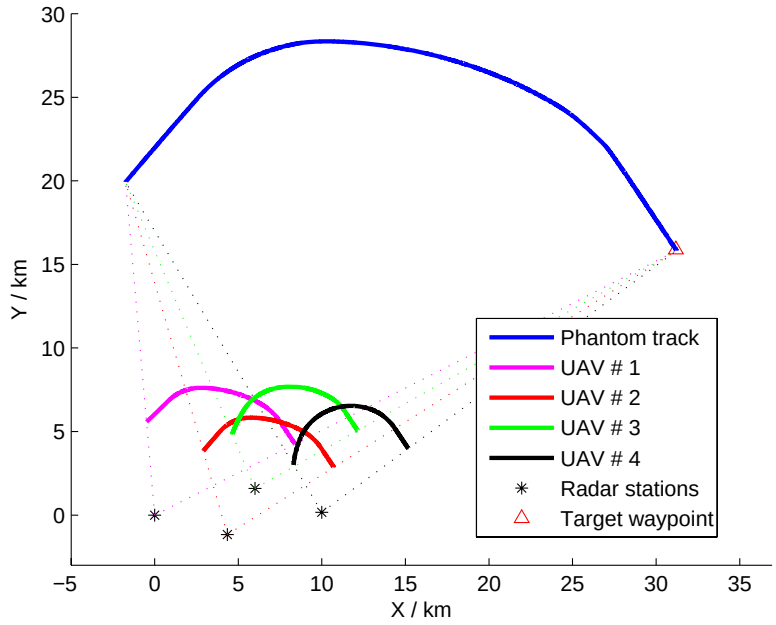

Fig. 6. Simulation results of trajectories for a team of four UAVs engaging four radars generating a coherent phantom track.

then the phantom track trivially evolves towards the goal waypoint in a straight line. The algorithm produces controls that are piecewise constant and result in continuous but non smooth speed and steer controls for the individual UAVs and this can be seen in Fig.7. However this is justified since this was a kinematic study only, where we did not take mass or inertia of the UAVs into consideration. In general, the computation time of the algorithm was an order of magnitude less than the real-time over which the algorithm was implemented. As mentioned earlier in the introduction of Chapter I, formulating this in the framework of a constrained optimization problem would require nonlinear programming methods to arrive at the trajectory solutions. Such an approach would not have been amenable to real-time control nor would it have been scalable in the number of agents.

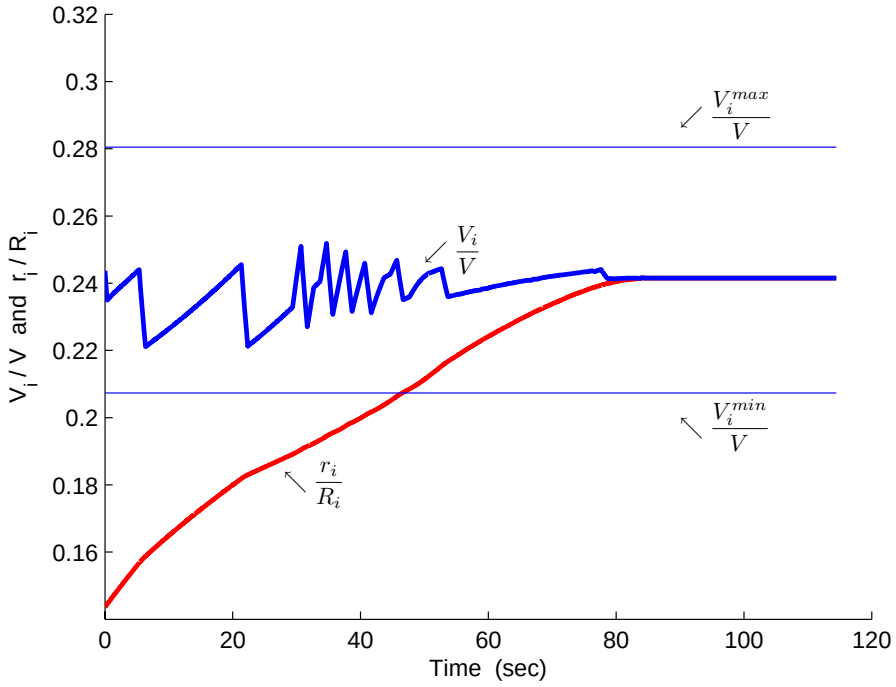

Fig. 7. Convergence of $\frac{r_i}{R_i}$ to $\frac{V_i}{V}$ for the 4-th UAV.

While the analysis and results given in this chapter are specific to radar deception and hides much of the geometry of the problem, it nevertheless motivates the intrinsic geometric formulation to formation control we present next.

CHAPTER III

PROPOSED APPROACH TO FORMATION CONTROL

In this chapter we present a motion planning algorithm for the class of problems considered in this study.

A. Formation Guidance

In formation control literature, we often come across the terms *formation guidance* and *formation tracking control*. Formation guidance is simply another term for trajectory generation in formation control where it is defined as the generation (or design) of reference trajectories to be used as the input for the formation agents' relative state tracking control law. Formation tracking control on the other hand refers to design techniques and associated stability/performance results for these relative state tracking control laws. The proposed approach to motion planning is on real-time reference trajectory generation as opposed to formation tracking. These reference trajectories are then to be simultaneously used as the input for the formation agents relative state tracking control law allowing the agents to track their reference trajectories online and in real-time.

Each of the three formation control problems we consider can be viewed as a multi-agent system $\mathcal{A}$ constrained to satisfy a formation constraint, which is a constraint on its configuration space. The configuration space of the multi-agent system $\mathcal{A}$ will have the structure of a smooth manifold which we shall call Q. Let $q \in Q$ denote the configuration of $\mathcal{A}$. The formation constraint on $\mathcal{A}$ will be a constraint on the configuration space Q and can be given by

$$C(q) = \mathbf{0}. \tag{3.1}$$

The objective is to design reference trajectories on Q satisfying the formation constraint $C(q) = \mathbf{0}$ that will also be dynamically feasible for the individual agents to track.

Explicitly incorporating the dynamic model, including all dynamic, operating and actuator constraints of the agents, in the design of the reference trajectories will ensure zero tracking error in the relative state tracking control stage, at least in theory. We say at least in theory, since this is with idealized assumptions of zero model uncertainty and zero disturbance. Explicit incorporation of the configuration constraints $C(q) = \mathbf{0}$ in the design of the reference trajectories will in theory result in zero error in the formation. But this is again with the assumption that zero tracking error can result in the tracking control stage. In actual implementation, model uncertainty and disturbance rejection is to be accounted through feedback in the tracking controllers, resulting in tracking errors (non zero) that will be functions of the model uncertainty, disturbance and performance of the feedback controller.

B. Agent Dynamics and Constraints

The individual agent trajectories of the multi-agent system are viewed as curves on the special Euclidean group $SE(n)$. We propose to design reference trajectories for these agents that capture the essential agent dynamics and constraints, but through a simplified dynamic model. For example, the dynamic capabilities of a four wheeled robot having many degrees of freedom and controls can be captured approximately but reasonably well through the much simpler unicycle model. The Unicycle model essentially captures the no slip condition of the wheeled robot while appropriate constraints on its higher level controls of speed, steer, force and torque can effectively capture the wheeled robot's actuator, operating and dynamic capabilities. This is the

reason why a lot of studies on wheeled robots, or even UAVs restricted to the plane, prefer to use the unicycle model to represent the agent dynamics.

Consider a general multi-agent system $\mathcal{A}$. Nonholonomic constraints of the agents in $\mathcal{A}$ are constraints on the velocities in the form of $C(\dot{q}, q) = \mathbf{0}$. Suppose these constraints will have an equivalent control form which will be affine in its controls.

$$\dot{q} = v^j f_j(q) \tag{3.2}$$

where $n = dim(Q),\ v^j \in \mathbb{R},\ j = 1, \ldots, m$ and $m < n$. Here v^j are control functions while f_j are vector fields on Q. In Eq.(3.2) and in the rest of this dissertation, we use the Einstein summation convention, also known as the tensor notation. For a multi-agent system $\mathcal{A}$ that does not have nonholonomic constraints, the system may still be written in the equivalent control form given above in Eq.(3.2) with $m = n$.

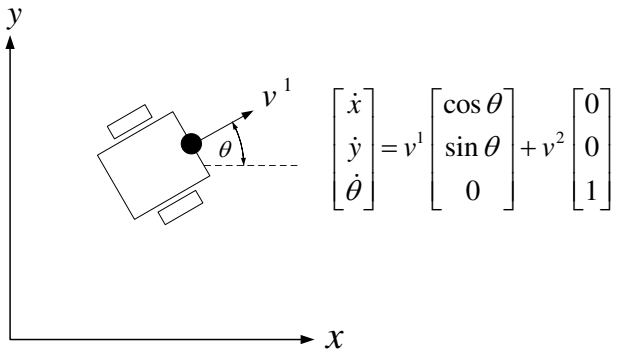

Fig. 8. Unicycle model, where (x, y): position, θ: orientation, v^1: speed, v^2: steer of unicycle.

We assume the agent dynamics of $\mathcal{A}$ can be represented through the above affine control form, $\dot{q} = v^j f_j(q)$. This control form is general enough to consider at least the commonly seen simplified vehicle models in formation control literature. For example the unicycle model shown in Fig.8, the simplified kinematic model of a UAV shown in Fig.9 and the single integrator model (dynamics of a holonomic robot) shown in

Fig.10 are all of the control affine form given by Eq.(3.2).

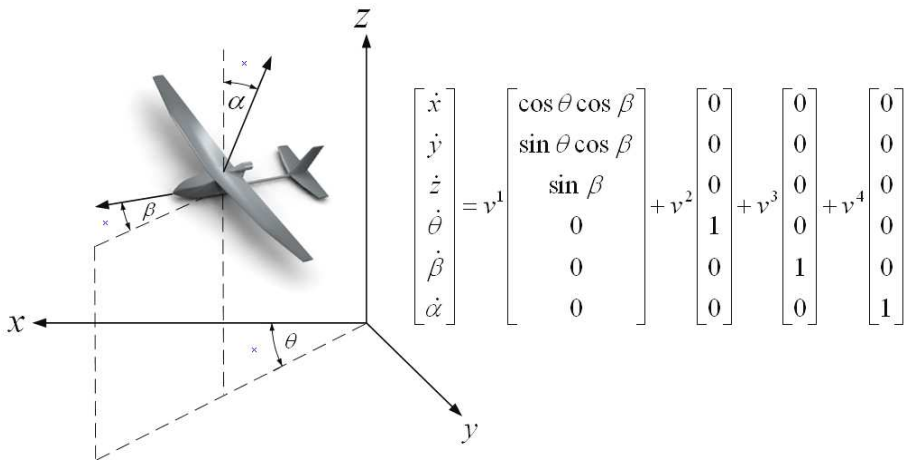

Fig. 9. Simplified UAV kinematic model, where (x, y, z): position, θ: heading angle, β: flight path angle, α: bank angle, v^1: speed, v^2: pitch, v^3: yaw and v^4: roll of UAV.

We propose to capture actuator and operating constraints of the agents through bounds on the control functions v^j and their first derivatives $\dot{v}^j$. These actuator and operating constraints, which are inequality constraints, can be compactly written as

$$(\mu, \dot{\mu}) \in \Pi, \quad \mu = \{v^1, \ldots, v^m\} \tag{3.3}$$

where Π is a compact set which does not necessarily have to have zero in its inclusion. Technically this can be stated as $\dot{q} = v^j f_j(q)$ being a drift system where the drift term is non-vanishing for $\mu \in \Pi$. The consideration of allowing Π to not have zero in its inclusion makes the above formalism general enough to consider a system $\mathcal{A}$ comprised of multi-agents whose operating constraints prohibit the system from coming to rest. An example being a multi-agent system comprised of fixed winged UAVs where the air speed must be maintained for the UAVs to remain aloft which is an operating limitation. Considering bounds on $\dot{\mu}$ allows us to treat the individual agents as

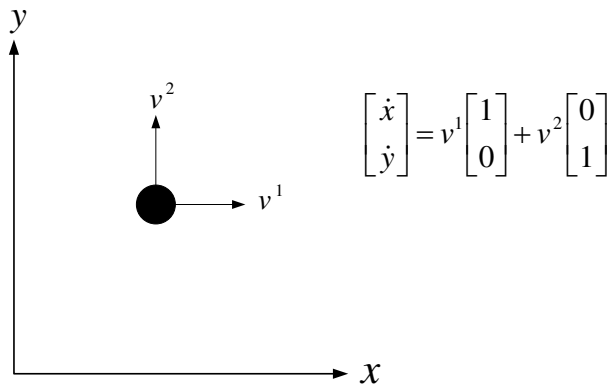

Fig. 10. Single integrator model of a mobile robot, where (x, y): position and v^1, v^2 are controls in the x, y directions.

having mass and inertia thus capturing their dynamic constraints more accurately. The agent dynamic constraints given by $\dot{q} = v^j f_j(q),\ (\mu, \dot{\mu}) \in \Pi$ can hence include nonholonomic, actuator and operating constraints, and take mass and inertia effects into consideration, making the above formulism powerful in capturing individual agent dynamics reasonably well.

Representing agent dynamics through a simplified dynamic model, while ensuring the essential constraints and limitations of the agent are captured reasonably well, makes the approach model independent and applicable to the class of problems we consider in formation control involving a variety of multi-agents from wheeled robots to UAVs. The accuracy with which the dynamic models of the individual agents are captured in the design of the reference trajectories will determine the degree of tracking error in the tracking control stage and ultimately in the degree of the error in formation. In actual implementation, model uncertainty and disturbances need to be accounted through feedback in the tracking controllers.

In 2D we prefer to employ the unicycle model for each of the agents making it applicable to wheeled robots and UAVs alike with controls v^j being the "speed",

"steer" of the agent while the first derivative of these controls, $\dot{v}^j$ will be associated with the "force" and "torque" acting on the agent. Actuator and operating constraints can be captured through bounds on these "speed", "steer", "force" and "torque" functions. If the application involves Hilare-type mobile robots, which have dynamics equivalent to a unicycle, the dynamic model is then explicitly and accurately captured in the design of the reference trajectories.

Each of the formation control problems of the class of problems we consider is assumed to be completely described, and hence defined, through a set of geometric constraints including a formation constraint of the form given by Eq.(3.1) and agent dynamic constraints of the form given by Eq.(3.2), Eq.(3.3). A feasible solution to the formation control problem is one that satisfies all these constraints.

C. Separation of the Problem for Distributed Control

Of the two approaches of centralized and decentralized coordinated motion planning for multi-agent systems, currently the dominant paradigm is the decentralized approach. There are two types of decentralized architectures; distributed architectures in which all agents are equal with respect to control, and hierarchical architectures which are locally centralized. The choice of architecture in the proposed motion planning algorithm is distributed control. We assume the multi-agent system to be homogeneous, meaning the dynamic capabilities and constraints of the individual agents are assumed identical. For distributed control of the multi-agent system $\mathcal{A}$ having N agents, we decouple the problem into N subproblems. From a geometric control point of view, this means the configuration and dynamic constraints given by $C(q) = 0,\ \dot{q} = v^j f_j(q),\ (\mu, \dot{\mu}) \in \Pi$ defining the formation control problem can be separated into N geometrically similar sets of constraints

$C(q_i) = 0,\ \dot{q}_i = v^j f_j(q_i),\ (\mu_i, \dot{\mu}_i) \in \Pi_i$ for $i = 1, \ldots, N$. Separating the multi-agent system into geometrically similar subsystems makes the approach and the resulting motion planning algorithm scalable in the number of agents in the system.

In the radar deception problem the phantom and each UAV makes up a separate subsystem where the coupling between the subsystems will be through the controls on the phantom. For consensus between the N subsystems, these controls (subset of the controls μ) need to have intrinsic meaning. In other words, these controls that couple the N subsystems should be independent of the coordinates of the subsystems.

For purposes of control, the agents in the multi-agent system for rigid formation keeping is viewed as forming a virtual structure (VS). Here the virtual structure consisting of the N agents is considered time invariant while each agent and a unique point on this VS defining the formation is treated as a separate subsystem. For convenience we consider the centroid of the VS as this unique point and assume virtual control over the VS as a whole. The coupling between the N subsystems will be through these controls on the VS. As in the radar deception problem, here too the controls that couple the N subsystems need to have intrinsic meaning for consensus amongst the N subsystems.

From a geometric control point of view, the formation reconfiguration problem is different from the rigid formation keeping problem only in that the VS made up of the multi-agent system is time varying. Here in the formation reconfiguration problem, each agent and the initial centroid (centroid of the VS at $t = t_0$) of the now time varying VS is considered a subsystem. Virtual control is assumed over the relative positions of each of the agents in the VS giving us control over the physical geometry of the time varying structure. Once again the controls that couple the N subsystems need to have intrinsic meaning for consensus.

We note that in the above three multi-agent systems, the controls that couple

the subsystems, controls on the phantom and on the VS, are only virtual controls, considered for the purpose of coordinated motion planning.

D. Constrained Dynamics

Having separated the problem into geometrically similar subproblems, next constrained dynamics are developed for the subsystem, which is the basis to the motion planning algorithm we present here. Constrained dynamics are formulated intrinsically to make it applicable to the class of problems considered and is presented in detail in the next chapter. We opt for tools from geometric mechanics to formulate the constrained dynamics due to the inherent geometry of constraints seen in the formation control problems we consider. The constrained dynamics are derived in a particular frame where the choice of frame for which these constrained dynamics are formulated is intimately associated with the affine control form $\dot{q}_i = v^j f_j(q_i)$ because of the particular manner in which we capture the actuator and operating constraints (through the set constraint $(\mu_i, \dot{\mu}_i) \in \Pi_i$). What this particular frame actually is, will be made clear in the proceeding chapter. The significance of deriving constrained dynamics in a particular frame is that we then have actuator and operating constraints appearing quite transparently in the constrained dynamic equations. This in turn facilitates control law design to satisfy these inequality constraints coming through actuator and operating limitations.

The use of concepts and tools from geometric mechanics is necessary for two reasons. One, the particular frame of choice is not a coordinate frame and it is the tools of geometric mechanics that come to our rescue in deriving the constrained dynamics exploiting the intrinsic geometry of the formation control problem. Second, it unifies a class of formation control problems through the intrinsic geometric formulation of

the governing constrained equations of motion.

E. Control Strategy for Consensus and Feasibility

A control law that would achieve consensus between all subsystems is identified and designed for a subset of the controls μ_i (by examining the constrained dynamics of the subsystem). Next we design two sets of control laws for the remaining of the control functions μ_i.

First solutions to these remaining control functions μ_i satisfying the dynamic constraints $((\mu_i, \dot{\mu}_i) \in \Pi_i)$ are identified and a control law is designed driving the subsystem towards these solutions. This control law focusing on the dynamic feasibility aspect of solutions is called the control law for feasibility. Note that this is different from the ideal case of designing a control law that would ensure dynamic feasibility by satisfying the set constraints $((\mu_i, \dot{\mu}_i) \in \Pi_i)$. Next a control law that would optimize the team goal is developed for the subsystem for these same remaining control functions. We propose a simple switching control strategy for motion planning for the multi-agent system based on these latter two control laws together with the control law for maintaining consensus. When actuator and operating constraints of all the subsystems are satisfied, feasibility is not an issue and the control law that optimizes the team goal is implemented on all the constrained subsystems. If actuator or operating constraints of even one of the subsystems are violated then the control law for feasibility is implemented on all the constrained subsystems to drive the system towards feasible solutions.

Instead of identifying solutions to μ_i that satisfy the dynamic constraints and designing a control law that would drive the subsystem towards these feasible solutions, if a control law is designed to guarantee feasible solutions then this control strategy

is guaranteed to produce dynamically feasible reference trajectories. We note here that for the three formation control problems considered in this study, we have only identified particular solutions for μ_i that are guaranteed to be feasible (as opposed to control laws that guarantee feasibility of solutions) and designed control laws that drive the system towards these feasible solutions. However, through simulation results for all three formation control problems considered in this study, we have shown that by appropriately tuning the control gains of the control law for feasibility, this control strategy can effectively produce dynamically feasible reference trajectories although there is no theoretical guarantee for feasibility of solutions.

Identifying a subset of control functions and designing control laws to achieve consensus and feasibility is quite subjective and heavily relies upon the form of the constrained dynamics developed. This is the reason why we restrict our comments to only the three formation control problems we consider, for each of which these steps are demonstrated.

F. Communication and Control Algorithm for Distributed Control

Synchronized and global communication is proposed for the control architecture of the motion planning algorithm. For the implementation of the switching control strategy, all that needs to be communicated amongst all the agents in the team is which controller to be used and for how long. The constrained dynamics takes care of the equality constraints corresponding to the formation and nonholonomic constraints while the switching control strategy takes care of the inequality constraints corresponding to actuator and operating constraints and this approach is amenable to real-time trajectory generation. Each agent in the multi-agent system is responsible for solving the constrained dynamics associated with its subsystem for distributed

control. The proposed communication/control algorithm is presented in the form of a flow-chart in Fig.11. The computations shown in the blocks (i),(ii) and (iii) of the flow-chart of Fig.11 are performed by each of the N-agents in parallel and as such increasing the number of agents in the system has minimal effect on the overall communication/computation time thus making the approach scalable. Communication amongst the agents need not be continuous and has to occur only once in each cycle of the receding horizon control strategy. For simplicity we have assumed that the algorithm step time δt is a constant and the algorithm incrementally steps forward in these step increments in a receding horizon framework. All the preceding sections of this chapter taken together describes the proposed motion planning algorithm.

From an implementation point of view, the biggest weakness in the proposed distributed control algorithm is the admittedly strong assumption of synchronized communication. We note that the distributed receding horizon control architecture is not technically decentralized, since a globally synchronous implementation requires centralized clock keeping. Communication topology, time delays, robustness in the communication architecture, local sensing and communication architectures as opposed to global communication are other issues we do not consider in this study. Nevertheless, these and other important issues in sensing and communication will need to be addressed before implementing the proposed motion planning algorithm on a multi robot test-bed.

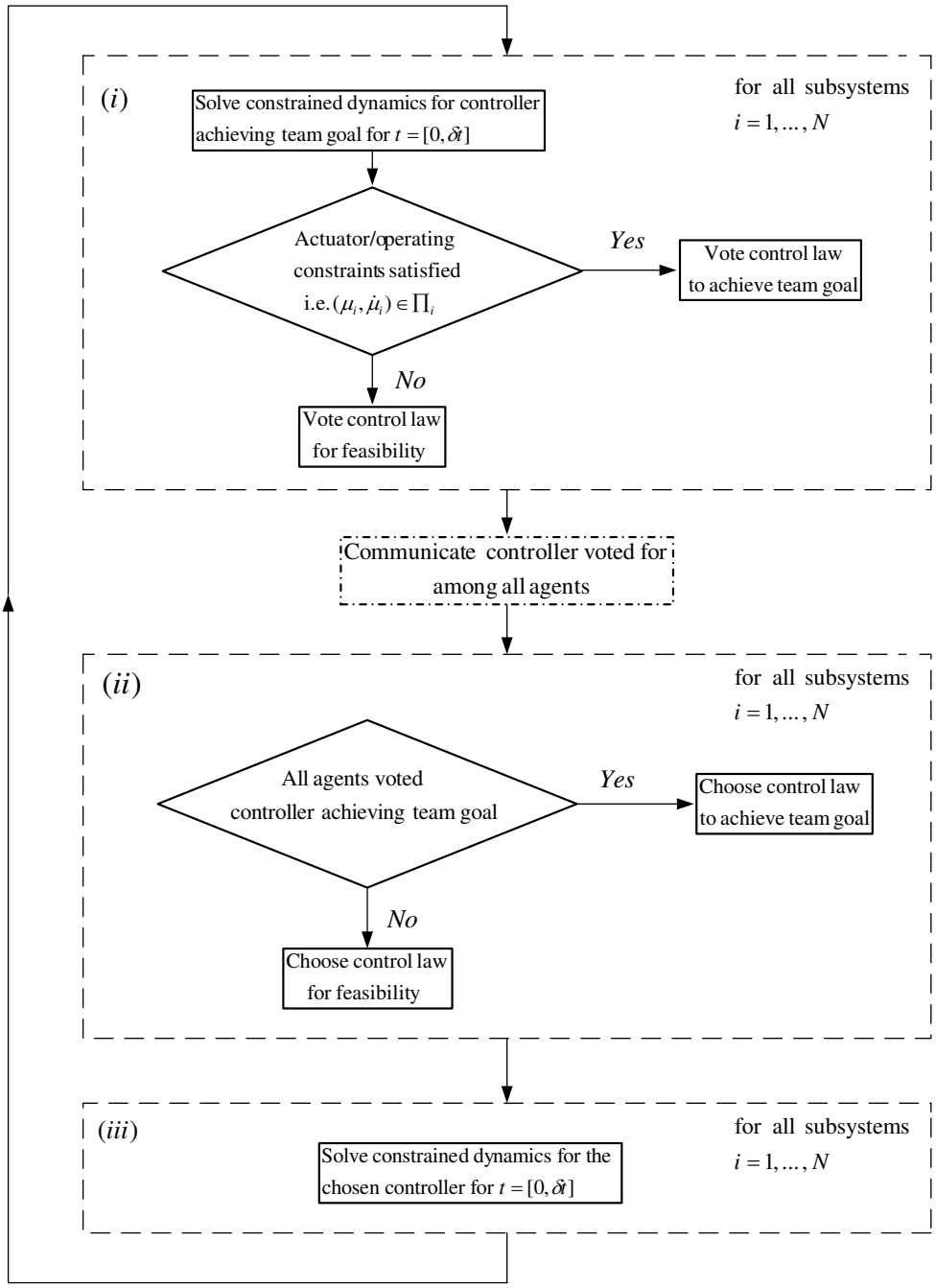

Fig. 11. Control/communication algorithm based on a switching control strategy.

CHAPTER IV

GEOMETRIC FORMULATION OF CONSTRAINED DYNAMICS

Consider a system $\mathcal{A}$ required to satisfy holonomic and nonholonomic constraints. Let Q be the configuration manifold of $\mathcal{A}$ and TQ, T^*Q its tangent and cotangent bundles respectively. A trajectory of the system $\mathcal{A}$ is a curve on Q, $\gamma : [a, b] \to Q$, whose tangent vector on Q along the curve γ we denote by γ'. For purposes of developing a motion planning algorithm for a class of formation control problems, this system $\mathcal{A}$ will represent the i-th subsystem, and Q its configuration space. Holonomic constraints on Q will capture the formation constraint while the nonholonomic constraints on Q will capture nonholonomic constraints of the agents in $\mathcal{A}$.

Let us next introduce some of the terminology used in the rest of this chapter. A system $\mathcal{A}$ constrained to satisfy these holonomic and nonholonomic constraints is termed the *constrained system* $\mathcal{A}$. When equations of motion satisfying these holonomic and nonholonomic constraints of $\mathcal{A}$ are derived at the velocity level, through a distribution, we term these as the *constrained kinematics*. When the equations of motion satisfying these constraints of $\mathcal{A}$ are derived at the dynamic level, corresponding to a metric on Q, we call them the *constrained dynamics*.

A. Constrained Kinematics

We refer the reader to [44, 45] for details of the differential geometric ideas used in this section. A map $\mathcal{C} : Q \mapsto \mathbf{0} \in \mathcal{R}^m$ captures all configuration constraints (holonomic) on Q. $\mathcal{M} = \mathcal{C}^{-1}(\mathbf{0}) = \{q \in Q \mid \mathcal{C}(q) = \mathbf{0}\}$ is an embedded submanifold of Q ($\mathcal{M} \subset Q$) and is the true configuration manifold of the constrained system $\mathcal{A}$. The differential of the map $\mathcal{C}$, denoted $d\mathcal{C}$, is a codistribution that annihilates the entire tangent space $T_q\mathcal{M}$ for every $q \in \mathcal{M}$ and uniquely identifies $T\mathcal{M}$. Thus for a vector $\mathbf{v}$ on Q,

$d\mathcal{C}(\mathbf{v}) = \mathbf{0}$ *iff* the vector $\mathbf{v}$ is on $\mathcal{M}$.

A distribution Δ on Q captures all nonholonomic constraints on Q. There is a unique annihilating codistribution $\Lambda = \{\boldsymbol{\alpha} \in T^*Q \mid \boldsymbol{\alpha}(\mathbf{v}) = 0;\ \forall \mathbf{v} \in \Delta\}$ on Q associated with Δ (Here we have made an abuse of notation by denoting the distribution as well as the set of vector fields taking their values in the distribution by the same symbol since it should be clear from the context which we mean). Let $\{\mathbf{e}_1, \cdots, \mathbf{e}_{rank(\Delta)}\}$ be a basis for the distribution Δ. Then $\gamma' = v^i \mathbf{e}_i$ is its equivalent control system form associated with the nonholonomic constraints and the nonholonomic constraints alone.

Note. For the three formation control problems we consider, this equivalent control form $\gamma' = v^i \mathbf{e}_i$ represents the individual agent kinematics (that need not satisfy the configuration constraints) and we propose to capture actuator and operating constraints of the individual agents through inequality constraints on the functions v^i and their first derivatives $\dot{v}^i$. In other words, actuator and operating constraints are captured through the set constraint $(\mu, \dot{\mu}) \in \Pi$ where $\mu = (v^1, \ldots, v^{rank(\Delta)})$ and Π is a compact set. Notice that the above set constraint depends on the choice of frame $\{\mathbf{e}_i\}$.

$\Omega = \{\boldsymbol{\alpha} \in T^*Q \mid \boldsymbol{\alpha} \in dC,\ \boldsymbol{\alpha} \in \Lambda\}$ is the intersection of the codistributions dC and Λ. There exists a unique distribution on Q, call it the constrained distribution $\mathcal{D} = \{\mathbf{v} \in T_qQ,\ \forall q \in Q \mid \Omega(\mathbf{v}) = \mathbf{0}\}$, associated with the annihilating codistribution Ω. A trajectory γ will satisfy both the holonomic and nonholonomic constraints *iff* its associated tangent vector γ' along γ is annihilated by Ω. i.e. *iff* $\Omega(\gamma') = \mathbf{0}$.

The vector γ' being annihilated by Ω is equivalent to having γ' be in the distribution $\mathcal{D}$. Hence a necessary condition for the trajectory γ to satisfy the holonomic and nonholonomic constraints on $\mathcal{A}$ is that the vector γ' along γ has to be in the distribution $\mathcal{D}$. We immediately see that, for such a γ to exist, we must have a

non-empty $\mathcal{D}$. This condition is given in terms of an algebraic rank condition on the matrix representation of Ω in [3] where a trajectory γ satisfying holonomic and nonholonomic constraints on $\mathcal{A}$ is equated to a feasible trajectory.

Kinematic control. If $\{\mathbf{X}_1, \ldots, \mathbf{X}_{rank(\mathcal{D})}\}$ is a basis for the distribution $\mathcal{D}$, then $\gamma^{'} = u^i \mathbf{X}_i$ describes the equivalent kinematic control system of the constrained system. In general it will not be possible to find a relationship between u^i and actuator/operating constraints $(\mu, \dot{\mu}) \in \Pi$ in the way we have defined them, and we turn to the dynamics of the constrained system.

To the best of our knowledge, [3] is the only meaningful study on the feasibility aspect to formation control. However, feasibility results of [3] are limited to kinematic systems only and do not consider dynamics-related effects other than through the consideration of nonholonomic constraints. For the formation control problems we consider, for a trajectory γ to be a feasible one, it has to have a non-empty $\mathcal{D}$ and also has to satisfy actuator and operating constraints captured through the set constraint $(\mu, \dot{\mu}) \in \Pi$ where $\gamma' = v^i \mathbf{e}_i$ with $\mu = (v^1, \ldots, v^{rank(\Delta)})$. The work presented in this study goes beyond the constrained kinematics presented in [3], to derive constrained dynamics and to consider dynamics related effects of the individual agents through actuator/operator constraints. Let us formally define what we mean by feasible solutions to $\mathcal{A}$.

Feasibility. *Necessary and sufficient conditions for the trajectory γ to be a feasible trajectory of $\mathcal{A}$ are;*

1. *The distribution $\mathcal{D}$ has to be non-empty.*

2. *γ' restricted to the distribution $\mathcal{D}$ with, $(\mu, \dot{\mu}) \in \Pi$*
   where $\gamma' = v^i \mathbf{e}_i$, $\mu = (v^1, \ldots, v^{rank(\Delta)})$.

B. Constrained Dynamics

The notion of an affine connection is used to derive the constrained dynamics. An affine *connection* or *covariant differentiation* is an operator ∇ that assigns to each pair consisting of a vector $\mathbf{x}$ at $q \in Q$ and a vector *field* $\mathbf{v}$ defined near q, a vector $\nabla_{\mathbf{x}}\mathbf{v}$ at q satisfying the following three properties [45];

$$\nabla_{\mathbf{x}}(a\mathbf{v} + b\mathbf{w}) = a\nabla_{\mathbf{x}}\mathbf{v} + b\nabla_{\mathbf{x}}\mathbf{w}$$

$$\nabla_{a\mathbf{x}+b\mathbf{y}}\mathbf{v} = a\nabla_{\mathbf{x}}\mathbf{v} + b\nabla_{\mathbf{y}}\mathbf{v}$$

$$\nabla_{\mathbf{x}}(f\mathbf{v}) = \mathbf{x}(f)\mathbf{v} + f\nabla_{\mathbf{x}}\mathbf{v}$$

for all vectors $\mathbf{x}$ and $\mathbf{y}$, vector fields $\mathbf{v}$ and $\mathbf{w}$, functions f, and real numbers a and b.

For the local coordinates $q = (q^1, \ldots, q^n)$ in a coordinate patch in Q, let $\boldsymbol{\partial_q} = (\partial_{q^1}, \ldots, \partial_{q^n})$ be its coordinate frame of vector fields that span every tangent space of Q and $\boldsymbol{dq} = (dq^1, \ldots, dq^n)$ its associated dual frame of covector fields (i.e. $dq^i(\partial_{q^j}) = \delta^i_j$). Also consider the frame of vector fields $\mathbf{e} = (\mathbf{e}_1, \ldots, \mathbf{e}_{rank(\Delta)}, \ldots, \mathbf{e}_n)$ where $\{\mathbf{e}_1, \ldots, \mathbf{e}_{rank(\Delta)}\}$ forms a basis for Δ and $\{\mathbf{e}_{rank(\Delta)+1}, \ldots, \mathbf{e}_n\}$ forms a basis for $\Delta^{\perp}$, the orthogonal compliment to Δ. The frame $\mathbf{e}$ has the associated frame of covector fields $\boldsymbol{\sigma} = (\sigma^1, \ldots, \sigma^n)$ on Q (i.e. $\mathbf{e}_i(\sigma^j) = \delta^i_j$). Then,

$$\gamma' = \dot{q}^k \partial_{q^k} = v^k \mathbf{e}_k.$$

where v^k includes the same functions that capture the actuator and operating limits as mentioned earlier.

The frame $\mathbf{e}$ is locally a coordinate frame *iff* $[\mathbf{e}_i, \mathbf{e}_j] = 0,\ \forall i, j$ in which case we can always find local coordinates $p = (p^1, \ldots, p^n)$ such that $\mathbf{e}_j = \partial_{p^j}$ and $\sigma^j = dp^j$. i.e. locally each σ^j will be exact. Here $[\mathbf{e}_i, \mathbf{e}_j]$ is the Lie bracket between the vector fields $\mathbf{e}_i, \mathbf{e}_j$. For the three problems considered in this study, the choice of $\mathbf{e}$ will be

such that it will not be a coordinate frame.

For a vector $\mathbf{x} = X^j \mathbf{e}_j$ and a vector field $\mathbf{v} = v^k \mathbf{e}_k$, the covariant derivative of $\mathbf{v}$ with respect to $\mathbf{x}$ is obtained through the properties of a connection as follows;

$$\begin{aligned} \nabla_{\mathbf{x}} \mathbf{v} &= X^j \mathbf{e}_j(v^k)\mathbf{e}_k + X^j \mathbf{e}_i \omega^i_{jk} v^k \\ &= \mathbf{e}_i\{dv^i(\mathbf{x}) + X^j \omega^i_{jk} v^k\} \\ &= \mathbf{e}_i\{dv^i(\mathbf{x}) + v^k \omega^i_{jk} \sigma^j(\mathbf{x})\} \\ &= \mathbf{e}_i\{dv^i + v^k \omega^i_k\}(\mathbf{x}) \end{aligned} \tag{4.1}$$

where the connection coefficients ω^i_{jk} and the connection 1-forms ω^i_k are defined by;

$$\begin{aligned} \nabla_{\mathbf{e}_j} \mathbf{e}_k &:= \mathbf{e}_i \omega^i_{jk} \\ \omega^i_k &:= \omega^i_{jk} \sigma^j \end{aligned} \tag{4.2}$$

and where we have used the fact that $\mathbf{x}(v^k) = dv^k(\mathbf{x})$.

Let $\mathbb{G}$ be the Riemannian metric on Q specified by the kinetic energy of the system $\mathcal{A}$. The Levi-Civita connection $\overset{\mathbb{G}}{\nabla}$ is the unique affine connection associated with $(Q, \mathbb{G})$, satisfying the following two properties $\forall \mathbf{x}, \mathbf{y}$;

$$\begin{aligned} \overset{\mathbb{G}}{\nabla} &= 0 \\ \overset{\mathbb{G}}{\nabla}_{\mathbf{x}} \mathbf{y} - \overset{\mathbb{G}}{\nabla}_{\mathbf{y}} \mathbf{x} &= [\mathbf{x}, \mathbf{y}]. \end{aligned} \tag{4.3}$$

The connection coefficients of the Levi-Civita connection $\overset{\mathbb{G}}{\Gamma}{}^i_{jk}$ are defined similarly by

$$\overset{\mathbb{G}}{\nabla}_{\partial_{q^j}} \partial_{q^k} := \partial_{q^i} \overset{\mathbb{G}}{\Gamma}{}^i_{jk} . \tag{4.4}$$

These connection coefficients $\overset{\mathbb{G}}{\Gamma}{}^i_{jk}$, which are called Christoffel symbols, are given in

the coordinates q by

$$\overset{\mathbb{G}}{\Gamma}{}^{i}_{jk} = \frac{1}{2}\mathbb{G}^{ir}\left(\frac{\partial \mathbb{G}_{jr}}{\partial q^k} + \frac{\partial \mathbb{G}_{kr}}{\partial q^j} - \frac{\partial \mathbb{G}_{jk}}{\partial q^r}\right)$$

where $\mathbb{G}^{ij}$ are defined by $\mathbb{G}_{ij}\mathbb{G}^{jk} = \delta^k_i$.

For a force represented by the one-form $F(t, \gamma'(t)) \in T^*Q$, a curve $\gamma : [a, b] \to Q$ satisfies the Lagrange-d'Alembert principle and is a solution of the system satisfying the constraints (holonomic and nonholonomic constraints captured through the distribution $\mathcal{D}$) *iff*

$$\nabla_{\gamma'(t)}\gamma'(t) = \lambda(t) + Y(\gamma(t))$$
$$P'(\gamma'(t)) = \mathbf{0}$$

where λ is in $\mathcal{D}^{\perp}$, the $\mathbb{G}$ orthogonal compliment to $\mathcal{D}$, Y is the vector field associated with the one-form F given by $Y = \mathbb{G}^{\sharp}(F)$, $\mathbb{G}^{\sharp} : T^*Q \to TQ$ is the isomorphism associated with the metric $\mathbb{G}$ mapping covector fields to vector fields, and $P' : TQ \to TQ$ is the $\mathbb{G}$ orthogonal projection map onto $\mathcal{D}^{\perp}$.

Taking the covariant derivative of $P'(\gamma'(t))$ leads us to another affine connection, the constrained affine connection $\overset{\mathcal{D}}{\nabla}$ given by

$$\overset{\mathcal{D}}{\nabla}_{\gamma'(t)}\gamma'(t) = \nabla_{\gamma'(t)}\gamma'(t) + (\nabla_{\gamma'(t)}P')(\gamma'(t)).$$

A property of $\overset{\mathcal{D}}{\nabla}$ is that it *restricts* to $\mathcal{D}$ meaning that $\overset{\mathcal{D}}{\nabla}_{X_1} X_2 \in \mathcal{D}$ for every $X_2 \in \mathcal{D}$.

In practice however, computation of $\overset{\mathcal{D}}{\nabla}$ can be quite troublesome and for computational convenience we instead consider the constrained connection given by;

$$\overset{A}{\nabla}_{\gamma'(t)}\gamma'(t) = \nabla_{\gamma'(t)}\gamma'(t) + A^{-1}\left(\left(\nabla_{\gamma'(t)}AP'\right)\left(\gamma'(t)\right)\right)$$

where A can be *any* invertible matrix [46]. Usually one would choose A to cancel out the denominator terms of P' that would cause computational problems in the

covariant differentiation of P'. It is shown in [46] (along with a proof) that this connection $\overset{A}{\nabla}$ too restricts to $\mathcal{D}$ and hence serves just as well as $\overset{\mathcal{D}}{\nabla}$ in determining the constrained equations of motion as long as $\gamma'(t_0) \in \mathcal{D}$.

A curve $\gamma : [a, b] \mapsto Q$ is a solution of the constrained system $\mathcal{A}$ *iff* $\gamma'(t_0) \in \mathcal{D}$ and γ satisfies;

$$\overset{A}{\nabla}_{\gamma'(t)} \gamma'(t) = P\left(Y(\gamma(t))\right)$$

where $Y = \mathbb{G}^{\#}(F)$ and $P : TQ \mapsto TQ$ is the $\mathbb{G}$ orthogonal projection map onto $\mathcal{D}$.

Let $\gamma' = \dot{q}^k \partial_{q^k} = v^k \mathbf{e}_k$ and using Eq.(4.1) we have $\overset{A}{\nabla}_{\gamma'} \gamma'$ given in the two frames $\mathbf{e}$, $\boldsymbol{\partial_q}$ as follows;

$$\begin{aligned}
\overset{A}{\nabla}_{\gamma'} \gamma' &= v^j \mathbf{e}_j(v^k)\mathbf{e}_k + v^j \mathbf{e}_i \overset{A}{\omega}{}^i_{jk} \, v^k \\
&= \mathbf{e}_k(dv^k(v^j \mathbf{e}_j) + v^j \overset{A}{\omega}{}^k_j \, (v^r \mathbf{e}_r)) \\
&= \mathbf{e}_k(\dot{v}^k + v^j \overset{A}{\omega}{}^k_j \, (\gamma'))
\end{aligned} \tag{4.5}$$

$$\begin{aligned}
\overset{A}{\nabla}_{\gamma'} \gamma' &= \dot{q}^j \partial_{q^j}(\dot{q}^k)\partial_{q^k} + \dot{q}^j \partial_{q^i} \overset{A}{\Gamma}{}^i_{jk} \, \dot{q}^k \\
&= \partial_{q^k}(d\dot{q}^k(\dot{q}^j \partial_{q^j}) + \dot{q}^j \overset{A}{\Gamma}{}^k_j \, (\dot{q}^r \partial_{q^r})) \\
&= \partial_{q^k}(\ddot{q}^k + \dot{q}^j \overset{A}{\Gamma}{}^k_j \, (\gamma'))
\end{aligned} \tag{4.6}$$

where the connection coefficients and the connection 1-forms of $\overset{A}{\nabla}$ in the two frames $\mathbf{e}$, $\boldsymbol{\partial_q}$ are defined by $\overset{A}{\nabla}_{\mathbf{e}_i} \mathbf{e}_j := \mathbf{e}_k \overset{A}{\omega}{}^k_{ij}$, $\overset{A}{\omega}{}^k_j := \overset{A}{\omega}{}^k_{rj} \, \sigma^r$ and $\overset{A}{\nabla}_{\partial_{q^i}} \partial_{q^j} := \partial_{q^k} \overset{A}{\Gamma}{}^k_{ij}$, $\overset{A}{\Gamma}{}^k_j := \overset{A}{\Gamma}{}^k_{rj} \, dq^r$ as usual. To actually compute $\overset{A}{\nabla}_{\gamma'} \gamma'$, we need to be able to compute the connection coefficients $\overset{A}{\omega}{}^k_{ij}$, $\overset{A}{\Gamma}{}^k_{ij}$.

Consider a type $(1, 1)$ tensor $\mathcal{P}$ with components $\mathcal{P}^i_j$. The components of the

covariant derivative of $\mathcal{P}$ with respect to $\mathbf{x}$, $\nabla_{\mathbf{X}}\mathcal{P}$, in the coordinate frame $\boldsymbol{\partial_q}$ are;

$$(\nabla_{\mathbf{x}}\mathcal{P})^i_j = \frac{\partial \mathcal{P}^i_j}{\partial q^k} X^k + \Gamma^i_{kr}\mathcal{P}^r_j X^k - \Gamma^r_{kj}\mathcal{P}^i_r X^k \tag{4.7}$$

where the connection coefficients Γ^i_{jk} are defined by $\nabla_{\partial_{q^j}}\partial_{q^k} := \partial_{q^i}\Gamma^i_{jk}$. The connection coefficients of $\overset{A}{\nabla}$ in the coordinate frame $\boldsymbol{\partial_q}$ are computed using Eq.(4.7) as;

$$\begin{aligned}\overset{A}{\Gamma}{}^i_{jk} = \ & \overset{\mathbb{G}}{\Gamma}{}^i_{jk} + (A^{-1})^i_r \frac{\partial (AP')^r_j}{\partial q^k} + (A^{-1})^i_r \ \overset{\mathbb{G}}{\Gamma}{}^r_{km} \ (AP')^m_j \\ & - (A^{-1})^i_r \ \overset{\mathbb{G}}{\Gamma}{}^m_{kj} \ (AP')^r_m.\end{aligned} \tag{4.8}$$

For the three problems considered in this study, the frame $\mathbf{e}$ will not be a coordinate frame. Hence we need to transform the connection 1-forms $\overset{A}{\Gamma}{}^j_k$ from the basis $\boldsymbol{\partial_q}$ to the basis $\mathbf{e}$ to compute the 1-forms $\overset{A}{\omega}{}^j_k$.

Define $\overset{A}{\nabla}\ \mathbf{e}_j(\mathbf{e}_i) := \overset{A}{\nabla}_{\mathbf{e}_j}\ \mathbf{e}_i = \mathbf{e}_k \overset{A}{\omega}{}^k_{ij}$. This can also be written in terms of a vector valued 1-form as $\mathbf{e}_k \otimes \overset{A}{\omega}{}^k_{rj}\ \sigma^r(\mathbf{e}_i) = \mathbf{e}_k \overset{A}{\omega}{}^k_{ij}$. However since $\overset{A}{\omega}{}^k_j := \overset{A}{\omega}{}^k_{rj}\ \sigma^r$ we have

$$\overset{A}{\nabla}\ \mathbf{e}_j = \mathbf{e}_k \otimes \overset{A}{\omega}{}^k_j \ .$$

Hence

$$\overset{A}{\nabla}\ \mathbf{e} = \mathbf{e}\ \overset{A}{\omega}$$

where $\overset{A}{\omega} := \begin{pmatrix} \overset{A}{\omega}{}^k_j \end{pmatrix}$ is the $n \times n$ matrix of connection 1-forms.

Since $\overset{A}{\nabla}$ is well defined, independent of basis, we have compatible $\overset{A}{\nabla}\ \mathbf{e} = \mathbf{e}\ \overset{A}{\omega}$ and $\overset{A}{\nabla}\ \boldsymbol{\partial_q} = \boldsymbol{\partial_q}\ \overset{A}{\Gamma}$ where $\overset{A}{\Gamma} := \begin{pmatrix} \overset{A}{\Gamma}{}^k_j \end{pmatrix}$.

Let $\mathbf{e} = \boldsymbol{\partial_q}\mathcal{S}$ be the change of basis where $\mathbf{e}_i = \partial_{q^j}\mathcal{S}^j_i$ and $\mathcal{S}$ is the non-singular

matrix whose (i,j)th element is $\mathcal{S}^i_j$. Then,

$$\begin{aligned}\overset{A}{\nabla}\mathbf{e} &= \overset{A}{\nabla}(\boldsymbol{\partial_q}\mathcal{S}) \\ &= (\overset{A}{\nabla}\boldsymbol{\partial_q})\mathcal{S} + \boldsymbol{\partial_q} d\mathcal{S} \\ &= \boldsymbol{\partial_q}\overset{A}{\Gamma}\mathcal{S} + \boldsymbol{\partial_q} d\mathcal{S}.\end{aligned}$$

But we also have

$$\overset{A}{\nabla}\mathbf{e} = \mathbf{e}\overset{A}{\omega} = \boldsymbol{\partial_q}\mathcal{S}\overset{A}{\omega}$$

We must then have

$$\overset{A}{\omega} = \mathcal{S}^{-1}\overset{A}{\Gamma}\mathcal{S} + \mathcal{S}^{-1} d\mathcal{S} \tag{4.9}$$

which is the transformation rule for the matrix of connection 1-forms. Notice that $\overset{A}{\Gamma}$ does not transform as would the components of a tensor since $\overset{A}{\Gamma}$ is in fact not a tensor.

Since $\mathbf{e} = \boldsymbol{\partial_q}\mathcal{S}$ we have $\boldsymbol{\sigma} = \mathcal{S}^{-1}\boldsymbol{dq}$. Let $\boldsymbol{\alpha}$ be a 1-form and $\boldsymbol{\alpha} = a^k dq^k = b^k\sigma^k$. This can be written as $\boldsymbol{\alpha} = \boldsymbol{a}\,\boldsymbol{dq} = \boldsymbol{b\sigma} = \boldsymbol{b}\mathcal{S}^{-1}\boldsymbol{dq}$ and we have $\boldsymbol{a} = \boldsymbol{b}\mathcal{S}^{-1}$ and hence

$$\boldsymbol{b} = \boldsymbol{a}\mathcal{S}$$

which is the transformation rule for 1-forms. This will be required in the actual computations of $\overset{A}{\omega}$ given in Eq.(4.9) to represent $\overset{A}{\omega}$ in the $\mathbf{e}$ frame.

The significance of deriving constrained dynamics $\overset{A}{\nabla}_{\gamma'}\,\gamma' = \mathbf{e}_k(\dot{v}^k + v^j\,\overset{A}{\omega}{}^k_j\,(\gamma'))$ in the $\mathbf{e}$ frame is that we then have the equations of motion of the constrained system exclusively in the functions μ, which also capture the actuator constraints of the individual agents, and configuration coordinates q. Note that in the above constrained dynamics, $v^{rank(\mathcal{D})}, \ldots, v^n$ will be identically zero since $\mathbf{e}_{rank(\mathcal{D})}, \ldots, \mathbf{e}_n \in \mathcal{D}^\perp$, to satisfy the nonholonomic constraints.

CHAPTER V

RADAR DECEPTION

The proposed motion planning algorithm outlined in Chapter-III is applied to the radar deception problem and verified in simulation in this chapter.

Consider the multi-agent system restricted to the 2D plane comprising of N-UAVs engaging N-radars. We propose the unicycle model to capture the dynamic, operating and actuator constraints of a UAV restricted to fly in the 2D plane. Let (x_i, y_i, θ_i) give the configuration of the i-th UAV where (x_i, y_i) is the position and θ_i its orientation. Assume an imaginary UAV whose trajectory will be considered the phantom trajectory to make the phantom trajectory realistically mimic the trajectory of an actual aircraft. Let (x, y, θ) be the position and orientation of this imaginary UAV. Let $(\bar{x}_i, \bar{y}_i)$ give the position of the i-th ground radar which is stationary by assumption. With the assumption of the ground radar network being a stationary one, $\bar{x}_i, \bar{y}_i$ will be constants for $i = 1, \ldots, N$.

The multi-agent system is then comprised of the N-UAVs, the corresponding N radars they engage and the imaginary UAV assigned for the phantom. The configuration of this multi-agent system can be given by the local coordinates

$$q_i = (x_1, y_1, \theta_1, \ldots, x_N, y_N, \theta_N, x, y, \theta)$$

and will have the structure of a smooth differentiable manifold having dimension $3(N + 1)$. The configuration of the multi-agent system involved in radar deception is illustrated in Fig.12, where only the imaginary UAV assigned for the phantom, and the 1st and the Nth UAV-radar pairs are shown.

The requirement that the N UAVs have to be in-line with their corresponding

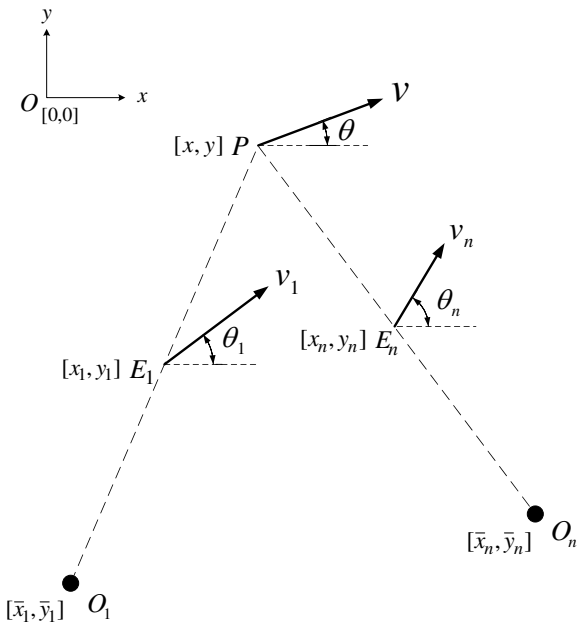

Fig. 12. Configuration of the radar deception problem where only the 1st, Nth and the imaginary UAV representing the phantom are shown.

radar and the phantom gives rise to configuration constraints

$$(x - \bar{x}_i)(y_i - \bar{y}_i) - (y - \bar{y}_i)(x_i - \bar{x}_i) = 0 \tag{5.1}$$

for $\forall\, i = 1, \ldots, N$.

The nonholonomic constraint of a unicycle representing the i-th UAV is

$$\dot{x}_i \sin\theta_i - \dot{y}_i \cos\theta_i = 0. \tag{5.2}$$

The equivalent control system corresponding to the above nonholonomic constraint, the unicycle kinematic model, is given by

$$\begin{aligned} \dot{x}_i &= v_i \cos\theta_i \\ \dot{y}_i &= v_i \sin\theta_i \\ \dot{\theta}_i &= w_i \end{aligned} \tag{5.3}$$

where v_i, w_i are the speed and steer controls.

Considering the i-th UAV to be of mass m_i and inertia J_i we also have the following;

$$\begin{aligned} \dot{v}_i &= \frac{1}{m_i} f_i \\ \dot{w}_i &= \frac{1}{J_i} \tau_i \end{aligned} \tag{5.4}$$

where f_i, τ_i are respectively the force and torque acting on the UAV. The above description that takes mass and inertia of the UAV into consideration, together with its kinematic model given by Eq.(5.3), describes the dynamics of the UAV.

Assuming the UAV to be fixed winged, its speed v_i will have to be lower bounded to avoid stall, a flight operating constraint on the UAV. Stability of the UAV and actuator limitations will upper and lower bound the steer w_i as well as the rate of steer $\dot{w}_i$. These bounds will in general be assumed symmetric about zero. Actuator limitations will impose an upper bound on the thrust force f_i on the UAV while the maximum attainable drag force will impose a lower bound on f_i. Although the upper bound of f_i will in general be different from its lower bound, we assume these to be symmetric for notational convenience. These actuator and operating constraints of the UAV are captured through the following constraints.

$$\begin{aligned} {v_i}^{min} \leq \quad v_i \quad &\leq {v_i}^{max} \\ -{w_i}^{max} \leq \quad w_i \quad &\leq {w_i}^{max} \\ -{f_i}^{max} \leq \quad f_i \quad &\leq {f_i}^{max} \\ -{\tau_i}^{max} \leq \quad \tau_i \quad &\leq {\tau_i}^{max} \end{aligned} \tag{5.5}$$

where $v_i^{max}, v_i^{min}, w_i^{max}, f_i^{max}, \tau_i^{max}$ are all positive constants.

We assume that the unicycle kinematic model given by Eq.(5.3), the inertia and mass effects captured through Eq.(5.4), and operating and actuator constraints

given by Eq.(5.5), will capture the dynamics of the i-th UAV restricted to the plane, reasonably well.

Similarly we have the following dynamical model for the imaginary UAV representing the phantom.

$$\begin{aligned} \dot{x} &= v\cos\theta \\ \dot{y} &= v\sin\theta \\ \dot{\theta} &= w \\ \dot{v} &= \frac{1}{m}f \\ \dot{w} &= \frac{1}{J}\tau \end{aligned} \tag{5.6}$$

$$\begin{aligned} v^{min} \leq \quad v \quad &\leq v^{max} \\ -w^{max} \leq \quad w \quad &\leq w^{max} \\ -f^{max} \leq \quad f \quad &\leq f^{max} \\ -\tau^{max} \leq \quad \tau \quad &\leq \tau^{max} \end{aligned} \tag{5.7}$$

where v, w are the speed and steer, m, J the mass and inertia and f, τ force and toque, and $v^{max}, v^{min}, w^{max}, f^{max}, \tau^{max}$ are positive constants, all of which are virtual quantities of an imaginary UAV.

Next the multi-agent system is separated into geometrically equivalent N subsystems corresponding to the N radar-UAV pairs. Each subsystem (N of them) now only has two UAVs, one representing the phantom and the other the UAV engaging the radar. Consider the i-th such subsystem and call it $\mathcal{A}$. The configuration space of the i-th subsystem, shown in Fig.13, has the structure of a manifold Q, and we assign the local coordinates $q = (x, y, \theta, x_i, y_i, \theta_i)$. On the manifold Q, $\boldsymbol{\partial_q} = \{\frac{\partial}{\partial x}, \frac{\partial}{\partial y}, \frac{\partial}{\partial \theta}, \frac{\partial}{\partial x_i}, \frac{\partial}{\partial y_i}, \frac{\partial}{\partial \theta_i}\}$ is the coordinate basis for T_qQ and $\mathbf{dq} =$

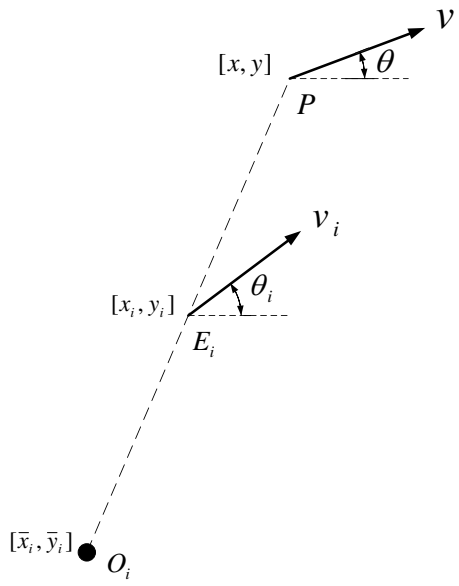

Fig. 13. Configuration of the i-th subsystem.

$\{dx, dy, d\theta, dx_i, dy_i, d\theta_i, d\phi\}$ its dual basis for T_q^*Q. The Riemannian metric corresponding to the kinetic energy of the system is $\mathbb{G} = m(dx \otimes dx + dy \otimes dy) + Jd\theta \otimes \theta + m_i(dx_i \otimes dx_i + dy_i \otimes dy_i) + J_i d\theta_i \otimes \theta_i$ where (m_i, J_i) are mass and inertia of the i-th agent and (m, J) the fictitious mass and inertia of the virtual UAV assigned to be the phantom. Since the multi-agent system is assumed to be restricted to the $2D$ plane, the potential energy of $\mathcal{A}$ is assumed zero. For computational convenience, and without loss of generality, we assume unit mass and inertia for both these UAVs. The inertia matrix associated with the Riemannian metric $\mathbb{G}$ is then the identity $[\mathbf{I}]_{6\times 6}$. Let us next proceed to derive the constrained dynamics of the i-th subsystem $\mathcal{A}$ as explained in the previous chapter.

Nonholonomic constraints on $\mathcal{A}$ are

$$\begin{aligned} \dot{x}\sin\theta - \dot{y}\cos\theta &= 0 \\ \dot{x}_i \sin\theta_i - \dot{y}_i \cos\theta_i &= 0. \end{aligned} \tag{5.8}$$

The annihilating codistribution associated with the above nonholonomic constraints of $\mathcal{A}$ is given by;

$$\Lambda : \begin{array}{l} \boldsymbol{\alpha}_1 = \sin\theta dx - \cos\theta dy \\ \boldsymbol{\alpha}_2 = \sin\theta_i dx_i - \cos\theta_i dy_i. \end{array}$$

The distribution Δ associated with the annihilating codistribution Λ is spanned by $\Delta = \{\mathbf{e}_v, \ldots, \mathbf{e}_{w_i}\}$ where

$$\begin{aligned} \mathbf{e}_v &= \cos\theta\frac{\partial}{\partial x} + \sin\theta\frac{\partial}{\partial y} \\ \mathbf{e}_w &= \frac{\partial}{\partial\theta} \\ \mathbf{e}_{v_i} &= \cos\theta_i\frac{\partial}{\partial x_i} + \sin\theta\frac{\partial}{\partial y_i} \\ \mathbf{e}_{w_i} &= \frac{\partial}{\partial\theta_i} \end{aligned}$$

and $\Delta^\perp$, the compliment of Δ, is spanned by $\Delta^\perp = \{\mathbf{e}_z, \mathbf{e}_{z_i}\}$ where

$$\begin{aligned} \mathbf{e}_z &= \mathbb{G}^\sharp(\boldsymbol{\alpha}_1) = \sin\theta\frac{\partial}{\partial x} - \cos\theta\frac{\partial}{\partial x} \\ \mathbf{e}_{z_i} &= \mathbb{G}^\sharp(\boldsymbol{\alpha}_2) = \sin\theta_i\frac{\partial}{\partial x_i} - \cos\theta_i\frac{\partial}{\partial y_i}. \end{aligned}$$

For a covector $\boldsymbol{\alpha} = \alpha_j dq^j$, and basis $\boldsymbol{\partial_q} = \{\frac{\partial}{\partial q^j}\}$, the computation of $\mathbb{G}^\sharp(\boldsymbol{\alpha})$ is as follows: $\mathbb{G}^\sharp(\boldsymbol{\alpha}) = \mathbb{G}^{ij}\alpha_j\frac{\partial}{\partial q^i}$ where $\mathbb{G}^{ij}\mathbb{G}_{jk} = \delta^i_k$.

The frame of vector fields $\{\mathbf{e}_v, \mathbf{e}_w, \mathbf{e}_{v_i}, \mathbf{e}_{w_i}, \mathbf{e}_z, \mathbf{e}_{z_i}\}$ span T_qQ on the manifold Q and hence is another basis for T_qQ. Associated with the frame $\mathbf{e} = \{\mathbf{e}_v, \mathbf{e}_w, \mathbf{e}_{v_i}, \mathbf{e}_{w_i}, \mathbf{e}_z, \mathbf{e}_{z_i}\}$ is its dual frame $\boldsymbol{\sigma} = \{\sigma^v, \sigma^w, \sigma^{v_i}, \sigma^{w_i}, \sigma^z, \sigma^{z_i}\}$.

The tangent vector on Q associated with a trajectory curve γ is given by $\gamma' = \dot{x}\frac{\partial}{\partial x} + \dot{y}\frac{\partial}{\partial y} + \dot{\theta}\frac{\partial}{\partial\theta} + \dot{x}_i\frac{\partial}{\partial x_i} + \dot{y}_i\frac{\partial}{\partial y_i} + \dot{\theta}_i\frac{\partial}{\partial\theta_i} = v\mathbf{e}_v + w\mathbf{e}_w + v_i\mathbf{e}_{v_i} + w_i\mathbf{e}_{w_i} + z\mathbf{e}_z + z_i\mathbf{e}_{z_i}$ in the two frames $\boldsymbol{\partial_q}$ and $\mathbf{e}$. Note that the functions v, w, v_i, w_i of $\gamma' = v\mathbf{e}_v + w\mathbf{e}_w + v_i\mathbf{e}_{v_i} + w_i\mathbf{e}_{w_i} + z\mathbf{e}_z + z_i\mathbf{e}_{z_i}$ are the same speed and steer controls corresponding to the dynamic

models of the i-th and the phantom UAV. The actuator and operating constraints acting on $\mathcal{A}$, given by Eq.(5.5), Eq.(5.7), can be written concisely as follows

$$(\mu_i, \dot{\mu}_i) \in \Pi_i \tag{5.9}$$

where $\mu_i = (v, w, v_i, w_i)$ and Π_i is a compact set.

The map $\mathcal{C} : Q \mapsto \mathbf{0} \in \mathcal{R}^m$ capturing the configuration constraint on $\mathcal{A}$ is

$$(x - \bar{x}_i)(y_i - \bar{y}_i) - (y - \bar{y}_i)(x_i - \bar{x}_i) = 0 \tag{5.10}$$

and the differential of this map, $d\mathcal{C}$, is given by the 1-form

$$d\mathcal{C} : \quad \boldsymbol{\beta}_1 = (y_i - \bar{y}_i)dx - (x_i - \bar{x}_i)dy - (y - \bar{y}_i)dx_i + (x - \bar{x}_i)dy_i.$$

The intersection of the annihilating codistributions Λ and $d\mathcal{C}$ gives the unique annihilating codistribution $\Omega : \Lambda \oplus d\mathcal{C}$ and has the following matrix representation in the $\boldsymbol{\partial_q}$ basis;

$$[\Omega]_{\boldsymbol{\partial_q}} = \begin{bmatrix} \sin\theta & -\cos\theta & 0 & 0 & 0 & 0 \\ 0 & 0 & 0 & \sin\theta_i & -\cos\theta_i & 0 \\ (y_i - \bar{y}_i) & -(x_i - \bar{x}_i) & 0 & -(y - \bar{y}_i) & (x - \bar{x}_i) & 0 \end{bmatrix} \tag{5.11}$$

The distribution $\mathcal{D}$ associated with the annihilating codistribution Ω is spanned by the following vector fields (which is the null space of the above matrix representation of Ω);

$$\begin{aligned} \mathbf{x}_1 &= h_i \cos\theta \frac{\partial}{\partial x} + h_i \sin\theta \frac{\partial}{\partial y} + h \cos\theta_i \frac{\partial}{\partial x_i} + h \sin\theta_i \frac{\partial}{\partial y_i} \\ \mathbf{x}_2 &= \frac{\partial}{\partial \theta} \\ \mathbf{x}_3 &= \frac{\partial}{\partial \theta_i} \end{aligned} \tag{5.12}$$

where

$$\begin{aligned} h &\triangleq (x_i - \bar{x}_i)\sin\theta - (y_i - \bar{y}_i)\cos\theta \\ h_i &\triangleq (x - \bar{x}_i)\sin\theta_i - (y - \bar{y}_i)\cos\theta_i. \end{aligned} \tag{5.13}$$

Vector fields $\mathbf{x}_4 = \mathbb{G}^\sharp(\alpha_1)$, $\mathbf{x}_5 = \mathbb{G}^\sharp(\alpha_2)$ and $\mathbf{x}_6 = \mathbb{G}^\sharp(\beta_1)$ span $\mathcal{D}^\perp$, the $\mathbb{G}$-orthogonal compliment to the distribution $\mathcal{D}$.

$$\begin{aligned} \mathbf{x}_4 &= \sin\theta\frac{\partial}{\partial x} - \cos\theta\frac{\partial}{\partial y} \\ \mathbf{x}_5 &= \sin\theta_i\frac{\partial}{\partial x_i} - \cos\theta_i\frac{\partial}{\partial y_i} \\ \mathbf{x}_6 &= (y_i - \bar{y}_i)\frac{\partial}{\partial x} - (x_i - \bar{x}_i)\frac{\partial}{\partial y} - (y - \bar{y}_i)\frac{\partial}{\partial x_i} + (x - \bar{x}_i)\frac{\partial}{\partial y_i} \end{aligned} \tag{5.14}$$

Let us next compute $P^{'}$, the $\mathbb{G}$-orthogonal projection map onto $\mathcal{D}^\perp$. In the basis $\{\mathbf{x}_1, \ldots, \mathbf{x}_6\}$, $P^{'}$ has the matrix representation;

$$\left[P^{'}\right]_{\mathbf{x}} = \begin{bmatrix} 0 & 0 & 0 & 0 & 0 & 0 \\ 0 & 0 & 0 & 0 & 0 & 0 \\ 0 & 0 & 0 & 0 & 0 & 0 \\ 0 & 0 & 0 & 1 & 0 & 0 \\ 0 & 0 & 0 & 0 & 1 & 0 \\ 0 & 0 & 0 & 0 & 0 & 1 \end{bmatrix} \tag{5.15}$$

Let $\mathbf{x} = \boldsymbol{\partial_q}\mathcal{R}$ be the change of basis where $\mathbf{x}_i = \frac{\partial}{\partial q^j}\mathcal{R}_i^j$ and $\mathcal{R}$ is the non-singular

matrix whose (i,j)th element is $\mathcal{R}^i_j$.

$$\mathcal{R} = \begin{bmatrix} h_i\cos\theta & 0 & 0 & \sin\theta & 0 & (y_i - \bar{y}_i) \\ h_i\sin\theta & 0 & 0 & -\cos\theta & 0 & -(x_i - \bar{x}_i) \\ 0 & 1 & 0 & 0 & 0 & 0 \\ h\cos\theta_i & 0 & 0 & 0 & \sin\theta_i & -(y - \bar{y}_i) \\ h\sin\theta_i & 0 & 0 & 0 & -\cos\theta_i & (x - \bar{x}_i) \\ 0 & 0 & 1 & 0 & 0 & 0 \end{bmatrix} \tag{5.16}$$

Matrix representation of P' in the $\boldsymbol{\partial_q} = \{\frac{\partial}{\partial x}, \ldots, \frac{\partial}{\partial \theta_i}\}$ basis is given by $[P']_{\boldsymbol{\partial_q}} = \mathcal{R}[P']_{\mathbf{x}}\mathcal{R}^{-1}$. The projection map P, the $\mathbb{G}$-orthogonal projection onto $\mathcal{D}$, in the basis $\boldsymbol{\partial_q}$ is simply $[P]_{\boldsymbol{\partial_q}} = I - [P']_{\boldsymbol{\partial_q}}$ where I is the identity.

We choose $A = (h^2 + h_i^2)I$ to eliminate the denominator terms of P'. Then $[AP']_{\boldsymbol{\partial_q}}$ is

$$\begin{bmatrix} h_i^2\sin\theta^2 + h^2 & -h_i^2\sin\theta\cos\theta & 0 & -hh_i\cos\theta_i\cos\theta & -hh_i\sin\theta_i\cos\theta & 0 \\ -h_i^2\sin\theta\cos\theta & h_i^2\cos\theta^2 + h^2 & 0 & -hh_i\cos\theta_i\sin\theta & -hh_i\sin\theta_i\sin\theta & 0 \\ 0 & 0 & 0 & 0 & 0 & 0 \\ -hh_i\cos\theta\cos\theta_i & -hh_i\sin\theta\cos\theta_i & 0 & h^2\sin\theta_i^2 + h_i^2 & -h^2\sin\theta_i\cos\theta_i & 0 \\ -hh_i\cos\theta\sin\theta_i & -hh_i\sin\theta\sin\theta_i & 0 & -h^2\sin\theta_i\cos\theta_i & h^2\cos\theta_i^2 + h_i^2 & 0 \\ 0 & 0 & 0 & 0 & 0 & 0 \end{bmatrix}$$

Recall that the choice of A does not affect the dynamics of system $\mathcal{A}$. The above choice of A simplifies the computation of the connection coefficients $\overset{A}{\Gamma}{}^i_{jk}$ a great deal by eliminating the denominator terms of P' without which the computation of partial differentiation of Eq.(4.8) would have made the symbolic computations of the connection coefficients $\overset{A}{\Gamma}{}^i_{jk}$ simply intractable.

Since the Riemannian metric $\mathbb{G}$ is constant, we also have

$$\overset{\mathbb{G}}{\Gamma}{}^{i}_{jk} = 0 \quad for \quad \forall\, i,j,k.$$

Remark. This further simplifies the computation of connection coefficients $\overset{A}{\Gamma}{}^{i}_{jk}$ and is exactly the reason why we consider the holonomic constraints in the distribution rather than working with the true configuration manifold, the embedded submanifold $\mathcal{C}^{-1}(\mathbf{0})$ of Q. On the embedded submanifold $\mathcal{C}^{-1}(\mathbf{0})$, the Riemannian metric would have been a tensor field on Q rather than a constant, and would have resulted in nonzero, and cumbersomely lengthy, connection coefficient terms $\overset{\mathbb{G}}{\Gamma}{}^{i}_{jk}$.

However since $\overset{\mathbb{G}}{\Gamma}{}^{i}_{jk} = 0$ and since A is diagonal, from Eq.(4.8) we have

$$\overset{A}{\Gamma}{}^{i}_{jk} = (A^{-1})^{i}_{r}\frac{\partial (AP')^{r}_{j}}{\partial q^{k}} = \frac{1}{(h^2+h_i^2)}\frac{\partial (AP')^{i}_{j}}{\partial q^{k}}. \tag{5.17}$$

As an example let us show the connection coefficients of $\overset{A}{\Gamma}{}^{x}_{x} = \overset{A}{\Gamma}{}^{x}_{xx}\,dx + \overset{A}{\Gamma}{}^{x}_{yx}\,dy + \overset{A}{\Gamma}{}^{x}_{\theta x}\,d\theta + \overset{A}{\Gamma}{}^{x}_{x_i x}\,dx_i + \overset{A}{\Gamma}{}^{x}_{y_i x}\,dy_i + \overset{A}{\Gamma}{}^{x}_{\theta_i x}\,d\theta_i$;

$$\begin{aligned}
\overset{A}{\Gamma}{}^{x}_{xx} &= 2\sin^2\theta\sin\theta_i((x-\bar{x}_i)\sin\theta_i - (y-\bar{y}_i)\cos\theta_i)\\
\overset{A}{\Gamma}{}^{x}_{yx} &= -2\cos\theta\sin\theta\sin\theta_i((x-\bar{x}_i)\sin\theta_i - (y-\bar{y}_i)\cos\theta_i)\\
\overset{A}{\Gamma}{}^{x}_{\theta x} &= 0\\
\overset{A}{\Gamma}{}^{x}_{x_i x} &= \sin\theta_i\cos\theta_i\cos\theta((y_i-\bar{y}_i)\cos\theta - (x_i-\bar{x}_i)\sin\theta)\\
\overset{A}{\Gamma}{}^{x}_{y_i x} &= \sin^2\theta_i\cos\theta((y_i-\bar{y}_i)\cos\theta - (x_i-\bar{x}_i)\sin\theta)\\
\overset{A}{\Gamma}{}^{x}_{\theta_i x} &= 0.
\end{aligned}$$

The force acting on $\mathcal{A}$, along a curve γ on Q, is given by the covector

$$F = f\cos\theta dx + f\sin\theta dy + \tau d\theta + f_i\cos\theta_i dx_i + f_i\sin\theta_i dy_i + \tau_i d\theta_i$$

and the vector field associated with this covector F is give by $Y = \mathbb{G}^\sharp(F)$;

$$Y = f\cos\theta\frac{\partial}{\partial x} + f\sin\theta\frac{\partial}{\partial y} + \tau\frac{\partial}{\partial\theta} + f_i\cos\theta_i\frac{\partial}{\partial x_i} + f_i\sin\theta_i\frac{\partial}{\partial y_i} + \tau_i\frac{\partial}{\partial\theta_i}.$$

The projection map P in the basis $\boldsymbol{\partial_q}$ is $[P]_{\boldsymbol{\partial_q}} = I - [P^{'}]_{\boldsymbol{\partial_q}}$. Multiplying $[P]_{\boldsymbol{\partial_q}}$ on the right by the matrix representation of Y in the $\boldsymbol{\partial_q}$ basis, $[Y]_{\boldsymbol{\partial_q}} = [f\cos\theta, f\sin\theta, \tau, f_i\cos\theta_i, f_i\sin\theta_i, \tau_i]^\top$, gives the matrix representation of $P(Y(\gamma))$ and we have

$$\begin{aligned} P(Y(\gamma)) = {} & h_i\cos\theta(h_if + hf_i)\frac{\partial}{\partial x} + h_i\sin\theta(h_if + hf_i)\frac{\partial}{\partial y} + (h^2 + h_i^2)\tau\frac{\partial}{\partial\theta} \\ & + h\cos\theta_i(h_if + hf_i)\frac{\partial}{\partial x_i} + h\sin\theta_i(h_if + hf_i)\frac{\partial}{\partial y_i} + (h^2 + h_i^2)\tau_i\frac{\partial}{\partial\theta_i}. \end{aligned}$$

Constrained dynamics $\overset{A}{\nabla}_{\gamma'}\ \gamma^{'} = P(Y(\gamma))$ of $\mathcal{A}$ in the $\boldsymbol{\partial_q}$ frame are given as follows using Eq.(4.6).

$$\begin{aligned} \ddot{x} + \dot{x}\dot{x}\ \overset{A}{\Gamma}{}^{x}_{xx} + \dot{x}\dot{y}\ \overset{A}{\Gamma}{}^{x}_{yx} + \ldots + \dot{\theta}_i\dot{\theta}_i\ \overset{A}{\Gamma}{}^{x}_{\theta_i\theta_i} &= h_i\cos\theta(h_if + hf_i) \\ \ddot{y} + \dot{x}\dot{x}\ \overset{A}{\Gamma}{}^{y}_{xx} + \dot{x}\dot{y}\ \overset{A}{\Gamma}{}^{y}_{yx} + \ldots + \dot{\theta}_i\dot{\theta}_i\ \overset{A}{\Gamma}{}^{y}_{\theta_i\theta_i} &= h_i\sin\theta(h_if + hf_i) \\ \ddot{\theta} + \dot{x}\dot{x}\ \overset{A}{\Gamma}{}^{\theta}_{xx} + \dot{x}\dot{y}\ \overset{A}{\Gamma}{}^{\theta}_{yx} + \ldots + \dot{\theta}_i\dot{\theta}_i\ \overset{A}{\Gamma}{}^{\theta}_{\theta_i\theta_i} &= (h^2 + h_i^2)\tau \\ \ddot{x}_i + \dot{x}\dot{x}\ \overset{A}{\Gamma}{}^{x_i}_{xx} + \dot{x}\dot{y}\ \overset{A}{\Gamma}{}^{x_i}_{yx} + \ldots + \dot{\theta}_i\dot{\theta}_i\ \overset{A}{\Gamma}{}^{x_i}_{\theta_i\theta_i} &= h\cos\theta_i(h_if + hf_i) \\ \ddot{y}_i + \dot{x}\dot{x}\ \overset{A}{\Gamma}{}^{y_i}_{xx} + \dot{x}\dot{y}\ \overset{A}{\Gamma}{}^{y_i}_{yx} + \ldots + \dot{\theta}_i\dot{\theta}_i\ \overset{A}{\Gamma}{}^{y_i}_{\theta_i\theta_i} &= h\sin\theta_i(h_if + hf_i) \\ \ddot{\theta}_i + \dot{x}\dot{x}\ \overset{A}{\Gamma}{}^{\theta_i}_{xx} + \dot{x}\dot{y}\ \overset{A}{\Gamma}{}^{\theta_i}_{yx} + \ldots + \dot{\theta}_i\dot{\theta}_i\ \overset{A}{\Gamma}{}^{\theta_i}_{\theta_i\theta_i} &= (h^2 + h_i^2)\tau_i \end{aligned}$$

Notice that by looking at the above equations of motion satisfying the configuration and nonholonomic constraints of $\mathcal{A}$, it is not clear what control strategy would satisfy the actuator and operating constraints of $\mathcal{A}$. Since operating and actuator constraints of the UAVs are captured through the constraints $(\mu_i, \dot{\mu}_i) \in \Pi$ where $\mu_i = (v, w, v_i, w_i)$ with $\gamma' = v\mathbf{e}_v + w\mathbf{e}_w + v_i\mathbf{e}_{v_i} + w_i\mathbf{e}_{w_i} + z\mathbf{e}_z + z_i\mathbf{e}_{z_i}$ in the frame $\mathbf{e}$, we proceed to derive the constrained dynamics of $\mathcal{A}$ in this $\mathbf{e}$ frame.

Let $\mathbf{e} = \boldsymbol{\partial_q}\mathcal{S}$ be the change of basis where $\mathbf{e}_i = \frac{\partial}{\partial q^j}\mathcal{S}_i^j$ and $\mathcal{S}$ is the non-singular matrix whose (i,j)th element is $\mathcal{S}_j^i$.

$$\mathcal{S} = \begin{bmatrix} \cos\theta & 0 & 0 & 0 & -\sin\theta & 0 \\ \sin\theta & 0 & 0 & 0 & \cos\theta & 0 \\ 0 & 1 & 0 & 0 & 0 & 0 \\ 0 & 0 & \cos\theta_i & 0 & 0 & -\sin\theta_i \\ 0 & 0 & \sin\theta_i & 0 & 0 & \cos\theta_i \\ 0 & 0 & 0 & 1 & 0 & 0 \end{bmatrix} \tag{5.18}$$

The transformation rule for the matrix of connection 1-forms given by $\overset{A}{\omega} = \mathcal{S}^{-1}\ \overset{A}{\Gamma}\ \mathcal{S} + \mathcal{S}^{-1}d\mathcal{S}$ in Eq.(4.9), after some lengthy computations yield the following as the

only nonzero connection 1-forms;

$$
\begin{aligned}
\omega_v^v &= \frac{\sin(\theta-\theta_i)h}{h^2+h_i^2}\sigma^{v_i} \\
\omega_w^v &= \frac{2hh^{'}}{h^2+h_i^2}\sigma^v - \frac{h^{'}h_i}{h^2+h_i^2}\sigma^{v_i} - \frac{h_i^2}{h^2+h_i^2}\sigma^z \\
\omega_{v_i}^v &= \frac{2\sin(\theta-\theta_i)h}{h^2+h_i^2}\sigma^v - \frac{h_i\sin(\theta-\theta_i)}{h^2+h_i^2}\sigma^{v_i} \\
\omega_{w_i}^v &= -\frac{hh_i^{'}}{h^2+h_i^2}\sigma^{v_i} - \frac{hh_i}{h^2+h_i^2}\sigma^{z_i} \\
\omega_z^v &= -\sigma^w + \frac{h\cos(\theta-\theta_i)}{h^2+h_i^2}\sigma^{v_i} \\
\omega_{z_i}^v &= -\frac{2h\cos(\theta-\theta_i)}{h^2+h_i^2}\sigma^v + \frac{h_i\cos(\theta-\theta_i)}{h^2+h_i^2}\sigma^{v_i} \\
\omega_v^{v_i} &= \frac{h\sin(\theta-\theta_i)}{h^2+h_i^2}\sigma^v + \frac{2h_i\sin(\theta_i-\theta)}{h^2+h_i^2}\sigma^{v_i} \\
\omega_w^{v_i} &= -\frac{h^{'}h_i}{h^2+h_i^2}\sigma^v - \frac{hh_i}{h^2+h_i^2}\sigma^z \\
\omega_{v_i}^{v_i} &= \frac{h_i\sin(\theta_i-\theta)}{h^2+h_i^2}\sigma^v \\
\omega_{w_i}^{v_i} &= -\frac{hh_i^{'}}{h^2+h_i^2}\sigma^v + \frac{2h_ih_i^{'}}{h^2+h_i^2}\sigma^{v_i} - \frac{h^2}{h^2+h_i^2}\sigma^{z_i} \\
\omega_z^{v_i} &= \frac{h\cos(\theta-\theta_i)}{h^2+h_i^2}\sigma^v - \frac{2h_i\cos(\theta-\theta_i)}{h^2+h_i^2}\sigma^{v_i} \\
\omega_{z_i}^{v_i} &= \frac{h_i\cos(\theta-\theta_i)}{h^2+h_i^2}\sigma^v - \sigma^{w_i} \\
\omega_v^z &= \sigma^w + \frac{2h_i\sin(\theta_i-\theta)}{h^2+h_i^2}\sigma^z \\
\omega_w^z &= -\frac{h_i^2}{h^2+h_i^2}\sigma^v - \frac{hh_i}{h^2+h_i^2}\sigma^{v_i} + \frac{2hh^{'}}{h^2+h_i^2}\sigma^z \\
\omega_{v_i}^z &= \frac{2h\sin(\theta-\theta_i)}{h^2+h_i^2}\sigma^z \\
\omega_{w_i}^z &= \frac{2h_ih_i^{'}}{h^2+h_i^2}\sigma^z \\
\omega_z^z &= -\frac{2h_i\cos(\theta-\theta_i)}{h^2+h_i^2}\sigma^z
\end{aligned}
\tag{5.19}
$$

$$
\begin{aligned}
\omega^{z}_{z_i} &= -\frac{2h\cos(\theta-\theta_i)}{h^2+h_i^2}\sigma^{z} \\
\omega^{z_i}_{v} &= \frac{2h_i\sin(\theta_i-\theta)}{h^2+h_i^2}\sigma^{z_i} \\
\omega^{z_i}_{w} &= \frac{2hh^{'}}{h^2+h_i^2}\sigma^{z_i} \\
\omega^{z_i}_{v_i} &= \sigma^{w_i} + \frac{2h\sin(\theta-\theta_i)}{h^2+h_i^2}\sigma^{z_i} \\
\omega^{z_i}_{w_i} &= -\frac{hh_i}{h^2+h_i^2}\sigma^{v} - \frac{h^2}{h^2+h_i^2}\sigma^{v_i} + \frac{2h_ih_i^{'}}{h^2+h_i^2}\sigma^{z_i} \\
\omega^{z_i}_{z} &= -\frac{2h_i\cos(\theta-\theta_i)}{h^2+h_i^2}\sigma^{z_i} \\
\omega^{z_i}_{z_i} &= -\frac{2h\cos(\theta-\theta_i)}{h^2+h_i^2}\sigma^{z_i}
\end{aligned}
$$

where

$$
\begin{aligned}
h^{'} &\triangleq (x_i-\bar{x}_i)\cos\theta + (y_i-\bar{y}_i)\sin\theta \\
h_i^{'} &\triangleq (x-\bar{x}_i)\cos\theta_i + (y-\bar{y}_i)\sin\theta_i.
\end{aligned}
$$

The force F along γ, is given by the following covector in the frame $\boldsymbol{\sigma}$

$$F = f\sigma^{v} + \tau\sigma^{w} + f_i\sigma^{v_i} + \tau_i\sigma^{w_i}$$

and the tangent vector field $Y = \mathbb{G}^{\sharp}(F)$ associated with this covector F is

$$Y = fe_v + \tau e_w + f_i e_{v_i} + \tau_i e_{w_i}.$$

Let $\mathbf{x} = \mathbf{e}\mathcal{Z}$ be the change of basis where $\mathcal{Z} = \mathcal{S}^{-1}\mathcal{R}$ with $\mathbf{x} = \boldsymbol{\partial_q}\mathcal{R}$ and $\mathbf{e} = \boldsymbol{\partial_q}\mathcal{S}$. Matrix representation of the projection map P in the $\mathbf{e}$ basis is given by $[P]_{\mathbf{e}} = \mathcal{Z}[P]_{\mathbf{x}}\mathcal{Z}^{-1}$. Recall that $[P]_{\mathbf{x}} = I - [P^{'}]_{\mathbf{x}}$. The projection of Y onto the distribution $\mathcal{D}$ is then

$$P(Y(\gamma)) = \frac{h_i(h_if+hf_i)}{(h^2+h_i^2)}e_v + \tau e_w + \frac{h(h_if+hf_i)}{(h^2+h_i^2)}e_{v_i} + \tau_i e_{w_i}. \tag{5.20}$$

The constrained dynamics in the frame $\mathbf{e}$ are then as follows where $\gamma' = v\mathbf{e}_v + w\mathbf{e}_w + v_i\mathbf{e}_{v_i} + w^i\mathbf{e}_{w_i} + z\mathbf{e}_z + z_i\mathbf{e}_{z_i}$;

$$\begin{aligned}
\dot{v} + v\omega_v^v(\gamma') + w\omega_w^v(\gamma') + \ldots + z_i\omega_{z_i}^v(\gamma') &= \frac{h_i(h_i f + h f_i)}{(h^2 + h_i^2)} \\
\dot{w} &= \tau \\
\dot{v}_i + v\omega_v^{v_i}(\gamma') + w\omega_w^{v_i}(\gamma') + \ldots + z_i\omega_{z_i}^{v_i}(\gamma') &= \frac{h(h_i f + h f_i)}{(h^2 + h_i^2)} \\
\dot{w}_i &= \tau_i \\
\dot{z} + v\omega_v^z(\gamma') + w\omega_w^z(\gamma') + \ldots + z_i\omega_{z_i}^z(\gamma') &= 0 \\
\dot{z}_i + v\omega_v^{z_i}(\gamma') + w\omega_w^{z_i}(\gamma') + \ldots + z_i\omega_{z_i}^{z_i}(\gamma') &= 0.
\end{aligned}$$

The choice of the frame $\mathbf{e}$ is such that $\mathbf{e}_z, \mathbf{e}_{z_i} \in \mathcal{D}^\perp$. For $\gamma'(0) \in \mathcal{D}$, we have $z(0) = z_i(0) = 0$ and since $\overset{A}{\nabla}$ restricts γ' to $\mathcal{D}$ the functions $z(t), z_i(t)$ will remain identically zero. Let us define $\eta_i \triangleq \frac{h_i(h_i f + h f_i)}{(h^2 + h_i^2)}$. The constrained dynamics of $\mathcal{A}$ in the frame $\mathbf{e}$ then reduce to

$$\begin{aligned}
\dot{v} + v\omega_v^v(\gamma') + w\omega_w^v(\gamma') + v_i\omega_{v_i}^v(\gamma') + w_i\omega_{w_i}^v(\gamma') &= \eta_i \\
\dot{w} &= \tau \\
\dot{v}_i + v\omega_v^{v_i}(\gamma') + w\omega_w^{v_i}(\gamma') + v_i\omega_{v_i}^{v_i}(\gamma') + w_i\omega_{w_i}^{v_i}(\gamma') &= \frac{h}{h_i}\eta_i \\
\dot{w}_i &= \tau_i.
\end{aligned}$$

The above equations when expanded using the connection 1-forms given in Eq.(5.19) result in the following form of the constrained dynamics.

$$\begin{aligned}
\dot{v} + vv_i\omega_{v_i v}^v + wv\omega_{vw}^v + wv_i\omega_{v_i w}^v + v_i v\omega_{vv_i}^v + v_i v_i\omega_{v_i v_i}^v + w_i v_i\omega_{v_i w_i}^v &= \eta_i \\
\dot{w} &= \tau \\
\dot{v}_i + vv\omega_{vv}^{v_i} + vv_i\omega_{v_i v}^{v_i} + wv\omega_{vw}^{v_i} + v_i v\omega_{vv_i}^{v_i} + w_i v\omega_{vw_i}^{v_i} + w_i v_i\omega_{v_i w_i}^{v_i} &= \frac{h}{h_i}\eta_i \\
\dot{w}_i &= \tau_i
\end{aligned} \tag{5.21}$$

Notice that the constrained dynamics of the i-th subsystem $\mathcal{A}$ in the $\mathbf{e}$ frame appear explicitly in the functions $\mu_i, \dot{\mu}_i, q_i$ where $\mu_i = (v, w, v_i, w_i)$ and q_i is the configuration. The functions v, w, τ are the only common functions to appear in each of the N such subsystems. For consensus, we require these functions v, w, τ to have the same value at any given time in each of the N such subsystems.

To ensure we have the same values for w, τ in each of the N subsystems simply means to have the same intrinsic control law for τ in each of them along with compatible initial conditions (since $\tau = \dot{w}$). By an intrinsic control law, we mean a control law which will be independent of the local coordinates q_i of its subsystem.

To ensure v has the same value in each of the N subsystems, consider the following control law for τ_i;

$$\tau_i = K_w(w_i^d - w_i) + \dot{w}_i^d \tag{5.22}$$

where

$$w_i^d = \frac{-vv_i\omega^v_{v_iv} - wv\omega^v_{vw} - wv_i\omega^v_{v_iw} - v_iv\omega^v_{vv_i} - v_iv_i\omega^v_{v_iv_i}}{v_i\omega^v_{v_iw_i}}.$$

The above control law that exponentially stabilizes w_i to w_i^d along with the initial condition $w_i(0) = w_i^d(0)$, reduces the first equation of constrained dynamics to

$$\dot{v} = \eta_i. \tag{5.23}$$

With the above control law for τ_i, to ensure we have the same value for v in each of the subsystems simply means to have the same intrinsic control law for $\eta_i = f$ (and hence the same value for η_i) in each of the N subsystems.

Implementing the same functions τ, f together with the above control law for τ_i on each of the N subsystems would then result in the same functions v, w, τ appearing in each of them, thus ensuring consensus between the subsystems. We now have

only two independent controls τ and f. We develop two sets of controllers for these functions τ and f, one for *feasibility* and the other to achieve the *team goal*.

A. Controls for Feasibility

From preliminary results of this same problem, presented in Chapter II, it was seen that when $w = 0$, actuator and operating constraints are satisfied, thus ensuring feasibility. We use this observation without analysis or proof here and simply verify it in simulations.

Consider the following controllers for the functions τ and f;

$$\tau = \begin{cases} -K_w w & if \quad |K_w w| \leq \tau^{max} \\ -sgn(w)\tau^{max} & else \end{cases} \tag{5.24}$$
$$f = 0$$

where the control law for τ asymptotically stabilizes w to zero.

B. Controls to Achieve Team Goal

The team goal is to generate a phantom trajectory moving towards the desired waypoint. We translate this goal to the requirement of orienting the phantom UAV towards the desired waypoint and propose the following control laws to achieve this team goal.

$$\tau = \begin{cases} K_w(w^d - w) + \dot{w}^d & if \quad |K_w(w^d - w) + \dot{w}^d| \leq \tau^{max} \\ sgn(K_w(w^d - w) + \dot{w}^d)\tau^{max} & else \end{cases}$$
$$f = \begin{cases} K_v(v^d - v) + \dot{v}^d & if \quad |K_v(v^d - v) + \dot{v}^d| \leq f^{max} \\ sgn(K_v(v^d - v) + \dot{v}^d)f^{max} & else \end{cases} \tag{5.25}$$

where,

$$\omega^d = K_{\beta-\theta}(\beta - \theta) + \dot{\beta}$$
$$v^d = \begin{cases} v^{min} & if \quad (\beta - \theta)\ is\ large \\ v^{max} & else \end{cases}$$

asymptotically stabilizing $(\beta - \theta)$ to zero and v to v_d in the two controllers. Here $\beta = \tan^{-1}\left(\frac{y_f - y}{x_f - x}\right)$ with (x_f, y_f) being the desired waypoint of the Phantom. Physically, $(\beta - \theta)$ is the angle between the desired waypoint of the phantom and its current heading and the objective is to orient the phantom UAV towards the desired waypoint.

In the control law for f, v^d is v^{min} when the angle $(\beta - \theta)$ is above a threshold value (i.e. when the phantom is not sufficiently oriented towards its final waypoint), and is v^{max} otherwise. The objective is to speed up the phantom UAV when oriented towards its desired waypoint and to slow down when not.

The constrained dynamics are solved for the time interval $t = [t, t + \delta t]$ using either the controls for feasibility or the controls for team goal, and this is repeated continuously from one time interval to the next. We assume δt to be fixed. The UAVs are responsible for computing their own trajectories as well as that of the phantom by solving the constrained dynamics of their corresponding subsystems. The proposed control strategy ensures that all the UAVs identically design the same phantom tra-

jectory thus achieving consensus. The distributed control architecture, shown in the form of a flow-chart in Fig.14, to generate reference trajectories implemented in a receding horizon approach is explained next.

C. Distributed Control Architecture

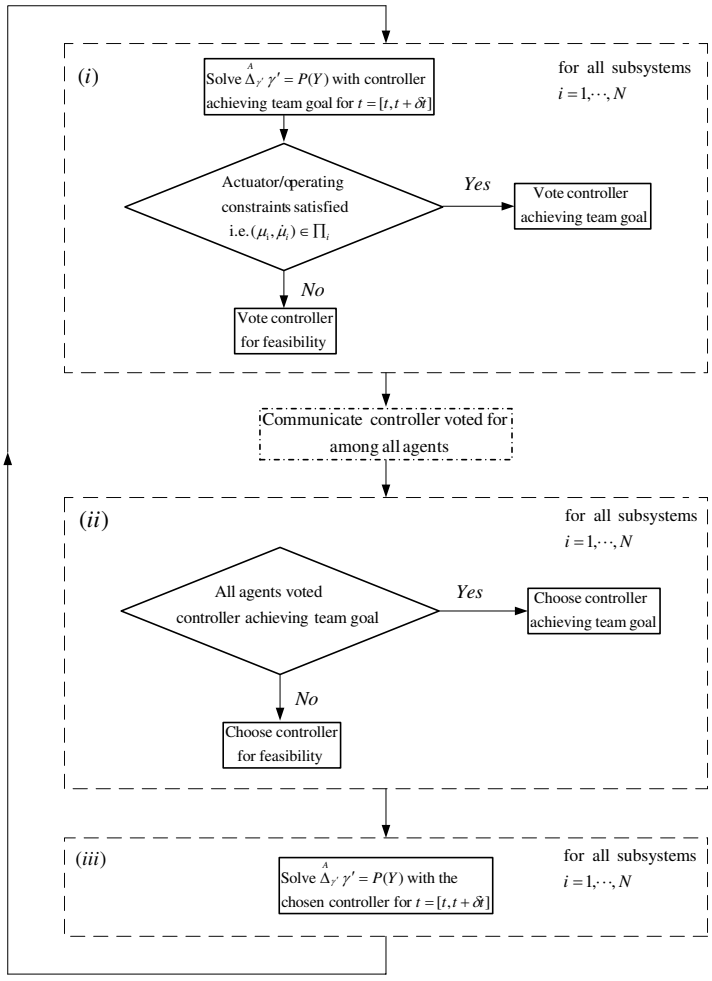

Fig. 14. Distributed control architecture.

Each of the N UAVs solves its corresponding constrained dynamics for the time interval $t = [t, t + \delta t]$ with controls to achieve the team goal first. Next they verify if

all actuator/operating constraints $(\mu_i, \dot{\mu}_i) \in \Pi_i$ were satisfied for their corresponding subsystems during this same time interval $[t, t + \delta t]$. Since constrained dynamics are solved in the functions μ_i, this step is straight forward. If all the actuator/operating constraints were satisfied in a particular subsystem, the corresponding UAV votes for the controls achieving the team goal. If any of the actuator/operating constraints were violated within $[t, t + \delta t]$, the UAV votes for the controls for feasibility. Recall that each of the subsystems need to implement identical control actions for τ, f for consensus. Hence each of the N UAVs communicates the type of controller it voted for and the entire team of UAVs picks a common controller to implement for the horizon interval $[t, t+\delta t]$. If even one of the N UAVs had voted for controls for feasibility, then all of the N UAVs chooses controls for feasibility to solve the constrained dynamics for $[t, t + \delta t]$. If on the other hand, all the N UAVs had voted for the controller for team goal, then each of the UAVs computes its trajectory for the time interval $[t, t + \delta t]$ using controls to achieve the team goal. Note that the phantom trajectory is designed (identically) by each of the N UAVs in addition to their own trajectory. This is a necessary redundancy in computation in the proposed distributed approach. The computations shown in the blocks (i), (ii) and (iii) of the flow-chart of Fig.14 are performed by each of the N UAVs in parallel and as such increasing the number of agents in the system has minimal effect on the overall communication/computation time thus making the approach scalable. Communication amongst the agents need not be continuous and has to occur only once in each cycle of the receding horizon control strategy. A severe drawback of this strategy however is that it requires synchronized control and communication among all its agents.

D. Simulation Results

Simulation results of this algorithm for the case of 4-UAVs engaging 4-radars are shown in Fig.15. Actuator and operating constraints on the phantom and the individual UAVs were assumed as follows. Phantom speed of $400 \pm 40m/s$, UAV speeds of $100 \pm 15m/s$ and minimum turn radii of $5000m$ and $1500m$ for the phantom and the UAVs, respectively. Force and toque bounds of $[-0.7N, 0.7N]$, and $[-0.04Nm, 0.04Nm]$, respectively, for the phantom and the UAVs. The force and torque are normalized quantities with the earlier assumption that mass and inertia of all the UAVs, including that of the imaginary UAV assigned for the phantom, are of unit magnitude. The time history of the functions v, w, v_i, w_i corresponding

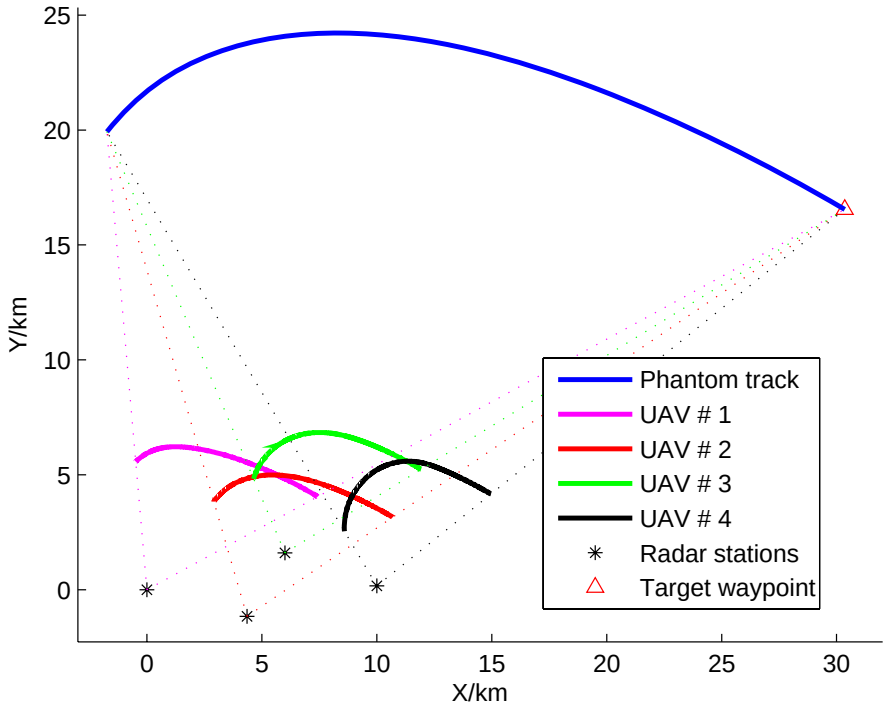

Fig. 15. Four UAVs deceiving a radar network of four radars through the generation of a phantom track.

to "speed" and "steer" of the UAVs and the phantom are shown in Fig.16, for the trajectory results shown in Fig.15. The lower and upper bounds of v, w, v_i, w_i are also shown. The normalized torque and force corresponding to each of the four UAVs

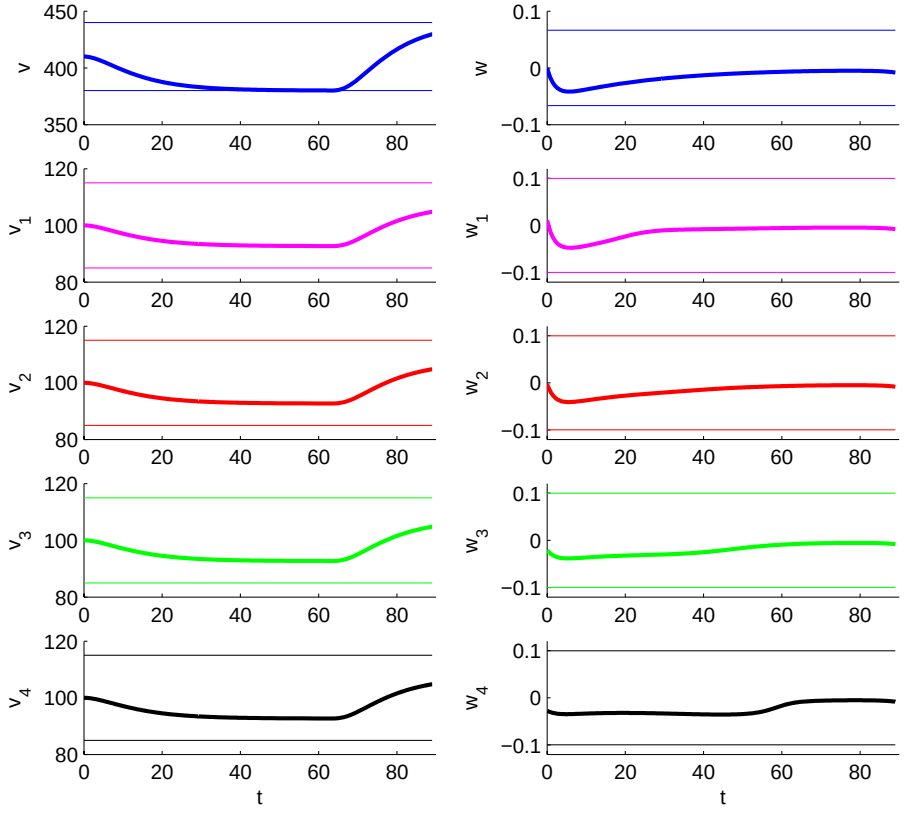

Fig. 16. Speed and steer, along with their upper and lower bounds, for each of the four UAVs and the UAV representing the phantom.

and the phantom UAV are illustrated in Fig.17 and here it is seen that the forces f_i and f remain identically the same. As mentioned in Chapter III, Section E, the control law for feasibility given in Eq.(5.24) only drives the system towards feasible solutions and hence does not provide a theoretical guarantee on satisfying the constraints $(\mu_i, \dot{\mu}_i) \in \Pi_i$ until after the controller stabilizes w to zero. However, simulation results suggest that these set constraints can be effectively satisfied even in

the transient stages of the controller (i.e. before w stabilizes to zero) by tuning the control gain K_w in Eq.(5.24). Simulation results given in Fig.16, Fig.17 verify that the set constraints $(\mu_i, \dot{\mu}_i) \in \Pi_i$ are satisfied and hence the reference trajectories designed are dynamically feasible to be tracked by each of the four UAVs.

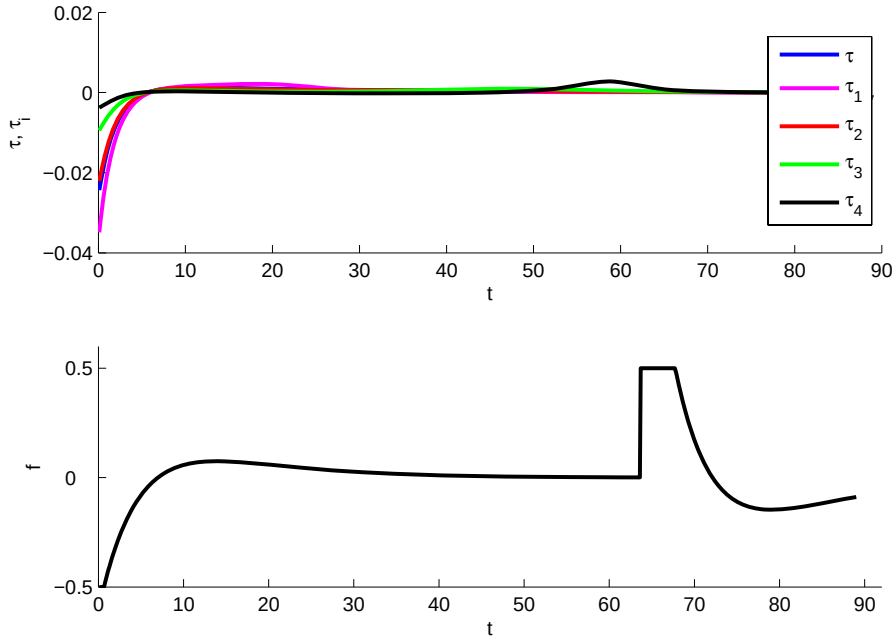

Fig. 17. Torque and force controls, for each of the four UAVs and the UAV representing the phantom.

The forces f_i and f remain identically the same since the control law for τ_i, given by Eq.(5.22), apparently forces $\frac{v_i}{v}$ to remain the same constant value. This is verified in Fig.18 which plots the ratios $\frac{v_i}{v}$ and $\frac{r_i}{R_i}$ against time for each of the UAVs, where r_i is the distance from the i-th UAV to its corresponding radar and R_i is the distance from the phantom to the same radar. As can be seen in Fig.18, the ratio $\frac{v_i}{v}$ remains constant with time while the ratios of $\frac{r_i}{R_i}$ all converge to it. This is a phenomena which was explained in the kinematic analysis of the radar deception problem presented in Chapter II. There it was shown that the convergence of $\frac{r_i}{R_i} \rightarrow \frac{v_i}{v}$ reduces the

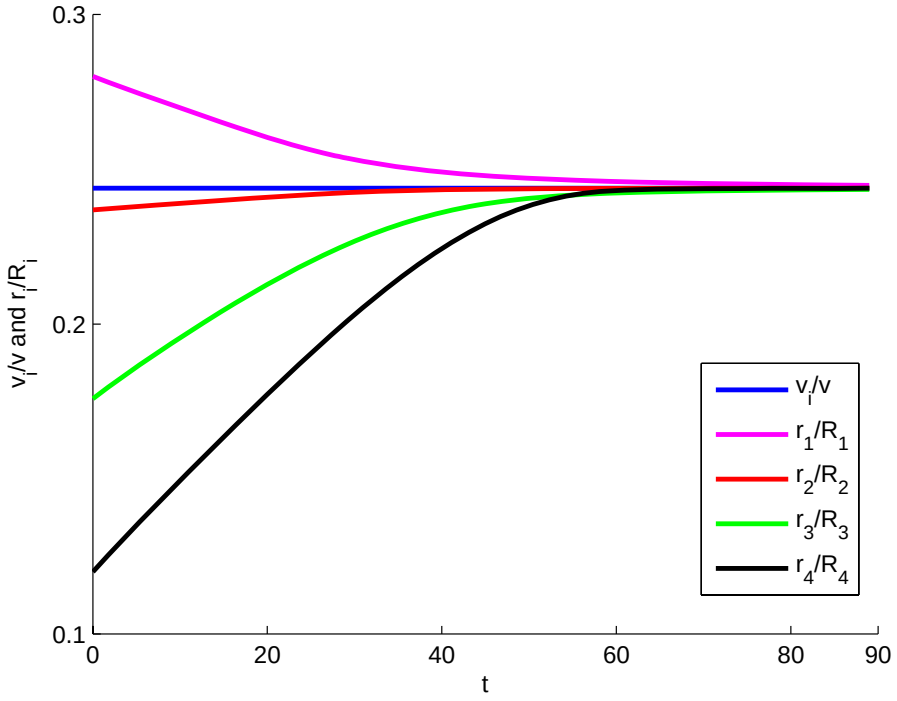

Fig. 18. The ratios of $\frac{v_i}{v}$ and $\frac{r_i}{R_i}$ for the four UAV-radar pairs.

dynamics of the multi-agent system to the dynamics of a single UAV, controllable on its configuration submanifold. In other words, all the four UAVs converge to a seemingly stable rigid formation maintaining parallel motion. The rigid formation it converges to is a contracted geometric copy (contracted by a factor of $\left(1 - \frac{v_i}{v}\right)$) of the geometric formation the network of radars make. If all four UAVs were to start out with initial conditions such that $\frac{r_i}{R_i} = \frac{v_i}{v}$, (i.e. with initial conditions such that it is already in the stable rigid formation), then the phantom UAV is controllable with all the UAVs in parallel motion, maintaining a rigid formation. This is illustrated in Fig.19. In general, the computation time of the algorithm was an order of magnitude less than the real-time over which the algorithm was implemented. The real-time corresponding to the trajectories shown in Fig.15 was 89 sec while the CPU time

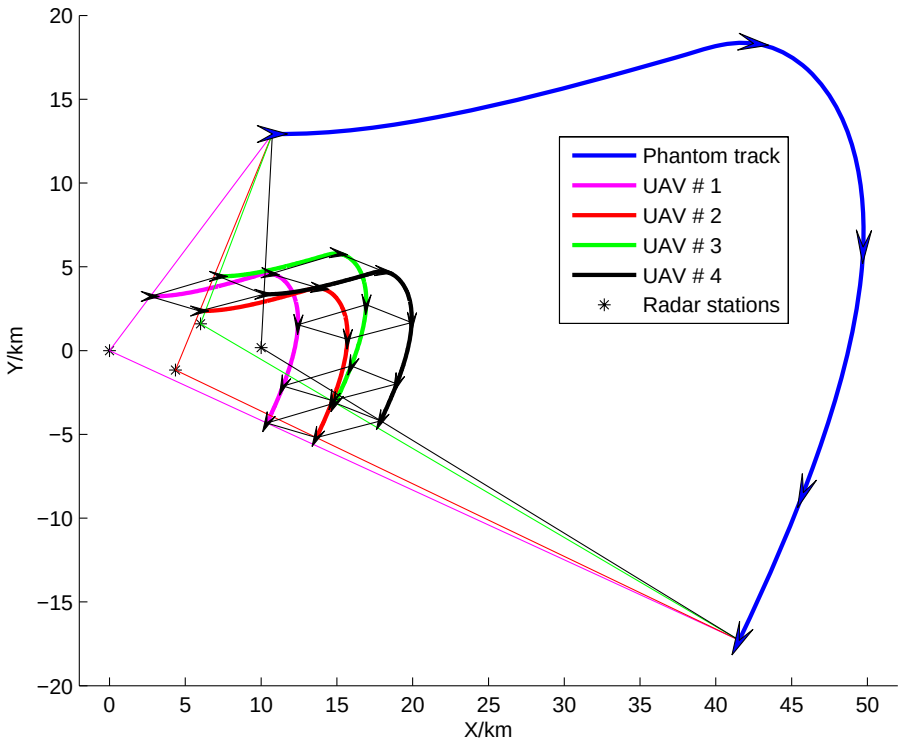

Fig. 19. Parallel motion of four UAVs maintaining a stable rigid formation, for initial conditions satisfying $\frac{r_i}{R_i} = \frac{v_i}{v}$.

(computation time) of each of the UAVs in the distributed control architecture was 7.5 sec.

Some of the key attributes of the motion planning algorithm verified through simulations for the radar deception problem are: (i) produces dynamically feasible reference trajectories (ii) scalable (iii) suited for real time computation (iv) communication (time and data) between agents is small (v) implementable as an autonomous team of agents (vi) the receding horizon approach has a feedback structure providing inherent robustness.

CHAPTER VI

RIGID FORMATION KEEPING

In this chapter, the proposed motion planning algorithm is applied to the rigid formation keeping problem and verified in simulation. Preliminary results of this problem can be found in [47, 48].

Consider N agents restricted to the plane making up a virtual structure (VS) with an arbitrary point O_c (the centroid of the VS). An orthogonal local coordinate frame B is assumed fixed to the VS at O_c and let $(b_{i,1}, b_{i,2})$ denote the place holder for the i-th agent in this B frame. These $b_{i,1}, b_{i,2}$ are assumed constant thereby forcing the VS to behave as a rigid formation. Once again we propose the unicycle model to capture the dynamic, operating and actuator constraints of an agent restricted to the 2D plane and the agents can be either wheeled robots or UAVs. Let (x, y) be local coordinates of O_c with respect to an inertial frame I and ϕ the orientation of the B frame with respect to I. Let (x_i, y_i) describe the position and θ_i the orientation of an i-th agent with respect to the frame I. Similarly let (x, y, θ) describe the position and orientation of a virtual agent at O_c.

The multi-agent system then comprises of the N-agents, the B frame and the virtual agent at O_c. The configuration of this multi-agent system has local coordinates

$$q = (x_1, y_1, \theta_1, \ldots, x_N, y_N, \theta_N, x, y, \theta, \phi)$$

and will have the structure of a smooth differentiable manifold having dimension $3N + 4$.

We have the following configuration constraints for the above multi-agent system;

$$\begin{aligned} x_i - x - b_{i,1}\cos\phi + b_{i,2}\sin\phi = 0 \\ y_i - y - b_{i,1}\sin\phi - b_{i,2}\cos\phi = 0. \end{aligned} \tag{6.1}$$

Agent constraints of the i-th agent and the virtual agent at O_c are captured through the following unicycle models;

$$\begin{aligned} \dot{x}_i &= v_i\cos\theta_i & \dot{x} &= v\cos\theta \\ \dot{y}_i &= v_i\sin\theta_i & \dot{y} &= v\sin\theta \\ \dot{\theta}_i &= w_i & \dot{\theta} &= w \end{aligned} \tag{6.2}$$

where v_i, w_i are the speed and steer controls of the i-th agent while v, w are that of the virtual agent.

Also assume the following virtual control over the orientation of the B frame;

$$\dot{\phi} = u \tag{6.3}$$

where u is the virtual steer control over the B frame.

Actuator and operating constraints are captured through the following constraints;

$$\begin{aligned} {v_i}^{min} &\leq v_i \leq {v_i}^{max} \\ -\frac{{w_i}^{max}}{v_i^{max}}v_i &\leq w_i \leq \frac{{w_i}^{max}}{v_i^{max}}v_i \\ v^{min} &\leq v \leq v^{max} \\ -\frac{w^{max}}{v^{max}}v &\leq w \leq \frac{w^{max}}{v^{max}}v. \end{aligned} \tag{6.4}$$

The control u being a virtual control we do not consider constraints over it. However we do consider constraints over the virtual steer and speed controls v, w corresponding to the virtual agent at O_c since we need to keep the formalism general enough to

allow this virtual agent be replaced by an actual agent. For convenience, we consider only actuator/operating constraints involving $\mu_i = (v, w, v_i, w_i)$ in this problem. Considering $\dot{\mu}_i$ in the formulation is quite straight forward, but would be at the expense of more symbolic computations.

Next the multi-agent system is decoupled into N-subsystems corresponding to the N agents. Consider the i-th subsystem, $\mathcal{A}$, made up of the i-th agent, the virtual agent at O_c and the B frame as shown in Fig.20. Here the vectors $\mathbf{r}_i = (x_i, y_i)$, $\mathbf{r} = (x, y)$ are in the inertial frame I while the vector $\mathbf{b}_i = (b_{i,1}, b_{i,2})$ is in the B frame and O_i denotes the place holder for the i-th agent. The manifold Q

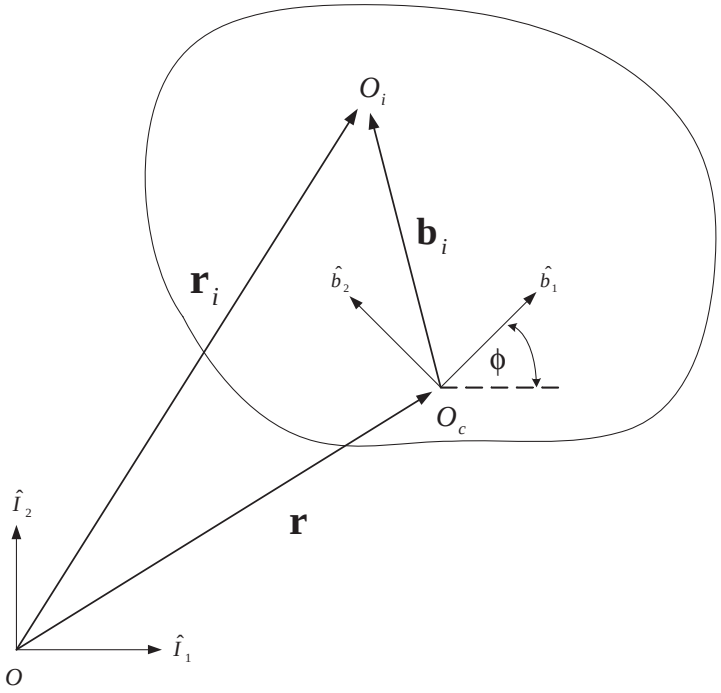

Fig. 20. Configuration of the i-th subsystem for the rigid formation keeping problem.

representing the i-th subsystem will have local coordinates $q_i = \{x, y, \theta, x_i, y_i, \theta_i, \phi\}$ where $\boldsymbol{\partial_q} = \{\frac{\partial}{\partial x}, \frac{\partial}{\partial y}, \frac{\partial}{\partial \theta}, \frac{\partial}{\partial x_i}, \frac{\partial}{\partial y_i}, \frac{\partial}{\partial \theta_i}, \frac{\partial}{\partial \phi}\}$ is the coordinate basis for T_qQ and $\boldsymbol{dq} = \{dx, dy, d\theta, dx_i, dy_i, d\theta_i, d\phi\}$ its dual basis for T_q^*Q. The Riemannian metric corre-

sponding to the kinetic energy of the system is $\mathbb{G} = m(dx \otimes dx + dy \otimes dy) + Jd\theta \otimes \theta + m_i(dx_i \otimes dx_i + dy_i \otimes dy_i) + J_i d\theta_i \otimes \theta_i + \tilde{J} d\phi \otimes d\phi$ where (m_i, J_i) are mass and inertia of the i-th agent, (m, J) the fictitious mass and inertia of the virtual agent and $\tilde{J}$ the fictitious inertia of the VS formation about O_c. As in the radar deception problem, for computational convenience, and without loss of generality, we assume $m, J, m_i, J_i, \tilde{J}$ to be of unit magnitude. The inertia matrix associated with the Riemannian metric $\mathbb{G}$ is then the identity $[\mathbf{I}]_{7\times 7}$. Next we proceed to derive the constrained dynamics of the i-th subsystem, $\mathcal{A}$.

Nonholonomic constraints on $\mathcal{A}$ are

$$\begin{aligned} \dot{x}\sin\theta - \dot{y}\cos\theta &= 0 \\ \dot{x}_i \sin\theta_i - \dot{y}_i \cos\theta_i &= 0. \end{aligned} \tag{6.5}$$

The annihilating codistribution associated with the above nonholonomic constraints of $\mathcal{A}$ is given by

$$\Lambda : \quad \begin{aligned} \boldsymbol{\alpha}_1 &= \sin\theta dx - \cos\theta dy \\ \boldsymbol{\alpha}_2 &= \sin\theta_i dx_i - \cos\theta_i dy_i. \end{aligned}$$

The distribution Δ associated with the annihilating codistribution Λ is spanned by $\Delta = \{\mathbf{e}_v, \ldots, \mathbf{e}_{w_i}\}$ where

$$\begin{aligned} \mathbf{e}_v &= \cos\theta \frac{\partial}{\partial x} + \sin\theta \frac{\partial}{\partial y} \\ \mathbf{e}_w &= \frac{\partial}{\partial \theta} \\ \mathbf{e}_{v_i} &= \cos\theta_i \frac{\partial}{\partial x_i} + \sin\theta_i \frac{\partial}{\partial y_i} \\ \mathbf{e}_{w_i} &= \frac{\partial}{\partial \theta_i} \end{aligned}$$

and $\Delta^{\perp}$, the compliment of Δ, is spanned by $\Delta^{\perp} = \{\mathbf{e}_u, \ldots, \mathbf{e}_{z_i}\}$ where

$$\begin{aligned}
\mathbf{e}_u &= \frac{\partial}{\partial u} \\
\mathbf{e}_z &= \mathbb{G}^{\sharp}(\boldsymbol{\alpha}_1) = \sin\theta \frac{\partial}{\partial x} - \cos\theta \frac{\partial}{\partial x} \\
\mathbf{e}_{z_i} &= \mathbb{G}^{\sharp}(\boldsymbol{\alpha}_2) = \sin\theta_i \frac{\partial}{\partial x_i} - \cos\theta_i \frac{\partial}{\partial y_i}.
\end{aligned}$$

The frame of vector fields $\mathbf{e} = \{\mathbf{e}_v, \mathbf{e}_w, \mathbf{e}_{v_i}, \mathbf{e}_{w_i}, \mathbf{e}_u, \mathbf{e}_z, \mathbf{e}_{z_i}\}$ span T_qQ on the manifold Q and hence is another basis for T_qQ. Associated with the frame $\mathbf{e}$ is its dual frame $\boldsymbol{\sigma} = \{\sigma^v, \sigma^w, \sigma^{v_i}, \sigma^{w_i}, \sigma^u, \sigma^z, \sigma^{z_i}\}$. The tangent vector on Q associated with a trajectory curve γ is given by $\gamma' = v\mathbf{e}_v + w\mathbf{e}_w + v_i\mathbf{e}_{v_i} + w_i\mathbf{e}_{w_i} + u\mathbf{e}_u + z\mathbf{e}_z + z_i\mathbf{e}_{z_i}$ in this $\mathbf{e}$ frame. The actuator and operating constraints acting on $\mathcal{A}$, given by Eq.(6.4), can be written concisely as follows.

$$\mu_i \in \Pi_i \tag{6.6}$$

The map $\mathcal{C} : Q \mapsto \mathbf{0} \in \mathcal{R}^m$ capturing the configuration constraint on $\mathcal{A}$ is

$$\begin{aligned}
x_i - x - b_{i,1}\cos\phi + b_{i,2}\sin\phi = 0 \\
y_i - y - b_{i,1}\sin\phi - b_{i,2}\cos\phi = 0
\end{aligned} \tag{6.7}$$

and the differential of this map, $d\mathcal{C}$, is given by the 1-forms

$$d\mathcal{C} : \quad \begin{aligned}
\boldsymbol{\beta}_1 &= dx - dx_i - (b_{i,1}\sin\phi + b_{i,2}\cos\phi)d\phi \\
\boldsymbol{\beta}_2 &= dy - dy_i + (b_{i,1}\cos\phi - b_{i,2}\sin\phi)d\phi.
\end{aligned}$$

The intersection of the annihilating codistributions Λ and $d\mathcal{C}$ gives the unique annihilating codistribution $\Omega : \Lambda \oplus d\mathcal{C}$ and has the following matrix representation in the

$\boldsymbol{\partial_q}$ basis;

$$[\Omega]_{\boldsymbol{\partial_q}} = \begin{bmatrix} \sin\theta & -\cos\theta & 0 & 0 & 0 & 0 & 0 \\ 1 & 0 & 0 & -1 & 0 & 0 & -(b_{i,1}\sin\phi + b_{i,2}\cos\phi) \\ 0 & 1 & 0 & 0 & -1 & 0 & (b_{i,1}\cos\phi - b_{i,2}\sin\phi) \end{bmatrix} \tag{6.8}$$

The distribution $\mathcal{D}$ associated with the annihilating codistribution Ω is spanned by the vector fields

$$\begin{aligned} \mathbf{x}_1 &= \frac{h_i\cos\theta}{\sin(\theta_i-\theta)}\frac{\partial}{\partial x} + \frac{h_i\sin\theta}{\sin(\theta_i-\theta)}\frac{\partial}{\partial y} + \frac{h\cos\theta_i}{\sin(\theta_i-\theta)}\frac{\partial}{\partial x_i} + \frac{h\sin\theta_i}{\sin(\theta_i-\theta)}\frac{\partial}{\partial y_i} + \frac{\partial}{\partial\phi} \\ \mathbf{x}_2 &= \frac{\partial}{\partial\theta} \\ \mathbf{x}_3 &= \frac{\partial}{\partial\theta_i} \end{aligned} \tag{6.9}$$

and $\mathcal{D}^{\perp}$ is spanned by

$$\begin{aligned} \mathbf{x}_4 &= \mathbb{G}^{\sharp}(\boldsymbol{\alpha}_1) = \sin\theta\frac{\partial}{\partial x} - \cos\theta\frac{\partial}{\partial y} \\ \mathbf{x}_5 &= \mathbb{G}^{\sharp}(\boldsymbol{\alpha}_2) = \sin\theta_i\frac{\partial}{\partial x_i} - \cos\theta_i\frac{\partial}{\partial y_i} \\ \mathbf{x}_6 &= \mathbb{G}^{\sharp}(\boldsymbol{\beta}_1) = \frac{\partial}{\partial x} - \frac{\partial}{\partial x_i} - (b_{i,1}\sin\phi + b_{i,2}\cos\phi)\frac{\partial}{\partial\phi} \\ \mathbf{x}_7 &= \mathbb{G}^{\sharp}(\boldsymbol{\beta}_2) = \frac{\partial}{\partial y} - \frac{\partial}{\partial y_i} + (b_{i,1}\cos\phi - b_{i,2}\sin\phi)\frac{\partial}{\partial\phi} \end{aligned} \tag{6.10}$$

where $h \triangleq b_{i,1}\cos(\theta-\phi) + b_{i,2}\sin(\theta-\phi)$ and $h_i \triangleq b_{i,1}\cos(\theta_i-\phi) + b_{i,2}\sin(\theta_i-\phi)$.

Let $\mathbf{x} = \boldsymbol{\partial_q}\mathcal{R}$ be the change of basis where $\mathbf{x}_i = \frac{\partial}{\partial q^j}\mathcal{R}_i^j$ and $\mathcal{R}_j^i$ is the (i,j)th element of $\mathcal{R}$. The projection map $P' : TQ \to TQ$ has the matrix representation $\left[P'\right]_{\mathbf{x}} = \begin{bmatrix} [\mathbf{0}]_{3\times3} & [\mathbf{0}]_{3\times4} \\ [\mathbf{0}]_{4\times3} & [\mathbf{I}]_{4\times4} \end{bmatrix}$ and $\left[P'\right]_{\boldsymbol{\partial_q}} = \mathcal{R}\left[P'\right]_{\mathbf{x}}\mathcal{R}^{-1}$ in the two basis $\mathbf{x}$ and $\boldsymbol{\partial_q}$.

Choosing $A = (h_i^2 + h^2 + \Theta)I$ to eliminate the denominator terms of P', we then

have $[AP^{'}]_{\boldsymbol{\partial_q}}$ to be

$$\begin{bmatrix}
(h_i^2\sin^2\theta + h^2 + \Theta) & (-h_i^2\cos\theta\sin\theta) & 0 & \\
(-h_i^2\cos\theta\sin\theta) & (h_i^2\cos^2\theta + h^2 + \Theta) & 0 & \\
0 & 0 & 0 & \\
(-hh_i\cos\theta\cos\theta_i) & (-hh_i\sin\theta\cos\theta_i) & 0 & \cdots \\
(-hh_i\sin\theta_i\cos\theta) & (-hh_i\sin\theta_i\sin\theta) & 0 & \\
0 & 0 & 0 & \\
(-h_i\cos\theta\sin(\theta_i-\theta)) & (-h_i\sin\theta\sin(\theta_i-\theta) & 0 &
\end{bmatrix}$$

$$\begin{bmatrix}
(-hh_i\cos\theta\cos\theta_i) & (-hh_i\sin\theta_i\cos\theta) & 0 & (h_i\sin(\theta-\theta_i)\cos\theta) \\
(-hh_i\sin\theta\cos\theta_i) & (-hh_i\sin\theta_i\sin\theta) & 0 & (h_i\sin(\theta-\theta_i)\sin\theta) \\
0 & 0 & 0 & 0 \\
\cdots\quad (h^2\sin^2\theta_i + h_i^2 + \Theta) & (-h^2\cos\theta_i\sin\theta_i) & 0 & (h\sin(\theta-\theta_i)\cos\theta_i) \\
(-h^2\cos\theta_i\sin\theta_i) & (h^2\cos^2\theta_i + h_i^2 + \Theta) & 0 & (h\sin(\theta-\theta_i)\sin\theta_i) \\
0 & 0 & 0 & 0 \\
(-h\cos\theta_i\sin(\theta_i-\theta)) & (-h\sin\theta_i\sin(\theta_i-\theta)) & 0 & (h^2+h_i^2)
\end{bmatrix}$$

where $\Theta \triangleq \sin^2(\theta_i - \theta)$.

Here too, as in the radar deception problem, the kinetic metric $\mathbb{G}$ is constant resulting in $\overset{\mathbb{G}}{\Gamma}{}^i_{jk} = 0 \quad for \quad \forall\ i,j,k$ and A is diagonal, and hence from Eq.(4.8) we have

$$\overset{A}{\Gamma}{}^i_{jk} = (A^{-1})^i_r \frac{\partial (AP^{'})^r_j}{\partial q^k} = \frac{1}{(h_i^2 + h^2 + \Theta)} \frac{\partial (AP^{'})^i_j}{\partial q^k}. \tag{6.11}$$

The constrained dynamics of $\mathcal{A}$ are derived in the $\mathbf{e}$ frame next. Let $\mathbf{e} = \boldsymbol{\partial_q}\mathcal{S}$ be the change of basis where $\mathbf{e}_i = \frac{\partial}{\partial q^j}\mathcal{S}^j_i$ and $\mathcal{S}$ is the non-singular matrix whose (i,j)th

element is $\mathcal{S}^i_j$.

$$\mathcal{S} = \begin{bmatrix} \cos\theta & 0 & 0 & 0 & 0 & -\sin\theta & 0 \\ \sin\theta & 0 & 0 & 0 & 0 & \cos\theta & 0 \\ 0 & 1 & 0 & 0 & 0 & 0 & 0 \\ 0 & 0 & \cos\theta_i & 0 & 0 & 0 & -\sin\theta_i \\ 0 & 0 & \sin\theta_i & 0 & 0 & 0 & \cos\theta_i \\ 0 & 0 & 0 & 1 & 0 & 0 & 0 \\ 0 & 0 & 0 & 0 & 1 & 0 & 0 \end{bmatrix} \tag{6.12}$$

The transformation rule for the matrix of connection 1-forms given by $\overset{A}{\omega} = \mathcal{S}^{-1}\ \overset{A}{\Gamma}\ \mathcal{S} + \mathcal{S}^{-1}d\mathcal{S}$ in Eq.(4.9), after some lengthy computations yield the following as the only nonzero connection 1-forms;

$$\omega^v_w = \frac{(2hh_\theta - \sin 2(\theta_i - \theta))}{h^2 + h_i^2 + \Theta}\sigma^v - \frac{h_i h_\theta}{h^2 + h_i^2 + \Theta}\sigma^{v_i} + \frac{h_i \cos(\theta_i - \theta)}{h^2 + h_i^2 + \Theta}\sigma^u - \frac{h_i^2}{h^2 + h_i^2 + \Theta}\sigma^z$$

$$\omega^v_{w_i} = \frac{\sin 2(\theta_i - \theta)}{h^2 + h_i^2 + \Theta}\sigma^v - \frac{hh_{\theta_i}}{h^2 + h_i^2 + \Theta}\sigma^{v_i} - \frac{(b_{i,1}\cos(2\theta_i - \theta - \phi) + b_{i,2}\sin(2\theta_i - \theta - \phi))}{h^2 + h_i^2 + \Theta}\sigma^u - \frac{hh_i}{h^2 + h_i^2 + \Theta}\sigma^{z_i}$$

$$\omega^v_u = -\frac{2hh_\theta}{h^2 + h_i^2 + \Theta}\sigma^v + \frac{h_i h_\theta + hh_{\theta_i}}{h^2 + h_i^2 + \Theta}\sigma^{v_i} + \frac{h_{\theta_i}\sin(\theta_i - \theta)}{h^2 + h_i^2 + \Theta}\sigma^u$$

$$\omega^v_z = -\sigma^w$$

$$\omega^{v_i}_w = -\frac{h_i h_\theta}{h^2 + h_i^2 + \Theta}\sigma^v - \frac{\sin 2(\theta_i - \theta)}{h^2 + h_i^2 + \Theta}\sigma^{v_i} + \frac{b_{i,1}\cos(2\theta - \theta_i - \phi) + b_{i,2}\sin(2\theta - \theta_i - \phi)}{h^2 + h_i^2 + \Theta}\sigma^u - \frac{hh_i}{h^2 + h_i^2 + \Theta}\sigma^z$$

$$\omega^{v_i}_{w_i} = -\frac{hh_{\theta_i}}{h^2 + h_i^2 + \Theta}\sigma^v + \frac{2h_i h_{\theta_i} + \sin 2(\theta_i - \theta)}{h^2 + h_i^2 + \Theta}\sigma^{v_i} - \frac{h\cos(\theta_i - \theta)}{h^2 + h_i^2 + \Theta}\sigma^u - \frac{h^2}{h^2 + h_i^2 + \Theta}\sigma^{z_i}$$

$$\omega^{v_i}_u = \frac{hh_{\theta_i} + h_i h_\theta}{h^2 + h_i^2 + \Theta}\sigma^v - \frac{2h_i h_{\theta_i}}{h^2 + h_i^2 + \Theta}\sigma^{v_i} + \frac{h_\theta \sin(\theta_i - \theta)}{h^2 + h_i^2 + \Theta}\sigma^u$$

$$\omega^{v_i}_{z_i} = -\sigma^{w_i}$$

$$\omega_w^u = \frac{h_i \cos(\theta_i - \theta)}{h^2 + h_i^2 + \Theta}\sigma^v + \frac{b_{i,1}\cos(2\theta - \theta_i - \phi) + b_{i,2}\sin(2\theta - \theta_i - \phi)}{h^2 + h_i^2 + \Theta}\sigma^{v_i} + \frac{2hh_\theta}{h^2 + h_i^2 + \Theta}\sigma^u - \frac{h_i \sin(\theta_i - \theta)}{h^2 + h_i^2 + \Theta}\sigma^z$$

$$\omega_{w_i}^u = -\frac{b_{i,1}\cos(2\theta_i - \theta - B) + b_{i,2}\sin(2\theta_i - \theta - B)}{h^2 + h_i^2 + \Theta}\sigma^v - \frac{h\cos(\theta_i - \theta)}{h^2 + h_i^2 + \Theta}\sigma^{v_i} + \frac{2h_i h_{\theta_i}}{h^2 + h_i^2 + \Theta}\sigma^u - \frac{h\sin(\theta_i - \theta)}{h^2 + h_i^2 + \Theta}\sigma^{z_i}$$

$$\omega_u^u = \frac{h_{\theta_i}\sin(\theta_i - \theta)}{h^2 + h_i^2 + \Theta}\sigma^v + \frac{h_\theta \sin(\theta_i - \theta)}{h^2 + h_i^2 + \Theta}\sigma^{v_i} - \frac{2(hh_\theta + h_i h_{\theta_i})}{h^2 + h_i^2 + \Theta}\sigma^u$$

$$\omega_v^z = \sigma^w$$

$$\omega_{v_i}^z = -\frac{h_i^2}{h^2 + h_i^2 + \Theta}\sigma^v - \frac{hh_i}{h^2 + h_i^2 + \Theta}\sigma^{v_i} - \frac{\sin(\theta_i - \theta)h_i}{h^2 + h_i^2 + \Theta}\sigma^u + \frac{2 * h * h_\theta - sin2(\theta_i - \theta)}{h^2 + h_i^2 + \Theta}\sigma^z$$

$$\omega_{w_i}^z = \frac{\sin 2(\theta_i - \theta) + 2h_i h_{\theta_i}}{h^2 + h_i^2 + \Theta}\sigma^z$$

$$\omega_u^z = -\frac{2hh_\theta + 2h_i h_{\theta_i}}{h^2 + h_i^2 + \Theta}\sigma^z$$

$$\omega_w^{z_i} = \frac{2hh_\theta - \sin 2(\theta_i - \theta)}{h^2 + h_i^2 + \Theta}\sigma^{z_i}$$

$$\omega_{v_i}^{z_i} = \sigma^{w_i}$$

$$\omega_{w_i}^{z_i} = -\frac{hh_i}{h^2 + h_i^2 + \Theta}\sigma^v - \frac{h^2}{h^2 + h_i^2 + \Theta}\sigma^{v_i} - \frac{h\sin(\theta_i - \theta)}{h^2 + h_i^2 + \Theta}\sigma^u + \frac{2h_i h_{\theta_i} + sin2(\theta_i - \theta)}{h^2 + h_i^2 + \Theta}\sigma^{z_i}$$

$$\omega_u^{z_i} = -\frac{2h_i h_{\theta_i} + 2hh_\theta}{h^2 + h_i^2 + \Theta}\sigma^{z_i}$$

where $h_\theta \triangleq \frac{\partial h}{\partial \theta}$ and $h_{\theta_i} \triangleq \frac{\partial h_i}{\partial \theta_i}$.

The vector field Y associated with the force F acting on $\mathcal{A}$, along a curve γ on Q, is give by $Y = \mathbb{G}^\sharp(F)$;

$$Y = f\mathbf{e}_v + \tau\mathbf{e}_w + f_i\mathbf{e}_{v_i} + \tau_i\mathbf{e}_{w_i} + \Gamma\mathbf{e}_u \tag{6.13}$$

where $f = \dot{v}, \tau = \dot{\theta}, f_i = \dot{v}_i, \tau_i = \dot{\theta}_i, \Gamma = \dot{\phi}$ with the earlier assumption that $m, J, m_i, J_i, \tilde{J}$ are all of unit magnitude.

Let $\mathbf{x} = \mathbf{e}\mathcal{Z}$ be the change of basis where $\mathcal{Z} = \mathcal{S}^{-1}\mathcal{R}$ with $\mathbf{x} = \boldsymbol{\partial_q}\mathcal{R}$ and

$\mathbf{e} = \boldsymbol{\partial_q}\mathcal{S}$. Matrix representation of the projection map P in the $\mathbf{e}$ basis is then given by $[P]_{\mathbf{e}} = \mathcal{Z}[P]_{\mathbf{x}}\mathcal{Z}^{-1}$ and the projection of Y onto the distribution $\mathcal{D}$ is

$$P(Y(\gamma)) = h_i\eta_i\mathbf{e}_v + \tau\mathbf{e}_w + h\eta_i\mathbf{e}_{v_i} + \tau_i\mathbf{e}_{w_i} - \sin(\theta-\theta_i)\eta_i\mathbf{e}_u$$

where

$$\begin{aligned}\eta_i = \{&b_{i,1}\sin(\theta-2\theta_i+\phi) + b_{i,1}\sin(\theta-\phi) - b_{i,2}\cos(\theta-\phi) + b_{i,2}\cos(\theta-2\theta_i+\phi))f\\ &+(b_{i,1}\sin(2\theta-\theta_i-\phi) + b_{i,1}\sin(\phi-\theta_i) + b_{i,2}\cos(\phi-\theta_i) - b_{i,2}\cos(2\theta-\theta_i-\phi))f_i\\ &-2\Theta\Gamma\}/\{2(h^2+h_i^2+\Theta)\sin(\theta-\theta_i)\}.\end{aligned}$$

The constrained dynamics in the frame $\mathbf{e}$ are as follows where $\gamma' = v\mathbf{e}_v + w\mathbf{e}_w + v_i\mathbf{e}_{v_i} + w^i\mathbf{e}_{w_i} + u\mathbf{e}_u + z\mathbf{e}_z + z_i\mathbf{e}_{z_i}$;

$$\begin{aligned}\dot{v} + w\omega_w^v(\gamma') + w_i\omega_{w_i}^v(\gamma') + u\omega_u^v(\gamma') + z\omega_z^v(\gamma') &= h_i\eta_i\\ \dot{w} &= \tau\\ \dot{v}_i + w\omega_w^{v_i}(\gamma') + w_i\omega_{w_i}^{v_i}(\gamma') + u\omega_u^{v_i}(\gamma') + z_i\omega_{z_i}^{v_i}(\gamma') &= h\eta_i\\ \dot{w}_i &= \tau_i\\ \dot{u} + w\omega_w^u(\gamma') + w_i\omega_{w_i}^u(\gamma') + u\omega_u^u(\gamma') &= \sin(\theta_i-\theta)\eta_i\\ \dot{z} + v\omega_v^z(\gamma') + w\omega_w^z(\gamma') + w_i\omega_{w_i}^z(\gamma') + u\omega_u^z(\gamma') &= 0\\ \dot{z}_i + w\omega_w^{z_i}(\gamma') + v_i\omega_{v_i}^{z_i}(\gamma') + w_i\omega_{w_i}^{z_i}(\gamma') + u\omega_u^{z_i}(\gamma') &= 0.\end{aligned} \tag{6.14}$$

Recall that for $\gamma'(0) \in \mathcal{D}$, $\overset{A}{\nabla}$ restricts γ' to $\mathcal{D}$. Once again the choice of the frame $\mathbf{e}$ is such that $\mathbf{e}_z, \mathbf{e}_{z_i} \in \mathcal{D}^\perp$ and the functions z, z_i will remain identically zero.

The next step is to design control laws for η_i, τ, τ_i of the above constrained system. For consensus of the N subsystems, the functions v, w, u must identically be the same

functions with respect to time in each of the N systems. Notice that

$$\eta_i = \frac{w\omega_w^v(\gamma') + w_i\omega_{w_i}^v(\gamma') + u\omega_u^v(\gamma') + f}{h_i}$$
$$w_i = \frac{\sin(\theta_i - \theta)\eta_i - (wv\omega_{vw}^u + wv_i\omega_{v_iw}^u + wu\omega_{uw}^u + uv\omega_{vu}^u + uv_i\omega_{v_iu}^u + uu\omega_{uu}^u) - \Gamma}{v\omega_{vw_i}^u + v_i\omega_{v_iw_i}^u + u\omega_{uw_i}^u}$$

would reduce the first and the fifth equations of the constrained dynamics to $\dot{v} = f$ and $\dot{u} = \Gamma$ respectively. Hence the following control laws are proposed to achieve consensus between the N subsystems.

$$\begin{aligned} \eta_i &= \frac{w\omega_w^v(\gamma') + w_i\omega_{w_i}^v(\gamma') + u\omega_u^v(\gamma') + f}{h_i} \\ \tau_i &= K_w(w_i^d - w_i) + \dot{w}_i^d \end{aligned} \tag{6.15}$$

where

$$w_i^d = \frac{\sin(\theta_i - \theta)\eta_i - (wv\omega_{vw}^u + wv_i\omega_{v_iw}^u + wu\omega_{uw}^u + uv\omega_{vu}^u + uv_i\omega_{v_iu}^u + uu\omega_{uu}^u) - \Gamma}{v\omega_{vw_i}^u + v_i\omega_{v_iw_i}^u + u\omega_{uw_i}^u}.$$

The above control laws of Eq.(6.15) along with initial conditions $w_i(0) = w_i^d(0)$ reduces the constrained dynamics to the following form.

$$\begin{aligned} \dot{v} &= f \\ \dot{w} &= \tau \\ \dot{v}_i + v_i(w_i - u)\frac{h_{\theta_i}}{h_i} - v(w - u)\frac{h_\theta}{h_i} &= \frac{h}{h_i}f \\ \dot{w}_i &= \tau_i \\ \dot{u} &= \Gamma \end{aligned} \tag{6.16}$$

Implementing the same functions f, τ, Γ together with the above control laws for η_i, τ_i on each of the N subsystems would result in identical functions v, w, u with respect to time appearing in each of them, thus ensuring consensus between the subsystems. We develop two sets of controllers for the functions f, τ, Γ; one for *feasibility* and the

other to achieve the *team goal*.

A. Controls for Feasibility

Solving either of the last two equations in the constrained dynamics of Eq.(6.14) with $\dot{z} = 0$ (or $\dot{z}_i = 0$) results in the identity $h_i u = \sin(\theta_i - \theta)v$. This identity along with Eq.(6.15) implies that v_i approaches v and w_i approaches w as both u and Γ approach zero (assuming $v \neq 0$). Hence controllers that achieve $v \in [v^{min}, v^{max}]$, $w, u = 0$ trivially satisfy actuator and operating constraints $\mu_i \in \Pi_i$, thus ensuring feasibility. The control law

$$\begin{aligned} \tau &= -K_w w \\ \dot{\Gamma} &= -K_\Gamma \Gamma \\ \dot{f} &= K_f(f_a - f) + \dot{f}_a \\ f_a &= K_v\Big(\frac{v^{min} + v^{max}}{2} - v\Big) \end{aligned} \tag{6.17}$$

exponentially stabilizes $w, u, \big(v - \frac{v^{min}+v^{max}}{2}\big)$ to zero. Hence the above control law along with the control law for τ_i given by Eq.(6.15), drives the system towards feasible solutions.

B. Controls to Achieve Team Goal

Let us consider a multi-agent system in a scouting scenario. The goal is to move the multi-agents in a rigid formation through a set of waypoints. The following control

law

$$
\begin{aligned}
\tau &= K_w(w^d - w) + \dot{w}^d \\
\dot{\Gamma} &= K_\Gamma(\Gamma_a - \Gamma) + \dot{\Gamma}_a \\
\Gamma_a &= K_u(u^d - u) + \dot{u}^d \\
\dot{f} &= K_f(f_a - f) + \dot{f}_a \\
w^d &= K_{\beta-\theta}(\beta - \theta) + \dot{\beta} \\
u^d &= K_{\theta-\phi}(\theta - \phi) + w \\
f_a &= K_v(v^d - v) \\
v^d &= \begin{cases} v^{min} & if\ \ formation\ \ is\ \ turning \\ v^{max} & else \end{cases}
\end{aligned}
\tag{6.18}
$$

exponentially stabilizes $(\beta-\theta), (\theta-\phi)$ and (v^d-v) to zero where $\beta = \arctan\left(\frac{y_f-y}{x_f-x}\right)$ with (x_f, y_f) being the desired waypoint of the rigid formation. Then $(\beta - \theta)$ is the angle between the desired waypoint of the formation and its current heading and the objective is to orient the formation towards the desired waypoint. The objective of the choice of v^d is to slow down the formation when negotiating a turn and speed up when not. The control laws given above along with the control law for τ_i given in Eq.(6.15) drives the system to achieve the team goal.

The same distributed control strategy proposed in the radar deception problem is proposed here and implemented in a receding horizon framework. The constrained dynamics described by Eq.(6.16) are solved for the time interval $t = [t, t + \delta t]$ using either the controls for feasibility or the controls for team goal, and this is repeated continuously from one time interval to the next.

C. Simulation Results

Figure 21 shows simulation results of the motion planning algorithm for six agents moving through a given set of waypoints while maintaining formation emulating a scouting scenario. These waypoints are specified for the geometric center O_c of the rigid formation which coincides with the origin of the B frame as explained earlier. These waypoints need to be specified sufficiently far apart from one another for the formation to successfully move through them. The spacing between agents in the rigid formation is $0.5m$ and agent speeds of $[0.2, 1.0]m/s$, and minimum turn radii of $0.4m$ are assumed to be the only actuator and operating constraints of the agents. The time history of the functions v, w, v_i, w_i corresponding to "speed" and "steer" for each of the six agents for the above results are shown in Fig.22. The lower and upper bounds of v_i, w_i are also shown and it can be seen that these functions v_i, w_i stay within their bounds. The real-time corresponding to the trajectories shown in Fig.21 was 48 sec while the CPU time (computation time) of each of the UAVs in the distributed control architecture was 3 sec.

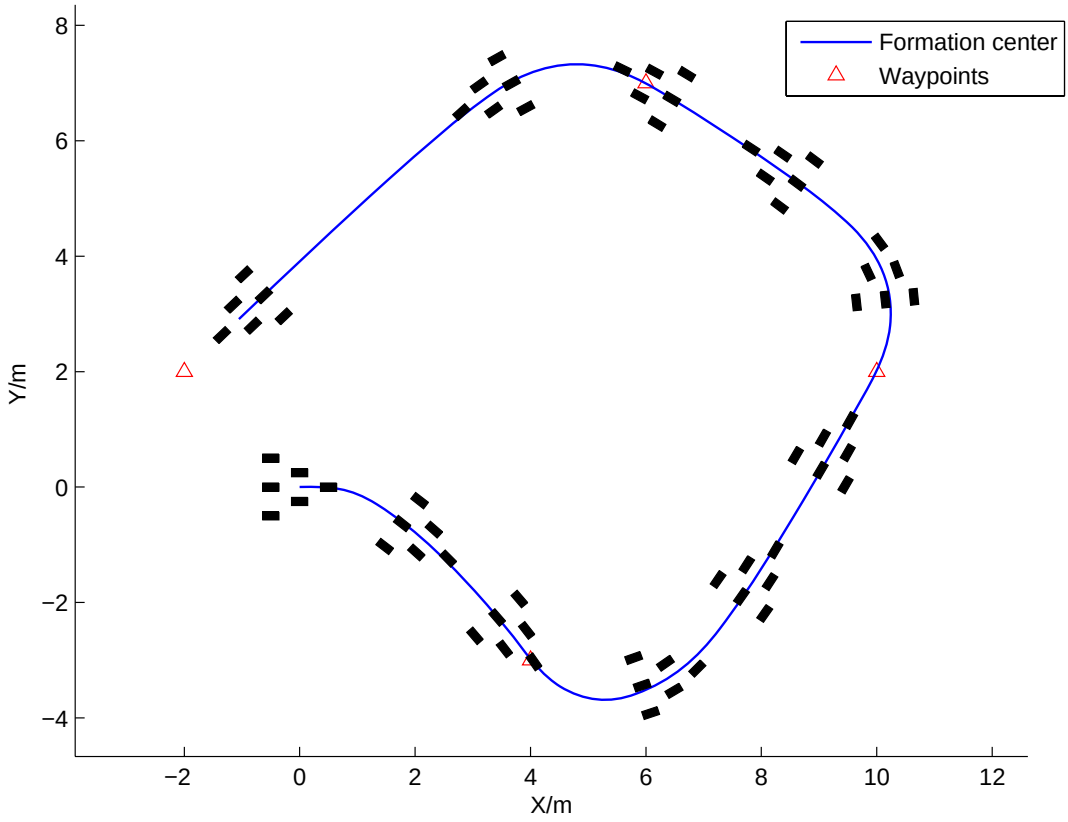

Fig. 21. Formation keeping motion for six mobile agents.

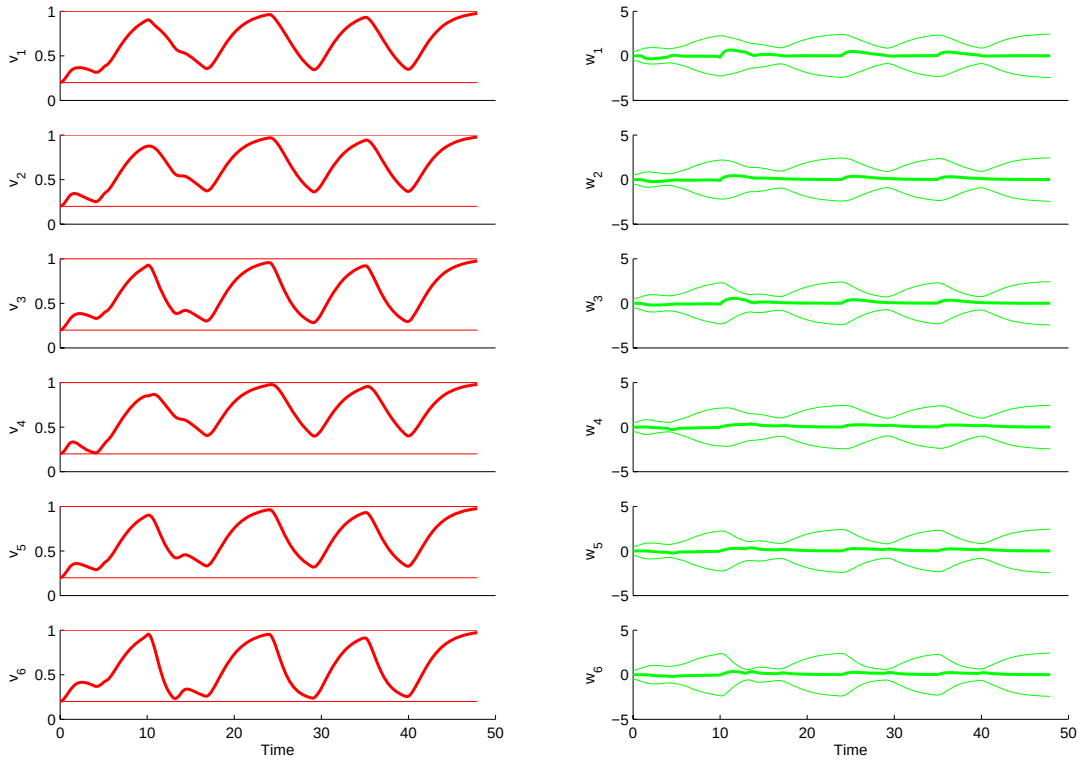

Fig. 22. "Speed" and "steer" controls for each of the six agents for the coordinated motion shown in Fig.21.

CHAPTER VII

FORMATION RECONFIGURATION

This chapter presents results of the motion planning algorithm applied to the formation reconfiguration problem.

The configuration of the formation reconfiguration problem is identified by adopting the same approach we did in the rigid formation keeping problem in the previous chapter. The only difference is that the VS made up of N agents restricted to the plane is now considered time varying. Once again let O_c be an arbitrary point on the VS (the centroid of the VS at time t_0 for example). An orthogonal local coordinate frame B is assumed fixed to the VS at O_c and let $(b_{i,1}, b_{i,2})$ denote the place holder for the i-th agent in this B frame. Here, $(b_{i,1}, b_{i,2})$ are assumed to be time varying allowing the VS to reconfigure with time. Let (x_i, y_i, θ_i) describe the position and orientation of an i-th agent with respect to an inertial frame I while (x, y, θ) describes the position and orientation of a virtual agent at O_c. Let ϕ describe the orientation of the B frame with respect to I.

The multi-agent system is decoupled into N-subsystems corresponding to the N agents, where the i-th subsystem, $\mathcal{A}$, comprises of the i-th agent, the virtual agent at O_c and the B frame. The manifold Q representing the i-th subsystem will have local coordinates $q_i = \{x, y, \theta, x_i, y_i, \theta_i, b_{i,1}, b_{i,2}, \phi\}$.

Configuration constraints of the i-th subsystem are

$$\begin{aligned} x_i - x - b_{i,1}\cos\phi + b_{i,2}\sin\phi = 0 \\ y_i - y - b_{i,1}\sin\phi - b_{i,2}\cos\phi = 0. \end{aligned} \tag{7.1}$$

Once again the dynamics of the i-th and the virtual agent at O_c are captured through

the following unicycle models

$$\begin{aligned} \dot{x}_i &= v_i \cos\theta_i & \dot{x} &= v\cos\theta \\ \dot{y}_i &= v_i \sin\theta_i & \dot{y} &= v\sin\theta \\ \dot{\theta}_i &= w_i & \dot{\theta} &= w \end{aligned} \tag{7.2}$$

along with actuator and operating constraints $u_i \in \Pi_i$

$$\begin{aligned} {v_i}^{min} \leq \quad v_i \quad &\leq {v_i}^{max} \\ -\frac{{w_i}^{max}}{{v_i}^{max}} v_i \leq \quad w_i \quad &\leq \frac{{w_i}^{max}}{{v_i}^{max}} v_i \\ v^{min} \leq \quad v \quad &\leq v^{max} \\ -\frac{w^{max}}{v^{max}} v \leq \quad w \quad &\leq \frac{w^{max}}{v^{max}} v. \end{aligned} \tag{7.3}$$

The following virtual controls are also assumed for control over the orientation of the B frame and control over the position of the i-th agent in the B frame;

$$\begin{aligned} \dot{\phi} &= u \\ \dot{b}_{i,1} &= u_{i,1} \\ \dot{b}_{i,2} &= u_{i,2}. \end{aligned} \tag{7.4}$$

Note that the above formalism differs from the rigid formation keeping problem only in that $b_{i,1}, b_{i,2}$ are considered time varying hence adding two extra coordinates to the configuration space Q of the i-th subsystem. Deriving its constrained dynamics will be similar to that of the rigid formation keeping problem of the previous chapter. Instead we follow an ad-hoc method to derive these constrained equations here. The main advantage is the ease of symbolic computations it offers while the disadvantage of course is the method being ad-hoc.

Consider the following which is the same as condition Eq.(7.1); provided that

Eq.(7.1) holds at some time instant (for example, t=0);

$$\begin{aligned} \dot{x_i} &= \dot{x} - \dot{\phi}(b_{i,1}sin\phi + b_{i,2}cos\phi) + \dot{b}_{i,1}cos\phi - \dot{b}_{i,2}sin\phi \\ \dot{y_i} &= \dot{y} + \dot{\phi}(b_{i,1}cos\phi - b_{i,2}sin\phi) + \dot{b}_{i,1}sin\phi + \dot{b}_{i,2}cos\phi. \end{aligned} \tag{7.5}$$

The above can be re-written using Eq.(7.2) and Eq.(7.4) to give the following.

$$\begin{aligned} v_i \cos\theta_i &= v\cos\theta - u(b_{i,1}\sin\phi + b_{i,2}\cos\phi) + u_{i,1}\cos\phi - u_{i,2}\sin\phi \\ v_i \sin\theta_i &= v\sin\theta + u(b_{i,1}\cos\phi - b_{i,2}\sin\phi) + u_{i,1}\sin\phi + u_{i,2}\cos\phi \end{aligned} \tag{7.6}$$

Equation (7.6) directly yields the following;

$$v\sin(\theta - \theta_i) = \left(u\ b_{i,2} - u_{i,1}\right)\sin(\phi - \theta_i) - \left(u\ b_{i,1} + u_{i,2}\right)\cos(\phi - \theta_i). \tag{7.7}$$

Taking the derivative of Eq.(7.7) with respect to time once, along with Eq.(7.2), Eq.(7.4) and Eq.(7.6) then yields;

$$\begin{aligned} v_i &= \{v\cos\theta - u(b_{i,1}\sin\phi + b_{i,2}\cos\phi) + u_{i,1}\cos\phi - u_{i,2}\sin\phi\} \ / \ \{\cos\theta_i\} \\ w_i &= \{v\ w\cos(\theta - \theta_i) + \dot{v}\sin(\theta - \theta_i) - \left(u^2 b_{i,1} + 2u\ u_{i,2} + \dot{u}b_{i,2} - \dot{u}_{i,1}\right)\sin(\phi - \theta_i) \\ &\quad - \left(u^2 b_{i,2} - 2u\ u_{i,1} - \dot{u}b_{i,1} - \dot{u}_{i,2}\right)\cos(\phi - \theta_i)\} \\ &\quad / \ \{v\cos(\theta - \theta_i) - \left(u\ b_{i,2} - u_{i,1}\right)\cos(\phi - \theta_i) - \left(u\ b_{i,1} + u_{i,2}\right)\sin(\phi - \theta_i)\}. \end{aligned} \tag{7.8}$$

The expression for w_i in Eq.(7.8) is the same as Eq.(7.7) as long as Eq.(7.7) holds for some time instant.

Then

$$\begin{aligned} \dot{v} &= f & & \\ & & \dot{x_i} &= v_i\cos\theta_i & \dot{x} &= v\cos\theta \\ \dot{w} &= \tau & & \\ & & \dot{y_i} &= v_i\sin\theta_i & \dot{y} &= v\sin\theta \\ \dot{u} &= \Gamma & & \\ & & \dot{\theta_i} &= w_i & \dot{\theta} &= w \\ \dot{u}_{i,j} &= G_{i,j} & & \end{aligned} \tag{7.9}$$

along with the expressions for w_i, v_i given in Eq.(7.8) describes the constrained dynamics of the i-th subsystem. Implementing the same functions f, τ, Γ on each of the N subsystems would achieve consensus.

Consider the following control law for $t = [t, t + \delta t]$;

$$\begin{aligned}
\tau &= K_w(w^d - w) + \dot{w}^d \\
\dot{\Gamma} &= K_\Gamma(\Gamma_a - \Gamma) + \dot{\Gamma}_a \\
\Gamma_a &= K_u(u^d - u) + \dot{u}^d \\
\dot{f} &= K_f(f_a - f) + \dot{f}_a \\
f_a &= K_v(v^d - v) + \dot{v}^d \\
\dot{G}_{a,(i,j)} &= K_G\left(G_{a,(i,j)} - G_{i,j}\right) + \dot{G}_{a,(i,j)} \\
G_{a,(i,j)} &= K_u\left(u^d_{i,j} - u_{i,j}\right) + \dot{u}^d_{i,j}.
\end{aligned} \tag{7.10}$$

We develop two sets of functions $v^d, w^d, u^d, u^d_{i,j}\ for\ j = 1, 2$ for the control law given above in Eq.(7.10), resulting in two sets of controllers; one to drive the system towards feasibility and the other to achieve the team goal.

A. Controls for Feasibility

Looking at Eq.(7.8) and Eq.(7.7) we see that v_i approaches v and w_i approaches w as $u, u_{i,1}, u_{i,2}, \dot{u}, \dot{u}_{i,1}, \dot{u}_{i,2}$ all approach zero (assuming $v \neq 0$). Hence the controls $v \in [v^{min}, v^{max}]$ and $w = u = u_{i,1} = u_{i,2} = 0$ satisfy $u_i \in \Pi_i;\ \forall i$, resulting in feasible

solutions. Hence the control law given in Eq.(7.10) along with

$$w^d = 0$$

$$u^d = 0$$

$$v^d = \frac{v^{min} + v^{max}}{2}$$

$$u^d_{i,j} = 0$$

exponentially stabilizes $w, u, u_{i,j}$ to zero and v to $(v^{min} + v^{max})/2$ driving the system towards feasibility.

B. Controls to Achieve Team Goal

The control laws to achieve the team task or the team goal depends on the task and the application at hand. Let us again consider the scouting scenario, where the goal is to move the multi-agent formation through a set of waypoints while changing the group formation on its way.

The control law given by Eq.(7.10) along with

$$w^d = K_{\beta-\theta}(\beta - \theta) + \dot{\beta}$$

$$u^d = K_{\theta-\phi}(\theta - \phi) + w$$

$$v^d = \begin{cases} v^{min} & if\ VS\ is\ turning \\ v^{max} & else \end{cases}$$

$$u^d_{i,j} = K_b \left(b^d_{i,j} - b_{i,j} \right) + \dot{b}^d_{i,j}$$

exponentially stabilizes $(\beta - \theta), (\theta - \phi), (b^d_{i,j} - b_{i,j})$ and $(v^d - v)$ to zero where $b^d_{i,j}$ describes the desired VS formation and where $\beta = \arctan\left(\frac{y_f - y}{x_f - x}\right)$ with (x_f, y_f) being the desired waypoint of the VS as earlier.

C. Simulation Results

Figure 23 shows simulation results for six agents moving through a given set of waypoints while maintaining formation and changing between predetermined formations as required. The predetermined formation configurations are specified for each of the desired waypoints and in the receding horizon approach only one desired waypoint and an associated desired formation configuration is visible to the algorithm at any given time. The control laws act to change the formation to a specific desired formation configuration only until the formation center reaches the associated waypoint, after which the algorithm only "sees" the next desired waypoint and its associated desired formation configuration. Hence for the successful transition between predetermined formation configurations, these associated waypoints need to be sufficiently far apart. Actuator and operating constraints are assumed to be the same as those for the rigid formation keeping results of the previous chapter. The simulation results are shown in the form of a series of superimposed snap shots of the coordinated multi agent motion. The functions v_i, w_i corresponding to "speed" and "steer" for each of the six agents are shown in Fig.24. The upper and lower bounds are also shown and once again it can be seen that these functions v_i, w_i stay within their bounds. The real-time corresponding to the trajectories shown in Fig.23 was 48 sec while the CPU time (computation time) of each of the UAVs in the distributed control architecture was 3 sec.

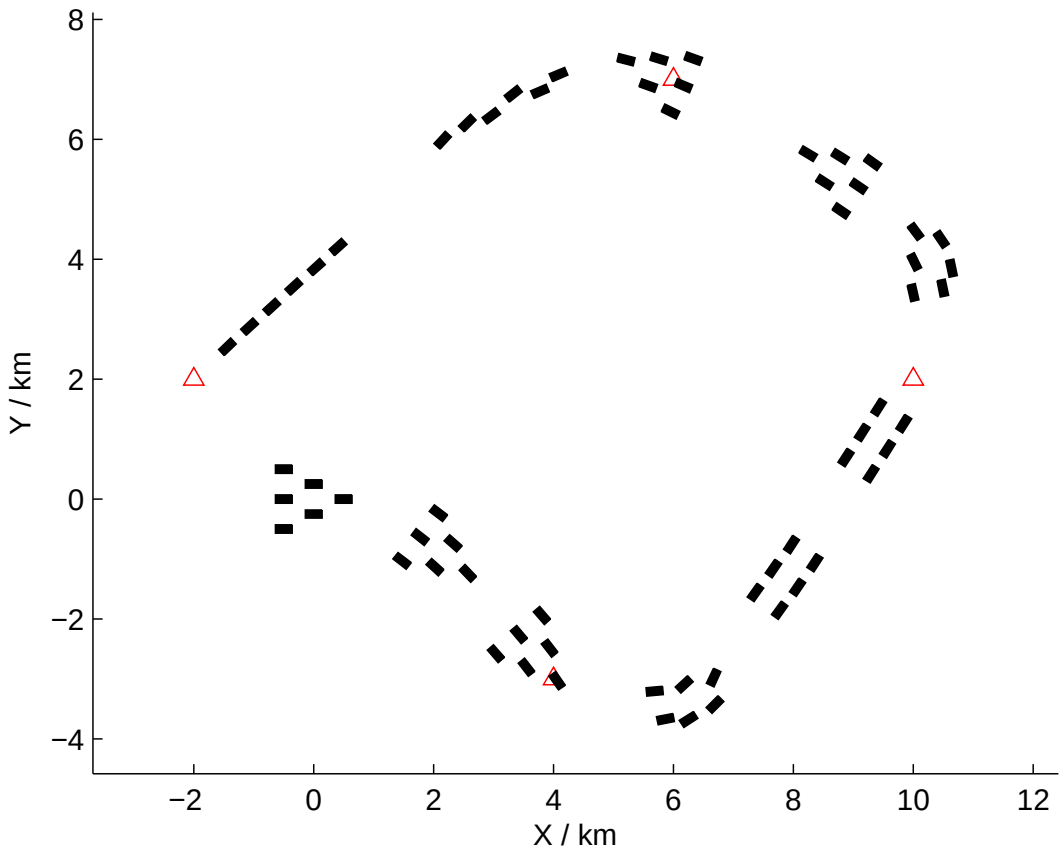

Fig. 23. Formation keeping and reconfiguration motion for six mobile agents.

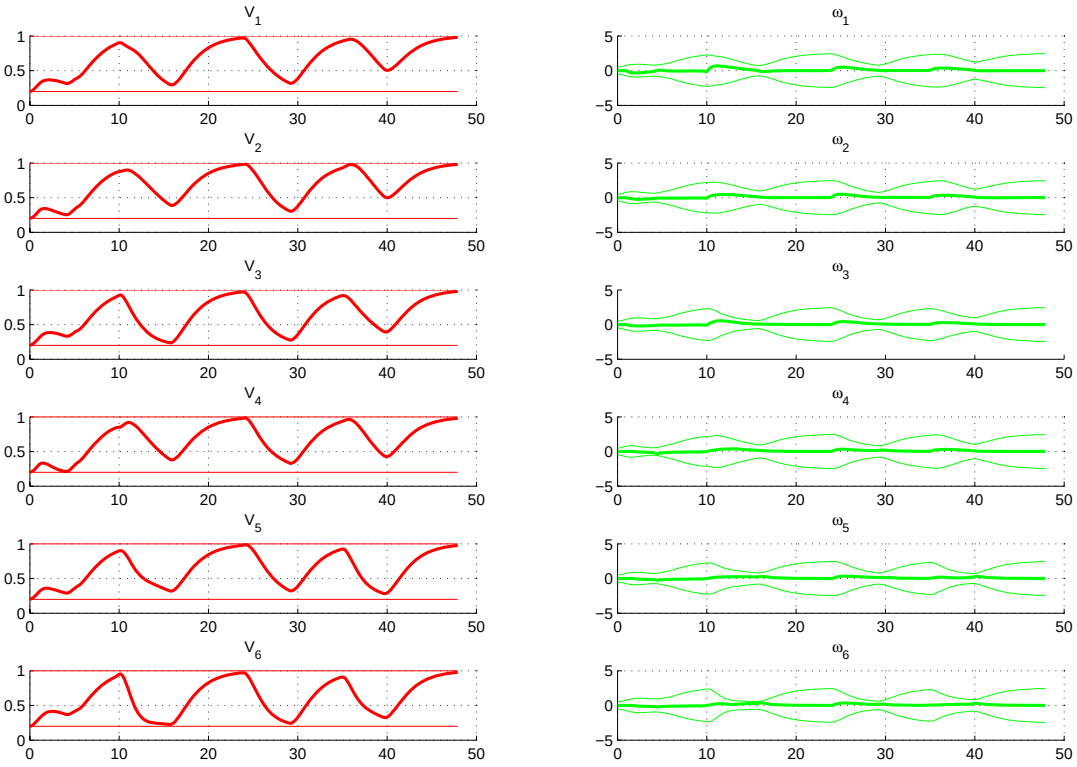

Fig. 24. "Speed" and "steer" controls for each of the six agents for the coordinated motion shown in Fig.23.

CHAPTER VIII

CONCLUSION

A class of problems in formation control is considered where an intrinsic geometric formulation of the associated constraints unifies the class of problems. The constraints can include nonholonomic, holonomic, actuator and operating constraints. A motion planning algorithm is presented for the class of problems advocating a change in paradigm to formation control by addressing both the key issues of dynamic feasibility and computational complexity. The approach to the algorithm is to embed the configuration and dynamic constraints of formation control into the design of reference trajectories to be used simultaneously by the tracking controllers of the individual agents. At the heart of the proposed approach is the explicit consideration of actuator and operating constraints of the individual agents and the derivation of constrained dynamics of the multi-agent system that makes these constraints transparent. Each of the three multi-agent formation control problems considered in this study is separated into geometrically similar subsystems for distributed control. In this distributed control architecture, each agent in the multi-agent system is responsible for the real-time computations associated with its subsystem. A control strategy ensures consensus between these subsystems and also addresses the dynamic feasibility aspect by addressing the inequality constraints that are not captured in the constrained dynamics. Deriving the constrained dynamics eliminates the need for nonlinear programming. This addresses the issue of computational complexity thereby making the approach amenable to real-time trajectory generation. Explicit consideration of actuator and operating limitations and nonholonomic constraints in the design of the reference trajectories addresses the important issue of dynamic feasibility. Global and synchronized communication is required for the implementation of the proposed algorithm.

Here global communication refers to the requirement of all the agents in the system having to communicate with all the rest of the agents in the multi-agent system. The derivation of constrained dynamics as well as the real-time trajectory generating algorithm is verified and validated through simulations for the radar deception, rigid formation keeping and formation reconfiguration examples.

From an implementation point of view, the weakest element in the proposed motion planning algorithm is the admittedly strong assumption of synchronized communication. Future research will look into the possibility of eliminating synchronized communication through an alternative control strategy, replacing the simple switching control strategy proposed in this study. Another interesting future research direction could be to consider capturing individual agent dynamic limitations through intrinsic geometric means as opposed to the proposed explicit consideration of the kinematic control form of the agents. An example would be energy shaping considerations or to directly control the intrinsic quantities of curvature, torsion and speed of individual agent trajectories to capture the dynamic limitations of agents including actuator and operating limits. Such an abstraction to capture individual agent dynamics, capabilities and operating constraints independent of exact agent dynamic models would be helpful, especially for formation control scenarios in the 3D.

REFERENCES

[1] Y. U. Cao, A. Fukunaga, A. Kahng, and F. Meng, "Cooperative mobile robotics: Antecedents and directions," in *Proc. 1995 IEEE/RSJ Int. Conf. Intell. Robot. Syst. (IROS 95)*, 1995, pp. 226-234.

[2] L. E. Parker, "Current state of the art in distributed autonomous mobile robotics," in *Distributed Autonomous Robotic Systems*, L. E. Parker, G. Bekey, and J. Barhen, Eds. Tokyo, Japan: Springer-Verlag, vol. 4, 2000, pp. 3-12.

[3] P. Tabuada, G. J. Pappas, and P. Lima, "Motion feasibility of multiagent formations," *IEEE Transactions on Robotics and Automation*, pp 387-392, 2005.

[4] H. Yamaguchi, T. Arai, and G. Beni, "A distributed control scheme for multiple robotic vehicles to make group formations", *Robot. Auton. Syst.*, vol. 36, no. 4, pp. 125-147, 2001.

[5] C. Belta and V. Kumar, "Motion generation for formations of robots: a geometric approach", in *IEEE Int. Conf. Robot. Automat.*, Seoul, Korea, 2001.

[6] J. P. Desai, J. P. Ostrowski, and V. Kumar, "Modeling and control of formations of nonholonomic mobile robots", *IEEE Trans. Robot. Automat.*, vol. 17, 2001, pp. 905-908.

[7] J.T. Betts, "Survey of Numerical Methods for Trajectory Optimization", *AIAA Journal of Guidance, Control, and Dynamics*, vol. 21, no. 2, pp. 193-207, 1998.

[8] M. B. Milam, K. Mushambi, and R. M. Murray, "A computational approach to real-time trajectory generation for constrained mechanical systems," in *Proc. IEEE Conf. Decision and Control*, Sydney, Australia, 2000, pp. 845-851.

[9] N. Faiz, S. K. Agrawal, and R. M. Murray, "Trajectory planning of differentially flat systems with dynamics and inequalities," *AIAA J. Guidance, Contr., Dynam.*, vol. 24, pp. 219-227, 2001.

[10] M. Pachter, P.R. Chandler, Reid A. Larson, K.B. Purvis, "Concepts for generating coherent radar phantom tracks using cooperative vehicles," in *AIAA Conf. Guidance, Navigation, and Control Conference*, Providence, RI, 2004.

[11] K.B. Purvis, P.R. Chandler, and M. Pachter, "Feasible flight paths for cooperative generation of a phantom radar track," *J, Guid. Control Dyn.*, vol. 29, no. 3, pp. 653-661, 2006.

[12] D.H.A. Maithripala, S. Jayasuriya, "Radar deception through phantom track generation", in *Proc. of 2005 American Control Conference*, Portland, OR, 2005, pp.4102-4106.

[13] P. K. C. Wang, "Navigation strategies for multiple autonomous robots moving in formation", *J. Robot. Syst.*, vol. 8, no. 2, pp. 177-195, 1991.

[14] J. P. Desai, J. P. Ostrowski, and V. Kumar, "Controlling formations of multiple mobile robots", in *Proc. 1998 IEEE Int. Conf. Robotics and Automation*, vol. 4, Leuven, Belgium, 1998, pp. 2864-2869.

[15] J. Desai,V.Kumar, and J. P. Ostrowski, "Control of changes in formation for a team of mobile robots", in *Proc. IEEE Int. Conf. Robotics and Automation*, Detroit, MI, 1999, pp. 1556-1561.

[16] M. A. Lewis and K.-H. Tan, "High precision formation control of mobile robots using virtual structures", *Auton. Robots*, vol. 4, pp. 387-403, 1997.

[17] M. Egerstedt and X. Hu, "Formation constrained multi-agent control", in *IEEE Int. Conf. on Robotics and Automation*, Seoul, Korea, 2001, pp. 3961-3967.

[18] B. J. Young, R. W. Beard, and J. M. Kelsey. "A control scheme for improving multi-vehicle formation maneuvers", in *Proc. of the American Control Conference*, 2001.

[19] T. Balch and R. Arkin, "Behavior-based formation control for multirobot systems", *IEEE Transactions on Robotics and Automation*, vol. 14, no. 6, pp. 926-39, 1998.

[20] F. E. Schneider, D. Wildermuth, and H.-L. Wolf, "Motion coordination in formations of multiple mobile robots using a potential field approach," in *Distributed Autonomous Robotic Systems*, L. E. Parker, G. Bekey, and J. Barhen, Eds. Tokyo, Japan: Springer-Verlag, vol. 4, 2000, pp. 305-314.

[21] C. Belta and V. Kumar, "Optimal motion generation for groups of robots: A geometric approach", *ASME J. Mech. Des.*, vol. 126, pp. 63-70, 2004.

[22] C. Belta and V. Kumar, "Abstraction and control for groups of robots", *IEEE Transactions on Robotics*, vol. 20, no. 5, pp. 865-875, 2004.

[23] E. W. Justh and P. S. Krishnaprasad, "Equilibria and steering laws for planar formations," *Systems and Control Letters*, vol. 52, no. 1, pp. 25-38, 2004.

[24] D. Paley, N. E. Leonard, and R. Sepulchre, "Oscillator models and collective motion: Splay state stabilization of self-propelled particles," in *Proc. 44th IEEE Conf. Decision and Control*, 2005, pp. 3935-3940.

[25] W. B. Dunbar and R. M. Murray, "Receding horizon control of multi-vehicle formations: A distributed implementation," in *Proc. of 43rd IEEE Conf. on*

Decision and Control, 2004, pp. 1995-2002.

[26] K.B. Purvis, P.R. Chandler, and M. Pachter, "Feasible flight paths for cooperative generation of a phantom radar track", *AIAA Conf. Guidance, Navigation, and Control Conference*, Providence, RI, 2004.

[27] M. J. Mears, "Cooperative electronic attack using unmanned air vehicles", in *Proc. of 2005 American Control Conference*, Portland, OR, 2005, pp. 3339-3347.

[28] D.H.A. Maithripala, S. Jayasuriya, M.J. Mears, "Real-time control of an autonomous control system based on feasibility analysis," in *Proc. of the 45th IEEE Conference on Decision and Control*, San Diago, CA, 2006.

[29] D.H.A. Maithripala, S. Jayasuriya, M.J. Mears, "Phantom track generation through cooperative control of multiple ECAVs based on feasibility analysis," *ASME Journal of Dynamical Systems Measurement and Control*, vol. 129, 2007, pp 708-715.

[30] K.B. Purvis, P.R. Chandler, "A review of recent algorithms and a new and improved cooperative control design for generating a phantom track", in *Proc. of 2007 American Control Conference*, Portland, NY, 2007.

[31] D.H.A. Maithripala, S. Jayasuriya, "Phantom track generation in 3D through cooperative control of multiple ECAVs based on geometric analysis," in *Proc of ICIIS*, Peradeniya, Sri Lanka, 2006.

[32] Chichka, D. F., Speyer, J. L., & Park, C. G., "Peak-seeking control with application to formation flight", in *Proc. of the 38th IEEE Conference on Decision and Control*, 1999.

[33] S. Singh, P. Chandler, C. Schumacher, S. Banda, and M. Pachter, "Adaptive feedback linearizing nonlinear close formation control of UAVs", in *Proc. 2000 Amer. Control Conf.*, Chicago, IL, 2000, pp. 854-858.

[34] F. Giulietti, L. Pollini, and M. Innocenti, "Autonomous formation flight", *IEEE Control Syst. Mag.*, vol. 20, pp. 34-44, 2000.

[35] M.J. Mataric, M. Nilsson and K.T. Simsarian, "Cooperative multi-robot box-pushing", in *Proc. of IEEE/RSJ IROS*, 1995, pp. 556-561.

[36] M. Dietl, J. S. Gutmann, and B. Nebel, "Cooperative sensing in dynamic environments," in *Proc. Int. Conf. Intelligent Robots and Systems (IROS)*, Maui, HI, 2001, pp. 1706-1713.

[37] D. J. Cook, P. Gmytrasiewicz, and L. B. Holder, "Decision-theoretic cooperative sensor planning", *IEEE Trans. Pattern Anal. Machine Intell.*, vol. 18, pp. 1013-1023, 1996.

[38] H. Yamaguchi, "A distributed motion coordination strategy for multiple nonholonomic mobile robots in cooperative hunting operations", *Robot. Auton. Syst.*, vol. 43, no. 4, pp. 257-282, 2003.

[39] K. Sugihara, I. Suzuki, "Distributed algorithms for formation of geometric patterns with many mobile robots," *Journal of Robotic Systems*, vol. 13, no. 3, pp. 127-139, 1996.

[40] G.W. Stimson, *"Introduction to Airborne Radar"*, SciTech Publishing, Raleigh, NC, 2nd ed., 1998.

[41] D. C. Schleher, *"Electronic Warfare"*, Artech House, New York, 1986.

[42] H.J. Sussmann, "A General Theorem on Local Controllability", *SIAM Journal on Control Optimization*, vol. 25, no. 1, pp. 158-194, 1987.

[43] L. E. Dubins, "On curves of minimal length with a constraint on average curvature and with prescribed initial and terminal positions and tangents", *Amer. J. Math.*, vol. 79, pp. 497-516, 1957.

[44] F. Bullo and A. Lewis, *Geometric Control of Mechanical Systems, ser. Number 49 in Texts in Applied Mathematics*, Springer-Verlag, 2004.

[45] T. Frankel, *The Geometry of Physics: An Introduction*, Cambridge University Press, 1997.

[46] A.D.Lewis, "Simple mechanical control systems with constraints," *IEEE Transactions on Automatic Control*, vol. 45, no. 8, pp. 1420-1436, 2000.

[47] D.H.A. Maithripala, S. Woo, S. Jayasuriya, "Rigid formation control of nonholonomic multi-agents," in *Proc. of the ASME International Mechanical Engineering Congress and Exposition*, Seattle, WA, 2007.

[48] D.H.A. Maithripala, S. Jayasuriya, "Rigid formation keeping and formation reconfiguration of multi-agent systems," in *Proc. of the 17th World Congress of International Federation of Automatic Control*, Soul, Korea, 2008.

VITA

D. H. Asanka Maithripala was born on March 03rd, 1976 in Sri Lanka. He received his B.S. in mechanical engineering from the University of Peradeniya, Sri Lanka in Nov, 2001 and his M.S. and Ph.D. in mechanical engineering from Texas A&M University, USA in Dec, 2005 and Aug, 2008. He may be contacted through Dr. Suhada Jayasuriya at the Department of Mechanical Engineering, Texas A&M University, College Station, TX 77843-3123.